# HYDROLOGICAL IMPACT OF BEAVER HABITAT RESTORATION IN THE MILWAUKEE RIVER WATERSHED

by

Syeda Mahmuda Noor

A Thesis Submitted in

Partial Fulfillment of the

Requirements for the Degree of

Master of Science

in Engineering

at

The University of Wisconsin-Milwaukee

May 2021

# ABSTRACT

HYDROLOGICAL IMPACT OF BEAVER HABITAT RESTORATION IN THE MILWAUKEE RIVER WATERSHED
by

Syeda Mahmuda Noor

The University of Wisconsin-Milwaukee, 2021
Under the Supervision of Professor Qian Liao

Flood is the most frequent natural disaster across the world which causes widespread destruction, loss of life, damage to property and infrastructure. There is a general assumption that beavers can help in flood mitigation by attenuating peak during large flood events though development of numerical model to analysis the impact of beaver dams on flood hydrograph is still uncommon. This study aims to combine beaver restoration strategy with a hydrologic model to assess the impact of beavers in peak flow attenuation. Based on the results of Beaver Restoration Assessment Tool (BRAT) and field survey 42 stream reaches were identified as suitable for beaver dam construction. To evaluate the impact of these beaver dams on the hydrographs of the stream flows, a numerical model was developed in the United States Army Core of Engineers-developed (USACE) Hydrologic Engineering Center Hydrologic Modeling System (HEC-HMS). Soil moisture accounting loss method was parameterized, calibrated and validated in HEC-HMS to capture the influence of soil moisture on peak flows. With beaver dams added as "reservoir" components model simulations were conducted with both past storm events and synthetic frequency storms. Four past storm events from the year 2010, 2014, 2018 and 2019 and six

frequency events between 10 and 100 year recurrence interval were applied to evaluate the impact of the dams at the eight observed locations (outlet of five sub-basins of the Milwaukee watershed and in three flood zones in the South Milwaukee river sub-basin) . The past storm simulation results showed that at these eight locations, average percentage of peak flow reduction ranged between 11% and 48%; and averaged percentage of volume reduction ranged between 15% and 48%. The frequency storm results showed average flood peak reduction ranged between 6% and 23% though volume reduction is not significant. In can be concluded from the analysis with both past storm events and frequency storm events that restoration of beaver habitats can help in peak flow attenuation.

To

my parents,

my husband,

and specially my son

## TABLE OF CONTENTS

## LIST OF FIGURES

## LIST OF TABLES

## ACKNOWLEDGMENTS

I would like to convey my endless gratitude to Professor Dr. Qian Liao for his relentless guidance and motivation during the research work. His patience and direction have been invaluable to me during this study.

I would like to thank Dr. Changshan Wu and Dr. Yin Wang for serving on my thesis committee.

I would also like to express appreciation to my parents, friends, and colleagues who all provided me support when I needed it most.

I would like to thank the Graduate School and the College of Engineering and Applied Science (CEAS) for bringing me to UWM panther family.

Finally, I would like to convey my heartiest thanks to my husband Muhammad Istiaque Haider and my son Taseen Intisam Haider for their enormous patience, sacrifice, support, and encouragement during this journey. I have no words to express my gratitude to them.

# CHAPTER 1

# INTRODUCTION

## 1.1 Background

Being highly prone to catastrophic aftermath including losses of life and damage to property and infrastructure, the risk of flooding remains a concern even in this modern era of intelligent infrastructures. Flooding has become a common occurrence in the last decades in the many regions of the world. Storms are increasing in intensity and frequency over the years due to rapid urban population growth, unplanned socioeconomic development, and undesirable climate change. Over the years, most efforts designed to reduce the effects of floods have focused on structural measures such as construction of dams or embankments (polders, levees, etc.) (C.Cuny 1991). Some of these large structural flood defenses are often rated as inappropriate over the period (Kundzecz 2002). Recently, nonstructural nature-based approaches are getting increasingly popular to reduce the impact of flooding (AR Nicholson 2012). Nicholson et al. 2012 demonstrated that the application of soft-engineered structures such as storage ponds, barriers, vegetation plantation and the setting of woody debris in the riparian zone in flood-prone areas had a great potential in managing flood hazard by altering flood flow in rural areas of UK. It is assumed that restoration of beavers, which are widely known for their dam building activities, can be adopted as a nature-based strategy in protecting valuable infrastructure from flood events. A recent study showed that water storage offered by the beaver ponds delayed downstream floodwater transmission during a large flood event in Canada. This study supports the assumption that reintroducing beaver as part of nature-

based restoration can help in flood peak attenuation during large flood events (Cherie J. Westbrook 2020).

Numerous scientific studies on beavers, over the past 30 years, have been acknowledged in study of the ecosystem benefits of beavers for biodiversity, water quality and flood abatement (Woo and Waddington 1990, Green and Westbrook 2009). River systems and watersheds with established beaver populations are much more resilient to floods. This is due to the effect of the dams and the resulting wetland complexes' ability to store and slow down water during peak high-water events (Nyssen, Pontzeele and Billi 2011, Puttock, et al. 2017, Meentemeyer and Butler 1999). Beaver dams can flatten the curve on hydrographs. Many studies have demonstrated that beavers and their dam building activities have profound impacts on the hydrology of a riverine system, such as: increasing the groundwater recharge (Westbrook, Cooper and Baker 2006); attenuating flow speed and increasing water temperature (Green and Westbrook 2009, Majerova, et al. 2015); increasing water loss through evaporation (Woo and Waddington 1990); promoting sedimentation and improving water quality (Meentemeyer and Butler 1999, Puttock, et al. 2017); and reducing flood peak flows (Nyssen, Pontzeele and Billi 2011). Fewer studies are found in literature that applied numerical models to assess beavers' hydrologic impact. MODFLOW model has been applied to investigate effects of beaver dams on regional groundwater flow through a wetland (Feiner and Lowry 2015). Hydraulic routing simulations were conducted to evaluate how beaver dams may attenuate peak flow from storms of various recurrence intervals (Beedle 1991). However, measurements and simulations estimating the influence of beaver dams on flood hydrograph and peak flows on a watershed scale are still rare.

The goal of the current study is to apply beaver restoration strategy as a natural flood mitigation approach and build a numerical model using HEC-HMS to assess the impact of beavers in peak flow attenuation. Many studies have adapted HEC-HMS as a planning tool for flood forecasting to reduce the damage of flooding. Meanwhile, GIS (geographic information systems) has become an integral part of hydrologic studies because it has the ability to capture, store, manipulate, analyze, and visualize the diverse sets of georeferenced data required for hydrologic modeling (James Oloche Oleyiblo 2010). GIS plays a major role in distributed hydrologic model parameterization. Several studies have incorporated ArcView GIS extension for watershed delineation and showed the suitability of HEC-HMS in predicting peak discharge accurately based on the available historic flood data (Joshi, et al. 2019, James Oloche Oleyiblo 2010, Salwa Ramly 2016, J.Harrower 2010). Anderson et al. (2002) adopted HEC-HMS with 48 hour ahead forecasted precipitation data to predict the reservoir inflows resulting from watershed runoff as a remedial approach to mitigate damage from flooding (M.L. Anderson 2002). Another study in the area of flood modeling has focused on coupling NEXRAD precipitation time series with GIS applications and hydrological modeling to produce a floodplain map (M.R. Knebl 2005). The most relevant reference in terms of technical approaches to this study is the application of beaver restoration strategy and development of hydrologic models to assess beaver impacts on water resources in the Jemez watershed in New Mexico (Caillat, et al. 2014).

While beaver restoration projects have been applied widely in the Mountain states and Western United States to protect riparian areas, however, it was never applied before in midwestern areas

of United States that are different in landscape and climate characteristics from the west (Pollock, et al. 2015). In this study, the HEC-HMS model combined with a Beaver Restoration and Assessment Tool (BRAT) was applied for the first time in Milwaukee River watershed in Wisconsin as a natural flood mitigation strategy, and the result showed that the restoration of beaver habitats can mitigate river flood flows, even for the urban areas at the lower end of the watershed.

## 1.2 Objectives

The primary objective of this study is to develop a modeling framework to assess the potential impacts of beaver constructed dams on the hydrological processes in the Milwaukee River watershed. Research activities included

1. To develop a GIS-based model to assess the potentials of beaver re-establishments in the watershed.
2. To develop and calibrate a hydrological model that can simulate infiltration, surface runoff, groundwater storage, and flows in the stream network of the watershed in response to precipitation events.
3. To develop hydraulic beaver dam models and evaluate their impacts on the hydrographs of river flows and flood mitigation through the calibrated hydrological model.

## 1.3 Thesis Organization

This thesis is organized into five chapters. The first chapter contains introductory information and an objectives of the paper. The second chapter includes a description of the study area as well as data collection and processing. The third chapter discusses briefly about the BRAT modeling and how the results from BRAT modeling along with field survey were used to identify suitable beaver dam locations. The fourth chapter provides an explanation of how the hydrologic models developed using arc-hydro tools and HEC-HMS. The fifth chapter presents and discusses model results. The sixth chapter contains a summary of the study and the conclusions reached.

# CHAPTER 2

# STUDY AREA AND DATA

## 2.1 Study Area

The study is carried out in Milwaukee watershed which is located in the southeastern Wisconsin. This watershed consists of three major rivers, namely Milwaukee, Menomonee and Kinnickinnic. The longest river is the Milwaukee river which flows from north and northwest to south, while the Menomonee flows from northwest to southeast. The northern portion of both rivers flow through rural areas and the southern portion flows through urban areas. The Kinnickinnic River, the shortest, flows through a heavily developed urban area from southwest to northeast. The Menomonee and Kinnickinnic rivers merge with the Milwaukee River, and then the Milwaukee River discharges into Lake Michigan. (Woonsup Choi 2016).

According to a Wisconsin Department of Natural Resources (WDNR) report (M. Burzynski 2001):

> *"The Milwaukee River Basin is located in portions of seven counties, contains (entirely or portions of) 13 cities, 32 towns, 24 villages and is home to about 1.3 million people. The Southern quarter of the basin is the most densely populated area in the state, holding 90 percent of the basin's population. The basin is divided into six watersheds (see* ***Error! Reference source not found.****). Three of the watersheds (Milwaukee River North, Milwaukee River East-West and Milwaukee River South) contain the Milwaukee River from start to finish and collectively occupy two-thirds of the basin area (584 square miles).*

*The other three watersheds (Cedar Creek, Menomonee River and Kinnickinnic River) are named after the major rivers they contain. Collectively the six watersheds contain about 500 miles of perennial streams, over 400 miles of intermittent streams, 35 miles of Lake Michigan shoreline, 57 named lakes and many small lakes and ponds. Wetlands encompass over 68,000 acres, or 12 percent of the basin land area.*

*The Natural Heritage Inventory (WDNR, 2000) has documented 16 endangered, 26 threatened and 65 special concern plant and animal species and 30 rare aquatic and terrestrial communities within the basin. The Southeastern Wisconsin Regional Planning Commission (SEWRPC) identified over 18,000 acres of high quality natural communities and critical species habitats remaining in the basin (SEWRPC, 1997). About 18 percent of the land area of the basin is covered by urban uses, while the remainder is considered rural. Agriculture is still dominant in the northern half of the basin."*

The East-West branch, North branch and Cedar Creek sub-basins are largely rural areas featured with extensive cover of grass land, farmland, forests and wetlands, and the Menomonee River, Kinnikinnic River and Milwaukee River South sub-basins have higher percentage of developed urban areas. The landscape of the Milwaukee river watershed is generally flat, and slopes of most river reaches are very mild except the main river in the South Milwaukee river sub-basin.

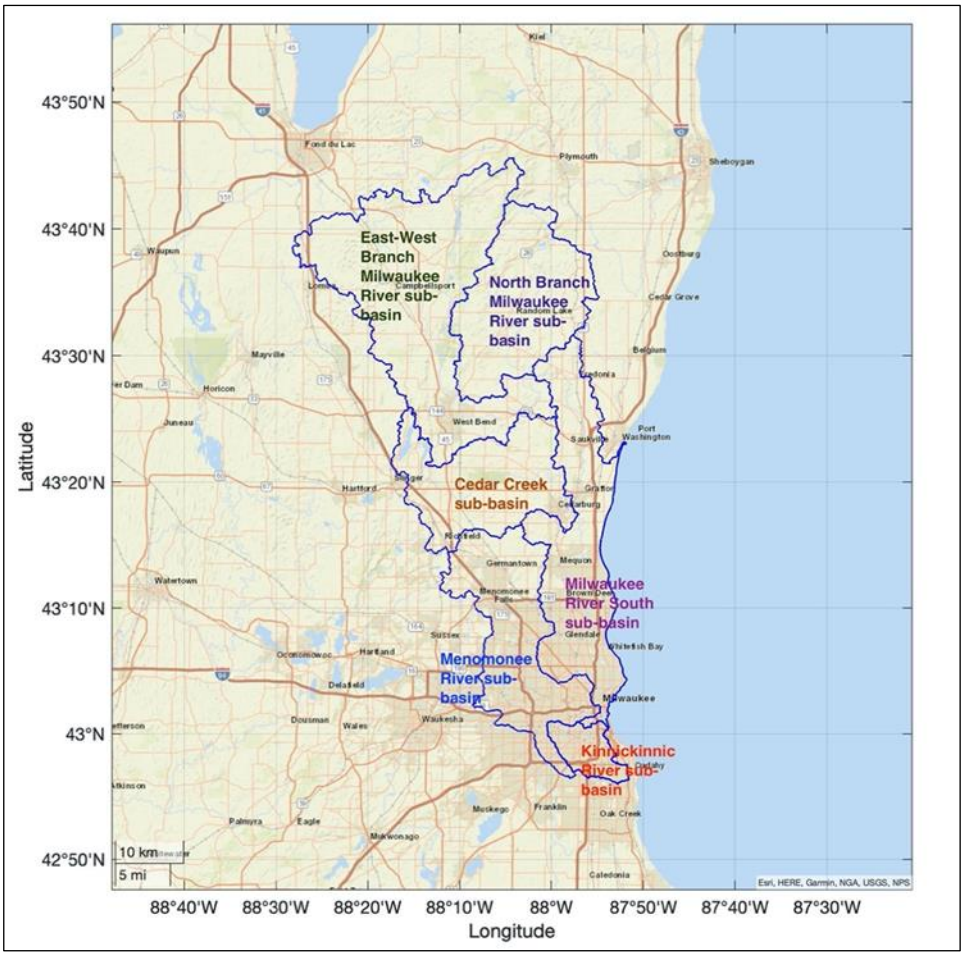


*Figure 2.1 Milwaukee river watershed and its six sub-watersheds*

## 2.2 Data Collection and Data Processing

### 2.2.1 Digital Elevation Model (DEM)

A digital elevation model is a 3D representation of ground surface topography or terrain. DEMs can be generated from ground surveys, digitizing existing hardcopy topographic maps or by photogrammetric methods. For this study, 1/3 arc-second (10-meter) resolution is used. Source

DEM data that covers the entire river basin included four mosaic patches were merged and then projected in the North American Datum (NAD) 1983 Universal Transverse Mercator (UTM) Zone 16N projection (**Error! Reference source not found.** (a)).

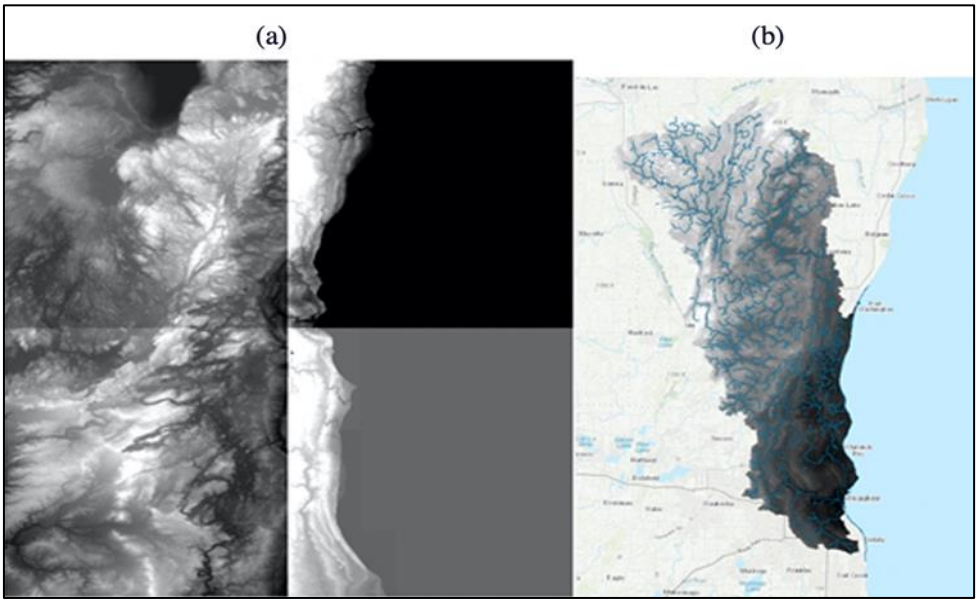


*Figure 2.2 (a) 10-m resolution DEM data from USGS (b) NHD flow network data of the Milwaukee River watershed.*

### 2.2.2 Stream Network and Watershed Boundary

The watershed boundary and stream network were obtained through USGS National Hydrograph Dataset (NHD) (https://www.usgs.gov/core-science-systems/ngp/national-hydrography) (**Error! Reference source not found.** (b)). This boundary was used to crop the DEM to reduce the computation efforts in the subsequent terrain process.

### 2.2.3 Land Cover Database (NLCD)

The hydrological modeling requires information about the percentage of impervious land area in each sub-basin. This information is provided by USGS's National Land Cover Database (NLCD) which can be directly downloaded from ArcGIS's online database (https://www.arcgis.com/home/item.html?id=1fdbb561c58b45c58f8f966c00c78ae6)

### 2.2.4 LANDFIRE Database

LANDFIRE database (https://www.landfire.gov/) provides the raster maps of vegetation types, including the existing (EVT) and historical (or potential, BPS) vegetation, which are required for BRAT modeling. LANDFIRE is a partnership between the wildland fire management programs of the United States Department of Interior, the USDA Forest Service and the Nature Conservancy. EVT and BPS maps were directly imported into ArcGIS with its online downloading tool.

### 2.2.5 SSURGO Database

Soil Survey Geographic (SSURGO) Database is required to develop the soil profile parameters required for Soil Moisture Accounting method in HEC-HMS. SSURGO datasets consist of map data, tabular data, and information about how the maps and tables were created. The extent of a SSURGO dataset is a soil survey area, which may consist of a single county, multiple counties, or parts of multiple counties. SSURGO map data were downloaded from the Web Soil Survey in ESRI® Shapefile format for all the seven counties (Milwaukee, Waukesha, Washington, Ozaukee, Fond du Lac, Sheboygan, and Dodge) that contain the entire Milwaukee River watershed.

However, SSUGO coverage does not include City of Milwaukee. Soil information for that particular area was derived from the STATGO database, which has a less spatial resolution than SSURGO.

### 2.2.6 Evapotranspiration Data

For a continuous year-round simulation of the precipitation, infiltration, surface runoff, stream flow, groundwater storage and discharge, water loss through evaporation of surface water and the transpiration through vegetation is an important component of the water budget. Combined evapotranspiration is often responsible for returning about 50~60% of the precipitation back to the atmosphere. Transpiration, a process of vegetation extracting water from the soil through the plant root system, usually causes much more water loss than evaporation. In HEC-HMS, evapotranspiration can be modeled with a number of options, including the energy balanced Penman Monteith method, physically based Priestely Taylor method as well as simple annual or monthly evapotranspiration method. All options account for the potential evapotranspiration, which is the upper limit based on atmospheric conditions, while the actual evapotranspiration rate in each subbasin is calculated based on the soil water limitation.

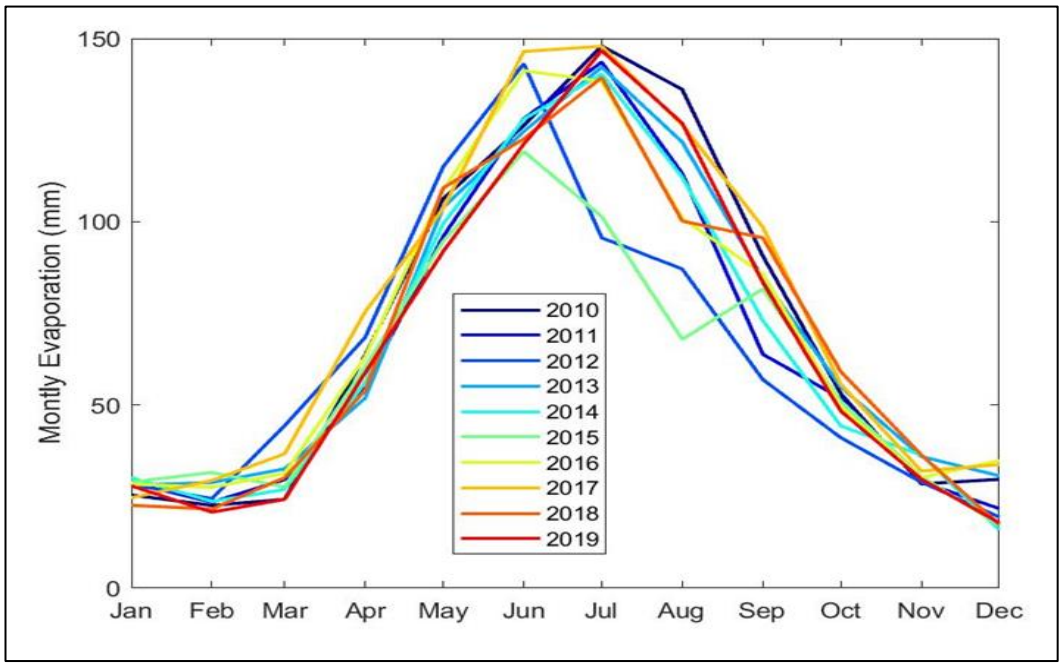


*Figure 2.3 Monthly average evaporation rate obtained from NCEP's NARR database for modeling the potential evapotranspiration in HEC-HMS*

In this study, a simple Monthly Average method was selected to model the evapotranspiration rate in mm of water depth per month. The North American Regional Reanalysis (NARR) is a product of NOAA's National Centers for Environmental Prediction (NCEP). NARR data provides various meteorological parameters, including evapotranspiration, from model simulations with assimilations from observational data. Monthly evaporation rates were extracted from the NARR database, interpolated and averaged over the Milwaukee River watershed area. *Figure 2.3* shows the monthly average evaporation depth between 2010 and 2019. These data were inputted in the HEC-HMS model.

### 2.2.7 Precipitation Data

Precipitation data are acquired from NOAA's National Centers for Environmental Information (NCEI) website (https://www.ncdc.noaa.gov/). Data used in this research are NCEI's land-based recording station data. Specifically, time sequence of precipitation depth (in inches) at every 15 minutes or hourly from multiple rain gauges around the Milwaukee River watershed were acquired. The entrance webpage for data request is https://www.ncdc.noaa.gov/cdo-web/datatools/lcd, which provides an interactive form allowing users to specify stations and date range for data download. Once the request is submitted, a follow-up email to users will provide a link for data download.

Local climate data (LCD) from the six stations between Jan 1st, 2010 and December 31st, 2019 were download from NCEI in "CSV" format. Names and geographic locations of the six rain gauges are listed in *Table 2.1*. An in-house MATLAB program was developed to read and parse all "CSV" files to extract time sequences of precipitation depth. The program also processed the raw data to time sequences with a fixed, 2-hour interval for model simulation runs. Data processed by MATLAB were exported to an EXCEL file, which will be subsequently processed for HEC-HMS import.

*Table 2.1 NOAA meteorologic stations selected for precipitation data input in HEC-HMS modeling*

| Name | WBAN | Latitude | Longitude | Location |
|---|---|---|---|---|
| **FOND DU LAC** | 04840 | 43.76944 | -88.49083 | FOND DU LAC COUNTY AIRPORT |
| **SHEBOYGAN** | 04841 | 43.76944 | -87.85056 | SHEBOYGAN CO MEMO AIRPORT |
| **WEST BEND** | 04875 | 43.41667 | -88.13333 | WEST BEND MUNICIPAL AIRPORT |
| **JUNEAU** | 04898 | 43.42639 | -88.70306 | DODGE COUNTY AIRPORT |
| **MILWAUKEE** | 14839 | 42.955 | -87.9044 | GENERAL MITCHELL INTERNATIONAL AIRPORT |
| **RACINE** | 94818 | 42.76111 | -87.81361 | JOHN H BATTEN AIRPORT |

The HEC-HMS software exchange input and output data through the Army Corps of Engineers' Hydrologic Center Data Storage System (HEC-DSS), which is a database system designed to efficiently store and retrieve scientific data that is typically sequential. Precipitation time sequences for the simulation were then converted into a DSS file. A Python tool, pydsstools (https://github.com/gyanz/pydsstools), was developed by HEC to facilitate automated data conversion and process. A set of in-house Python scripts which was developed for this study to convert input data (precipitation) and simulation results between DSS files and other data formats (such as EXCEL spreadsheet and MATLAB data storage files) for subsequent data analysis and presentation. *Figure 2.4* shows the map of the six selected rain gauges, and the precipitation time sequences in DSS data format which are visualized through the HEC-DSSVue tool.

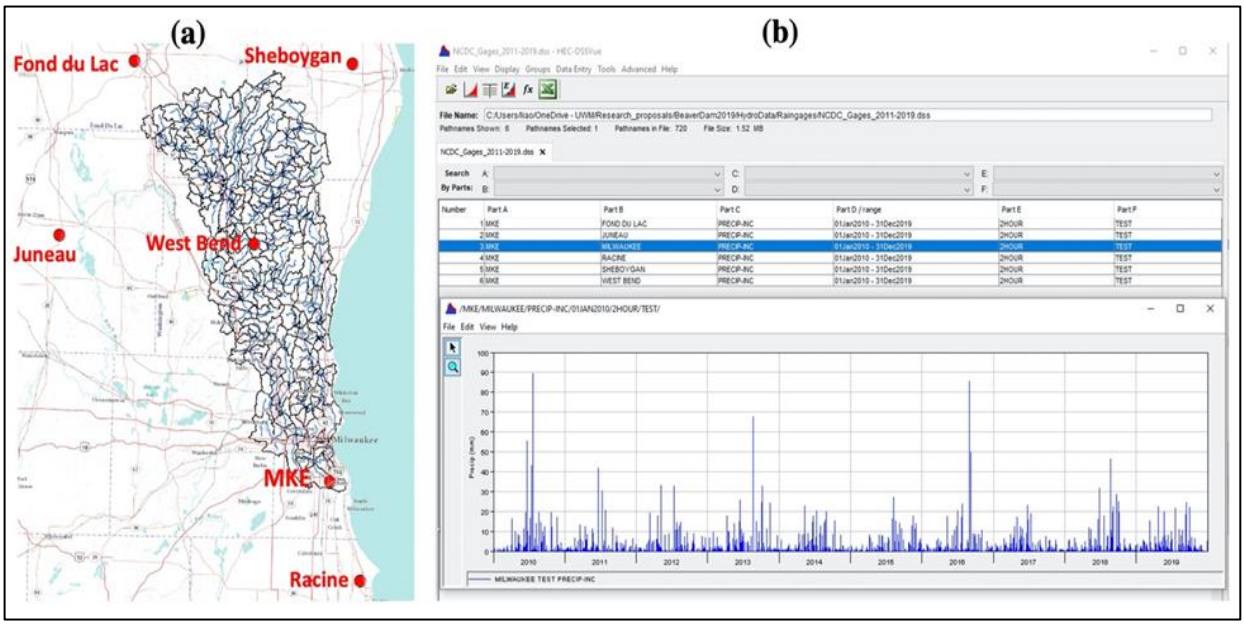


*Figure 2.4 (a) Locations of six NOAA rain gauges where precipitation data were extracted for HEC-HMS simulation. (b) Processed precipitation data converted in HEC-DSS format and visualized by HEC-DSSVue.*

### 2.2.8 Streamflow Data

Eleven stream gages within the Milwaukee River watershed were identified for the model calibration. Among the 11 stations, 1 of them is in the Cedar Creek sub-watershed; 3 in the Milwaukee River south sub-watershed; 5 in the Menomonee River sub-watershed; and 2 in the Kinnickinnic River sub-watershed. There are no USGS stream gages available in the East-West Branch and North Branch Milwaukee River sub-watersheds. The station number, name, location and the drainage areas of these gages are listed in *Table 2.2*. Locations of gages are also shown in *Figure 2.5*.

*Table 2.2 USGS stream gage stations identified for HEC-HMS model calibration*

| USGS station number | Station name | Latitude | Longitude | Drainage area ($mi^2$) | Sub-watershed |
|---|---|---|---|---|---|
| 04086500 | CEDAR CREEK NEAR CEDARBURG, WI | 43.3230556 | -87.97861111 | 120 | Cedar Creek |
| 04086600 | MILWAUKEE RIVER NEAR CEDARBURG, WI | 43.2802778 | -87.94250000 | 607 | Milwaukee River South |
| 040869416 | LINCOLN CREEK @ SHERMAN BOULEVARD AT MILWAUKEE, WI | 43.0975000 | -87.96694444 | 9.56 | Milwaukee River South |
| 04087000 | MILWAUKEE RIVER AT MILWAUKEE, WI | 43.1000000 | -87.90888889 | 696 | Milwaukee River South |
| 04087030 | MENOMONEE RIVER AT MENOMONEE FALLS, WI | 43.1727778 | -88.10388889 | 34.7 | Menomonee |
| 04087050 | LITTLE MENOMONEE RIVER NEAR FREISTADT, WI | 43.2066667 | -88.03833333 | 8 | Menomonee |
| 04087070 | LITTLE MENOMONEE RIVER AT MILWAUKEE, WI | 43.1236111 | -88.04361111 | 19.7 | Menomonee |
| 04087088 | UNDERWOOD CREEK AT WAUWATOSA, WI | 43.0500000 | -88.04611111 | 18.2 | Menomonee |
| 04087120 | MENOMONEE RIVER AT WAUWATOSA, WI | 43.0455556 | -87.99972222 | 123 | Menomonee |
| 040871488 | WILSON PARK CR @ ST. LUKES HOSPTL @ MILWAUKEE, WI | 42.9877778 | -87.95194444 | 11.34 | Kinnickinnic |
| 04087159 | KINNICKINNIC RIVER @ S. 11TH STREET @ MILWAUKEE, WI | 42.9975000 | -87.92638889 | 18.8 | Kinnickinnic |

The USGS stream stations recorded continuous stage and discharge data at every 15 minutes, which can be downloaded in various format following the web link: https://waterdata.usgs.gov/wi/nwis/current/?type=flow . An in-house MATLAB program was developed from this project to read in and parse the download page, and to convert flow series data into suitable formats (MATLAB data file or EXCEL spreadsheet) for subsequent analysis.


*Figure 2.5 Locations of USGS stream gage stations where stream flow rate data were extract for HEC-HMS model calibration*

# CHAPTER 3

# MODELING THE POTENTIALS OF BEAVER RESTORATION IN THE MILWAUKEE RIVER WATERSHED

## 3.1 Beaver Restoration and Assessment Tool (BRAT)

The Beaver Restoration and Assessment Tool (BRAT) (Macfarlane, et al. 2017) is an open-source model developed by Joseph Wheaton and William MacFarlance at the Utah State University (http://brat.joewheaton.org). The BRAT model was adapted for this project to estimate the likelihood of beaver dam building activity and the number and distribution of dams in the Milwaukee River watershed, based on the analysis of the stream network, vegetation cover, stream power under base flow high-flow conditions. Most parameters required to run the model are readily available from public resources, primarily from the US Geological Survey's (USGS) public database. Geodata have been collected and analyzed through GIS-based tools (e.g., ArcGIS and Geospatial Modeling addons) to generate modeling inputs to BRAT. Parameters for hydraulic regression models were specified based on the hydrological statistics of streams within and nearby the Milwaukee River basin and supplied to BRAT for simulation.

While BRAT has been applied successfully in western regions of the States, it has not been tested in the Midwest states that are significantly different in landscape and climate characteristics. Additional studies, including model development, parameterization, and validation with field observations, may be required to more realistically predict the capacity of the watershed to support

beaver dams and the potentials of beaver restoration. Therefore, the presented work should be considered as the first step to build a working framework for future research.

### 3.2 BRAT model configuration

BRAT is a stream network model that helps resources managers to plan and prioritize where beaver may build dams naturally, to estimate the capacity of the streamscape is to support their dam building activity, to predict where the potential for human-beaver conflicts may arise, and to highlight where and where-not beaver make sense as a conservation or restoration tool. The BRAT model estimates potential density of beaver dams along riverscape (dam count per length of stream) by evaluating the following factors (Macfarlane, et al. 2017):

- Existence of reliable water source (e.g., perennial vs ephemeral rivers)
- Riparian vegetation types that are favorable to foraging and dam building
- Vegetation within 100 m of stream to support expansion of dam complexes and maintain large colony
- The likelihood that channel-spanning dams could be built during low flows. (In the original BRAT model documentation, a low flow is defined as a base flow condition derived from a regional regression model)
- The likelihood that a beaver dam is likely to withstand typical floods (In the original BRAT model documentation, a typical flood is defined as the peak discharge of a 2-year flow)
- A suitable river that is not too large to restrict dam building or persistence.

A fuzzy inference modeling system is then applied to combine these factors to estimate beaver dam densities on each stream segment.

### 3.3 Model Results and Discussion

Model results suggested that vegetation type is the dominant factor that determines beaver potential capacity in the Milwaukee river watershed, as the difference between the outputs of vegetation-only and combined models is barely noticeable when comparing *Figure 3.1(a)* to *Figure 3.1(b)*. Specifically, mean beaver capacities averaged over all river segments are: 5.82 dams/km with the EVT-only model; 5.58 dams/km with the EVT-combined model; 9.00 dams/km with the BPS-only model; and 8.48 dams/km with the BPS-combined model. The landscape of the Milwaukee river watershed is generally flat, and slopes of most river reaches are very mild except the main river in the South Milwaukee river sub-basin. The hydrological condition is favorable for beavers at most river segments, which explains the minor difference between the vegetation-only and combined models. In this project, BRAT model results were used as a planning tool for field survey studies.

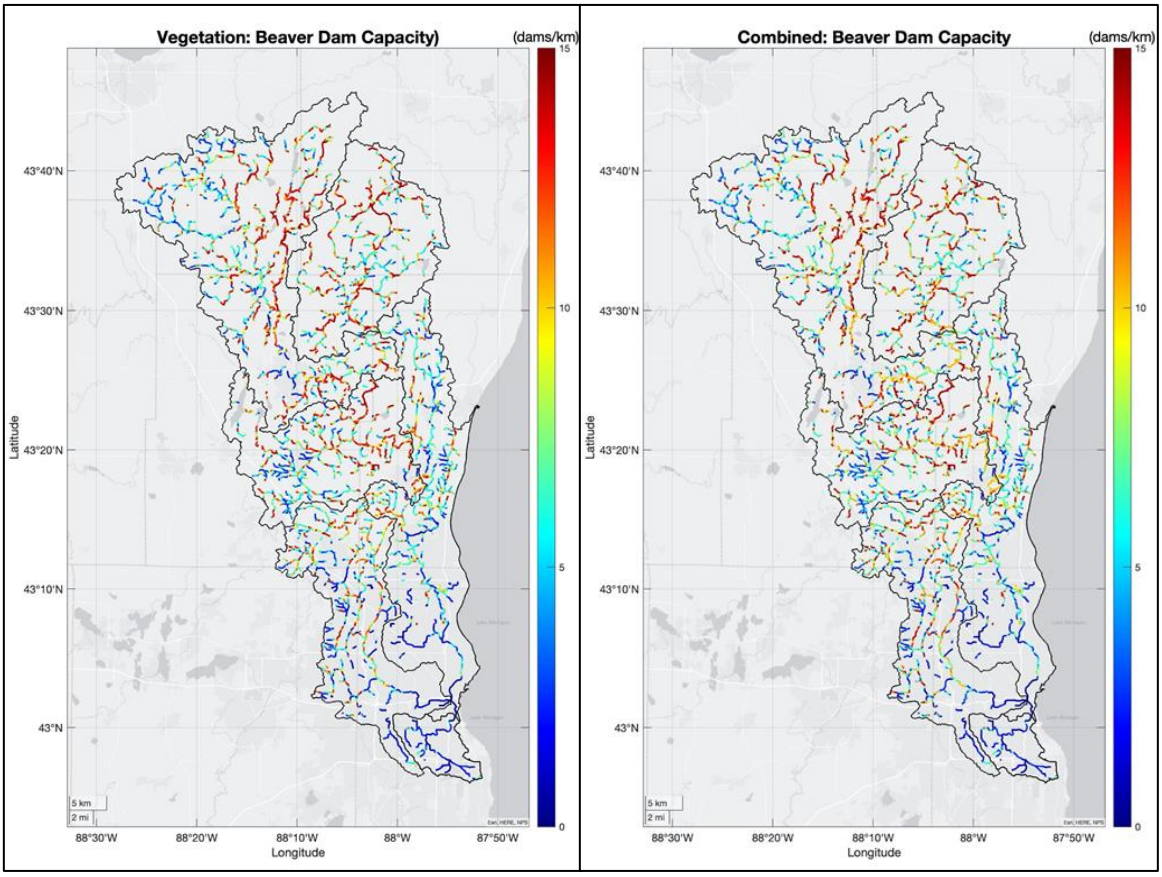


*Figure 3.1(a)Potential beaver capacity distribution as result of BRAT FIS model based on current vegetation cover (b) Potential beaver capacity distribution as result of BRAT FIS with vegetation (existing) and hydrologic factors combined model*

## 3.4 Beaver Dam Identification

According to BRAT modeling results and site evaluations an in-house MATLAB program was developed to identify the most likely locations for beavers to build dams based on topography (Digital Elevation Model- DEM) and aerial image. With this process, 42 dam locations were identified for the subsequent hydrologic modeling. Once the dam locations were determined, the program recorded the designed dam height and resulting dam length. Then a rating process was

conducted to calculate the change of ponding area and volume by setting water levels varying between 0 and the designed dam height This process produces Stage-Area and Stage-Volume rating curves for HEC-HMS modeling. These dams are distributed in 5 sub-watersheds, with

- 8 dams in the East-West Branch Milwaukee River watershed (East-West),
- 10 dams in the North Branch Milwaukee River watershed (North),
- 7 dams in the Cedar Creek watershed (Cedar),
- 9 dams in the Menomonee River watershed, and (Meno)
- 8 dams in the Milwaukee River South watershed (South).

(words in parentheses represent acronyms of each sub-watershed). No dams are identified as suitable for the Kinnikinnic River watershed. Locations of the 42 identified dams are shown in *Figure 3.2*. ***Error! Reference source not found.*** lists all identified dams, including their designed dam heights, dam lengths, ponding water surface areas and storage volumes with beaver dam.

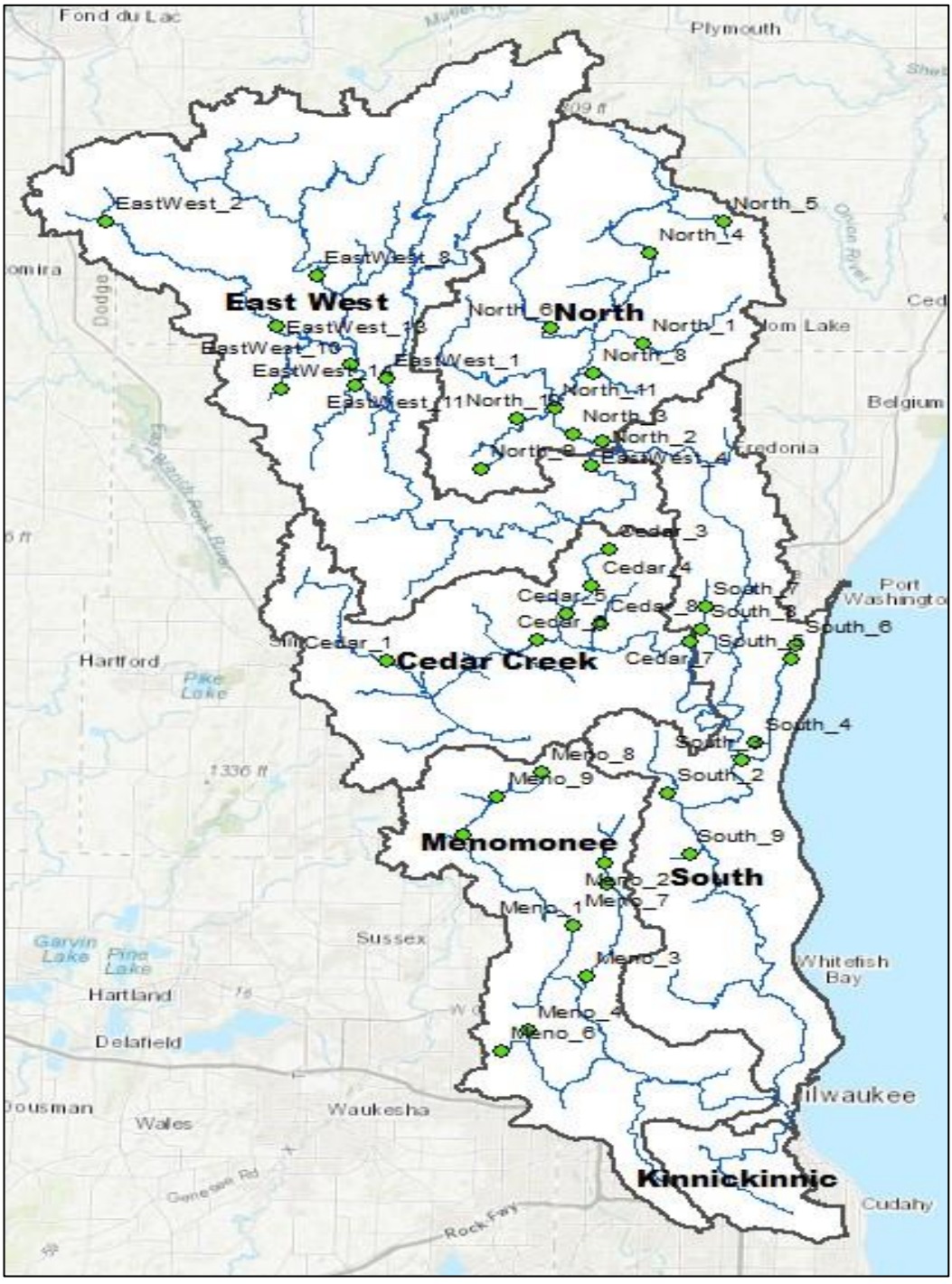


*Figure 3.2 Distribution of beaver dams identified for hydrologic modeling. Solid circles indicate dam locations and blue lines represent the stream network in the HEC-HMS model*

*Table 3.1 Summary table of all 42 identified beaver dams in five sub-basins of the Milwaukee River watershed, including designed dam heights, lengths, ponding water area and volume*

| ***East-West Branch Milwaukee River Sub-Watershed*** | | | | |
|---|---|---|---|---|
| Dam ID | Dam Height (m) | Dam Length (m) | Ponding Area (Acre) | Ponding Volume (Acre-m) |
| EastWest_1 | 0.3 | 17 | 14 | 5.6 |
| EastWest_2 | 0.5 | 62 | 8 | 4.0 |
| EastWest_4 | 0.6 | 54 | 10 | 16 |
| EastWest_8 | 0.3 | 54 | 13 | 6.7 |
| EastWest_10 | 0.3 | 50 | 11 | 12.4 |
| EastWest_11 | 1.2 | 16 | 7 | 7.3 |
| EastWest_13 | 0.45 | 35 | 8 | 5.0 |
| EastWest_14 | 0.3 | 37 | 13 | 4.0 |
| **Total Ponding Area (acre)** | | **84** | **Total Ponding Volume (Acre-m)** | **54.3** |

| ***North Branch Milwaukee River Sub-Watershed*** | | | | |
|---|---|---|---|---|
| Dam ID | Dam Height | Dam Length | Ponding Area (Acre) | Ponding Volume (Acre-ft) |
| North_1 | 0.3 | 43 | 10 | 8.9 |
| North_2 | 0.3 | 68 | 9 | 6.8 |
| North_3 | 0.8 | 36 | 7 | 7.8 |
| North_4 | 0.16 | 87 | 19 | 8.1 |
| North_5 | 0.15 | 27 | 12 | 6.3 |
| North_6 | 0.75 | 29 | 7 | 9.1 |
| North_8 | 0.18 | 79 | 17 | 5.8 |
| North_9 | 0.7 | 53 | 7 | 5.9 |
| North_10 | 0.7 | 52 | 7 | 7.5 |
| North_11 | 0.4 | 128 | 7 | 6.7 |
| **Total Ponding Area (acre)** | | **102** | **Total Ponding Volume (Acre-m)** | **73.0** |

| ***Cedar Creek Sub-Watershed*** | | | | |
|---|---|---|---|---|
| Dam ID | Dam Height | Dam Length | Ponding Area (Acre) | Ponding Volume (Acre-ft) |
| Cedar_1 | 0.15 | 64 | 16 | 10.8 |
| Cedar_3 | 0.24 | 51 | 9 | 2.3 |
| Cedar_4 | 0.4 | 59 | 8 | 5.0 |
| Cedar_5 | 0.5 | 64 | 7 | 5.0 |
| Cedar_6 | 0.12 | 54 | 20 | 18.8 |
| Cedar_7 | 0.7 | 36 | 6 | 4.3 |
| Cedar_8 | 0.7 | 51 | 5 | 3.8 |
| **Total Ponding Area (acre)** | | **71** | **Total Ponding Volume (Acre-m)** | **50.1** |

| ***Menomonee River Sub-Watershed*** | | | | |
|---|---|---|---|---|
| Dam ID | Dam Height | Dam Length | Ponding Area (Acre) | Ponding Volume (Acre-ft) |
| Meno_1 | 0.9 | 35 | 7 | 5.4 |
| Meno_2 | 0.28 | 53 | 12 | 5.9 |
| Meno_3 | 0.4 | 122 | 7 | 3.9 |
| Meno_4 | 0.6 | 48 | 8 | 7.4 |
| Meno_6 | 0.1 | 47 | 10 | 2.8 |
| Meno_7 | 0.2 | 42 | 8 | 4.1 |
| Meno_8 | 0.3 | 42 | 9 | 4.3 |
| Meno_9 | 0.36 | 61 | 5 | 1.0 |
| Meno_10 | 0.2 | 73 | 9 | 2.6 |
| **Total Ponding Area (acre)** | | **75** | **Total Ponding Volume (Acre-m)** | **37.3** |

| ***Milwaukee River South Sub-Watershed*** | | | | |
|---|---|---|---|---|
| Dam ID | Dam Height | Dam Length | Ponding Area (Acre) | Ponding Volume (Acre-ft) |
| South_2 | 0.5 | 58 | 5 | 4.0 |
| South_3 | 0.64 | 40 | 7 | 7.2 |
| South_4 | 0.42 | 30 | 7 | 3.2 |
| South_5 | 0.16 | 75 | 16 | 14.5 |
| South_6 | 0.12 | 104 | 12 | 2.5 |
| South_7 | 0.3 | 70 | 8 | 2.4 |
| South_8 | 0.5 | 67 | 6 | 5.5 |
| South_9 | 0.4 | 73 | 8 | 9.5 |
| **Total Ponding Area (acre)** | | **69** | **Total Ponding Volume (Acre-ft)** | **48.8** |

# CHAPTER 4

# MODELING HYDROLOGIC IMPACTS OF BEAVER RESTORATION IN MILWAUKEE RIVER WATERSHED

## 4.1 Hydrologic modeling framework: HEC-GeoHMS and HEC-HMS

Hydrograph processes across the Milwaukee River Basin, which includes watersheds of Milwaukee River, Menomonee River and Kinnickinnic River, were simulated with a Hydrologic Modeling System developed by the US Army Corps of Engineers Hydrologic Engineering Center (HEC-HMS). HEC-HMS is capable of simulating precipitation-runoff processes of dendritic watershed systems. Beaver dams were modeled as reservoir components in HEC-HMS.

To prepare inputs to HEC-HMS modeling, geo data were pre-processed with HEC-GeoHMS, which is an interface software between HEC-HMS and ArcGIS. These processes included delineating the watershed and its sub-basins, and reconditioning river channels. Hydrological parameters that are related to vegetation interception, soil infiltration and storage, groundwater storage, and the time of concentration of each sub-catchment were also analyzed and specified through the HEC-GeoHMS interface. Modeling procedures using HEC-GeoHMS and HEC-HMS are presented in detail in the following sections.

## 4.2 Model Preparation with Arc Hydro Tools

### 4.2.1 Basin pre-processing

The Milwaukee River Watershed was delineated using ArcHydro tools in the HEC-GeoHMS module on a 1/3 arc-second (10-meter) resolution Digital Elevation Model (DEM). First, the DEM was reconditioned through a "burning in" method for stream identification, i.e., the DEM cells that intersect with known drainage lines are artificially lowered such that streams, particularly those with low gradient and meanders, can be correctly identified. The NHD flow network of the Milwaukee River watershed was applied for the "burning in" process.

With the reconditioned DEM, the following procedures were carried out to reconstruct the flow network in the watershed:

- Flow direction raster map was calculated for every pixel of the DEM.
- Flow accumulation raster map was calculated to evaluate the drainage area of each "pixel" of the DEM.
- Streams were defined based on a specified minimum drainage area, which was set to 8 $km^2$ in this study, i.e., a pixel on the DEM is defined as part of a stream if its flow accumulation area is greater than 10 $km^2$. The specified minimum drainage area will eventually define the number of sub-basins to be created in the model.
- Stream segmentation process was carried out to link all defined "stream pixel" to linked stream network.

### 4.2.2 Watershed and sub-watershed delineation

Following the results from stream process, the entire watershed and sub-basins were delineated by taking a number of steps in HEC-GeoHMS: (1) Catchment grid delineation (2) Watershed polygon processing (3) Drainage line processing and (4) Adjoint catchments.

A final step was taken to define the Milwaukee River watershed based on a selected outflow point (***Error! Reference source not found.***). The outlet was selected to be at the confluence point of the Milwaukee River and the Kinnickinnic River. HEC-GeoHMS automatically tracks back to include all sub-basins that contributes to the flow at the outlet.

As a result, 135 sub-basins and 135 river reaches were defined in this model. The final number of sub-basins will be increased as some sub-basins will be sub-divided at locations where river gages and beaver dams are inserted in the flow network.

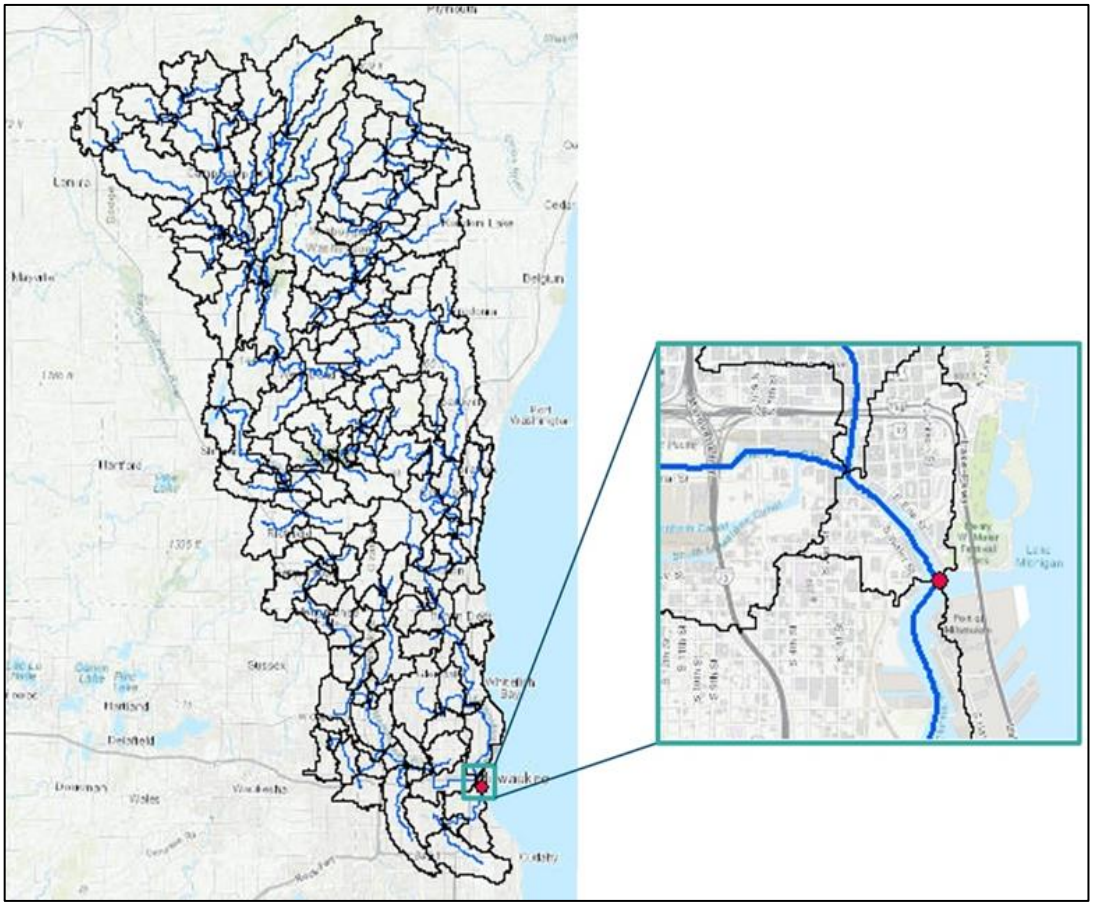

*Figure 4.1 Sub-basins and river reach segments identified from HEC-GeoHMS process, the entire Milwaukee River watershed was delineated based on the selection of outlet point where Milwaukee river discharge into the Milwaukee harbor (inserted figure)*

### 4.2.3 Placement of Beaver dams and stream gages

The location of 42 beaver dams were placed which were determined following BRAT modeling and field surveying studies (*Section 3.4* ). For the HEC-HMS model to recognize a beaver dam as portion of the stream regime, it is vital to make both an upstream and downstream connection to the dam and relative storage. Each dam is associated with an upstream river reach and a sub-basin so that the flow and the storage can be measured when the water travels through the dam.

Therefore, a subbasin was created manually using the "subdivide basin" in HEC-GeoHMS by inserting a dividing point at a beaver dam location (***Error! Reference source not found.*** *(a)*).The inserted point was then considered as a "junction" component in HEC-HMS. This junction point can be converted into a "reservoir" component subsequently to model the hydrologic impact of a beaver dam. In this study, "beaver dams" were inserted in HEC-GeoHMS for simulation cases with and without beavers. In the latter case, they were considered simply as a placeholder in terms of "junctions".

Similarly, USGS stream gauges were added to the map as junctions, which serves as placeholders for extracting simulated flow series to be compared with USGS flow data. As illustrated in *section 2.2.8*, 11 stream were selected for model calibration, which were placed in the watershed. ***Error! Reference source not found.****(b)* shows locations of beaver dams and stream gauges placed using the "subdivide basin" tool in HEC-GeoHMS.

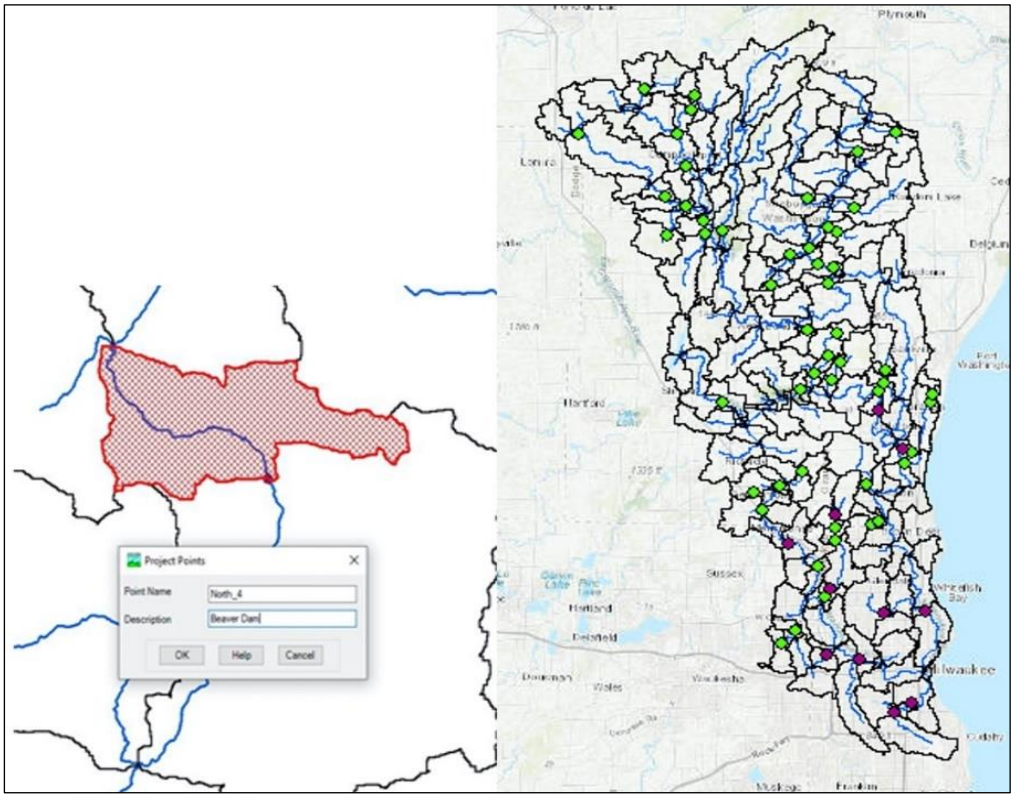


*Figure 4.2 (a) Placement of beaver dam using sub basin division tool (b) Location of Beaver dams (green diamond) and stream gauges (purple circles)*

### 4.2.4 Post-processing sub-basins and river reaches

Post-processes in Geo-HMS included calculations of river slope, basin slope, and longest flow path to collect geometric and topographic information of sub-basins for surface runoff transformation analysis. The longest flow path computes the length from the farthest point to the outlet for each sub-basin, which is used to estimate the time of concentration during processing of hydrologic parameters. In addition, basin centroids are identified for each sub-basin based on longest flow path method. Geographic coordinates, elevations and centroidal longest flow path of sub-basin centroids were calculated as well. In this study, precipitation on each sub-basin was

determined based on land-based rain gauge data using an "inverse distance" approach . Geographic coordinates of rain gauges used in this study were imported as a point layer in Geo-HMS for preparing the meteorological model components.

With physical characteristics of streams and sub-basins determined, TR55 flow path segments, TR55 flow path segment parameters are estimated in HEC-GeoHMS. For the TR-55 methodology, surface runoff process consists of sheet flow, concentrated flow and channel flows, with the corresponding lengths and slopes of flows computed in GeoHMS.

In the final step of the HEC-GeoHMS process, data were converted into a HEC-HMS input file, i.e., a "basin file" which is an ASCII file describes all HEC-HMS components. For this purpose, HEC-GeoHMS map layers were first converted into HMS units (SI Units), watershed schematic such as HMS link and HMS node were then added to the map before exporting to HEC-HMS input files (*Figure 4.3*). The layers for sub-basins and rivers were exported to GIS shape files and the attribute tables of longest flow path, basin centroids, HMSLink, HMSNode and project point are exported as excel files for the subsequent MATLAB analysis. In this study, MATLAB programs have been developed to post-process HEC-GeoHMS results and to generate ASCII files for HMS modeling inputs which include: (1) a "basin" file; (2) a precipitation "gage" file; and (3) a meteorological "met" file.

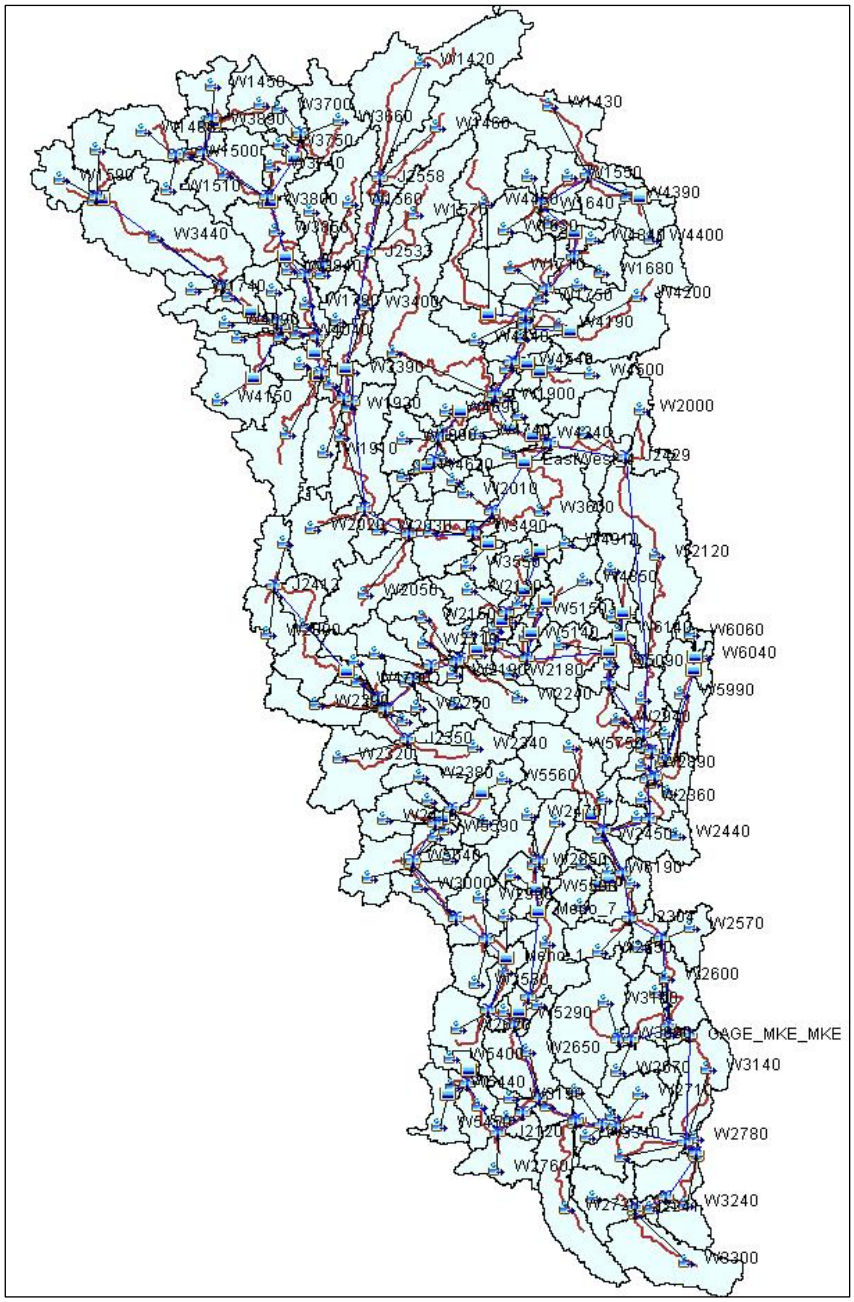


*Figure 4.3 HEC-HMS basin file of the Milwaukee River watershed as a result of HEC-GeoHMS processes.*

## 4.3 HMS Model Configuration

HEC-HMS is a distributed model for the simulation of complete hydrologic processes of dendritic watershed systems. A watershed is typically divided into “sub-basins” components from which water drains to “junction” points, and junctions are connected by streams or “reach” components. In a sub-basin, the model simulates losses due to surface storage, interception, infiltration and evapotranspiration; the transform process which produces surface runoff; and the groundwater storage and baseflow. The model also simulates routing (stream flow) process in reach components.

For this project, hydrologic processes in the Milwaukee River watershed are simulated with the following configurations:

- Hydrologic losses through infiltration, evapotranspiration, interception and detention were modeled using the simple surface, simple canopy and soil moisture accounting methods, respectively,
- Rainfall – runoff conversion was modeled by the Clark Unit Hydrograph method,
- Interflow and base flows due to groundwater seepage were modeled through a linear reservoir method,
- Routing of streamflow in river channels was modeled by the Muskingum-Cunge method.

The overall model framework and processes simulated are shown in *Figure 4.4*. Details of model configuration and parameterizations are presented in the following sections (from *Section 0* to *Section 4.8*) .

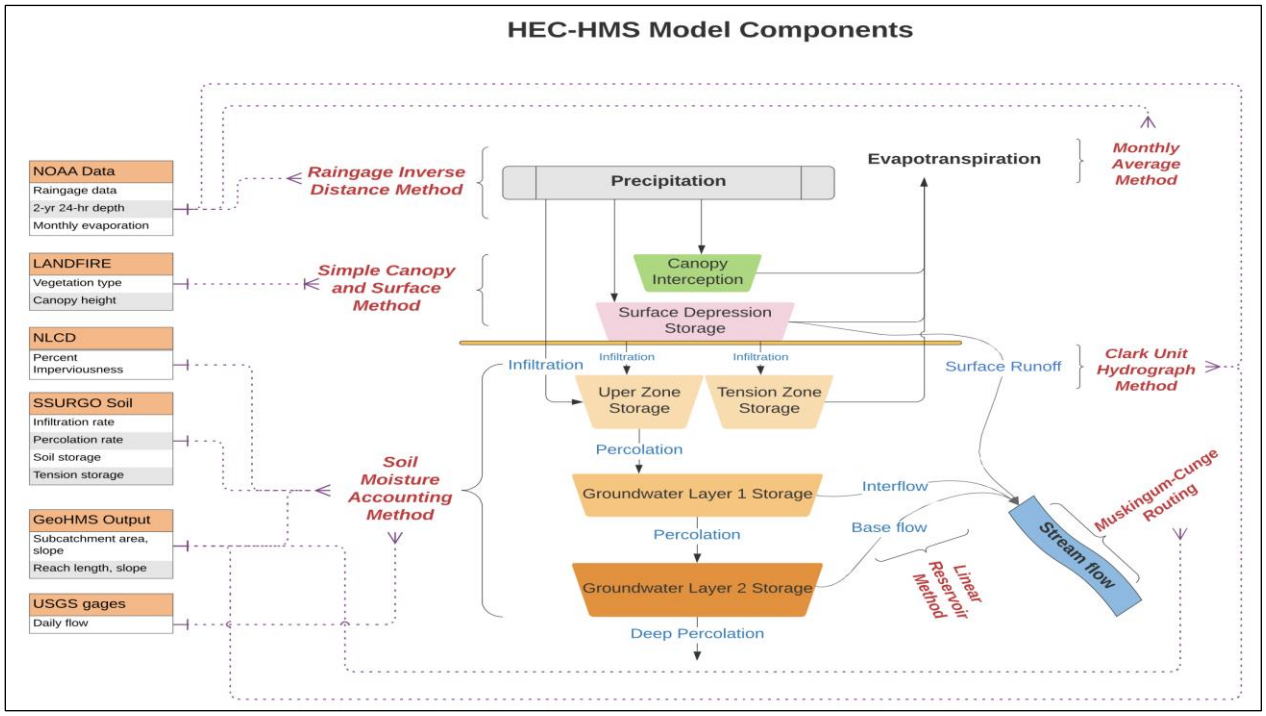


*Figure 4.4 Model framework and hydrologic processes simulated in the current study. Solid lines with arrows indicate flow directions of water cycles. Dashed lines with arrows represent data dependency for parameters of sub-model components.*

## 4.4 Soil Moisture Accounting (SMA) Algorithm for hydrologic losses

The Hydrologic Modelling System (HEC-HMS), developed by US Army Corps of Engineers Hydrologic Engineering Center was adopted for this study because it is designed for both continuous and event-based hydrologic modelling. Unlike event based, continuous hydrologic models consider soil moisture balance over a long time period and are appropriate for simulating daily, monthly and seasonal stream flow (Xuefeng Chu 2009, Flemming 2004). Though soil moisture has a significant impact on the hydrological processes of a watershed, it is rarely used for model simulation, because the structure of the model is very complex and it requires a large set of data which is often difficult to estimate (J. Holberg 2015, Yves Tramblay 2010). Flemming and

Neary (2004) derived the soil moisture parameters using the State Soil Geographic (STATSGO) database and geographic information system (GIS) software (Flemming 2004). Holberg (2015) explained the SMA method for both event based and continuous models (J. Holberg 2015). Recently, Samady (2017) adopted SMA algorithm for continuous hydrologic modeling to analyze the effects of drought on the lower Colorado river in Texas (Samady 2017).

### 4.4.1 Structure of Soil Moisture Accounting Algorithm

SMA is a continuous model that captures extensive loss determining how much and how fast precipitation will be lost to five different storage components including canopy-interception storage, surface-depression storage, soil profile storage and two groundwater storage. When precipitation starts, it first fills canopy storage. Once the canopy storage is filled, the additional precipitation, not captured by canopy interception and in excess of the infiltration rate, is held by shallow surface depressions. When the volume of these surface depressions is filled, the excess water flows over the land creating surface-runoff. After filling the canopy-interception storage and surface-depression storage, precipitation starts to infiltrate through soil profile storage. Soil profile storage is divided into two regions, the upper zone and tension zone. Precipitation fills the tension zone first and then it moves to the upper zone. From the soil profile storage precipitation percolates into the first layer of groundwater storage. Excess percolation to the first layer of groundwater storage percolates to the second layer of groundwater storage. Stored water can percolate from second layer of groundwater storage to a deep aquifer and is considered lost from the system *(Figure 4.5).*

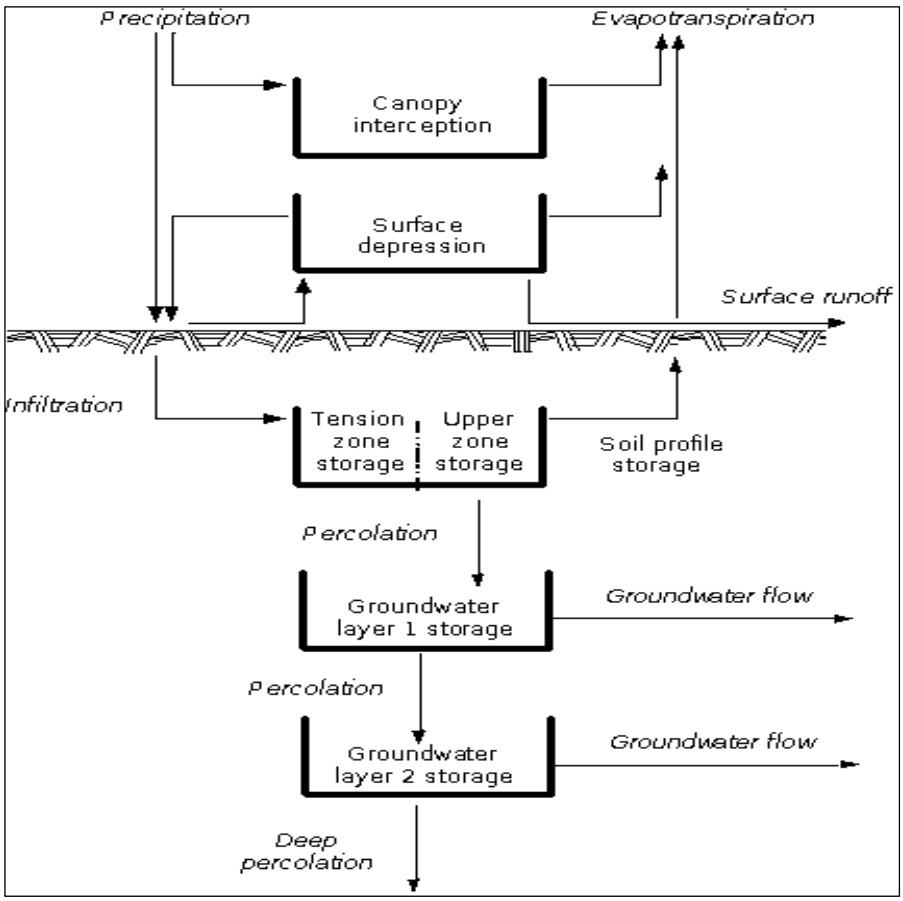


*Figure 4.5 Continuous Soil Moisture Accounting Algorithm (adapted from HEC-HMS)*

### 4.4.2 Estimation of Parameters for SMA Method

The SMA-based model requires a total of 14 parameters; eight are estimated from soil, LANDFIRE and land use data (maximum canopy storage, maximum infiltration rate, maximum percolation rate, maximum soil profile storage, maximum tension zone storage, surface depression storage, percentage imperviousness land surface), two from streamflow recession analysis (groundwater 1 storage coefficient and groundwater 2 storage coefficient), and four are calibrated

(groundwater 1 maximum storage, groundwater 2 maximum storage, groundwater 1 maximum percolation rate, groundwater 2 maximum percolation rate.)

4.4.2.1 Parameters estimated from LANDFIRE and land cover database

- Percentage Imperviousness of Land Surface

  Percent imperviousness has great impact on peak flow because impervious surfaces do not allow rainwater to enter into the soil through infiltration. The percentage of impervious land area was obtained from NLCD database (*Section 2.2.3*). The downloaded data was projected, cropped, and exported as a raster map. A MATLAB program was built to compute the regional average of the raster images for each sub-basin of the HEC-HMS model.

- Maximum Canopy Storage

  Canopy is a sub-basin component in HMS, which represents the presence of plants and vegetation in the landscape that can intercept precipitation and reduce runoff. The intercepted water can evaporate between storm events. Moreover, plants extract water from soil through transpiration. The combination of evaporation and transpiration is known as the evapotranspiration, which represent an important hydrologic loss term. A "Simple Canopy" method was selected to model this process in the present study. Specifically, a maximum canopy storage in terms of equivalent water depth was assigned for each sub-basin. The storage value was estimated from the LANFIRE vegetation data. The LANDFIRE data (Existing Vegetation Type) that were used in BRAT modeling were also

used to estimate the canopy storage. A lookup table was created to relate the type of vegetation to a storage depth, which were ranged between 0 ~ 3 mm in this study.

All precipitation is intercepted until the storage capacity is full. Excess precipitation will fall to the surface and go through the surface storage and infiltration processes subsequently. Between storm events, the canopy storage will be depleted at a rate set by the potential evapotranspiration rate. After the canopy storage is emptied, water will be extracted from soil for additional evapotranspiration. The “Tension Reduction” method was applied in this study to model this process, where water was first extracted from the gravity zone at the full rate defined by the evapotranspiration rate, then water will be extracted from the tension zone at a reduced rate. This method was selected as it can work along with the soil moisture account method.

*Figure 4.6* shows the process raters images of the percentage of impervious land and the canopy storage distribution.

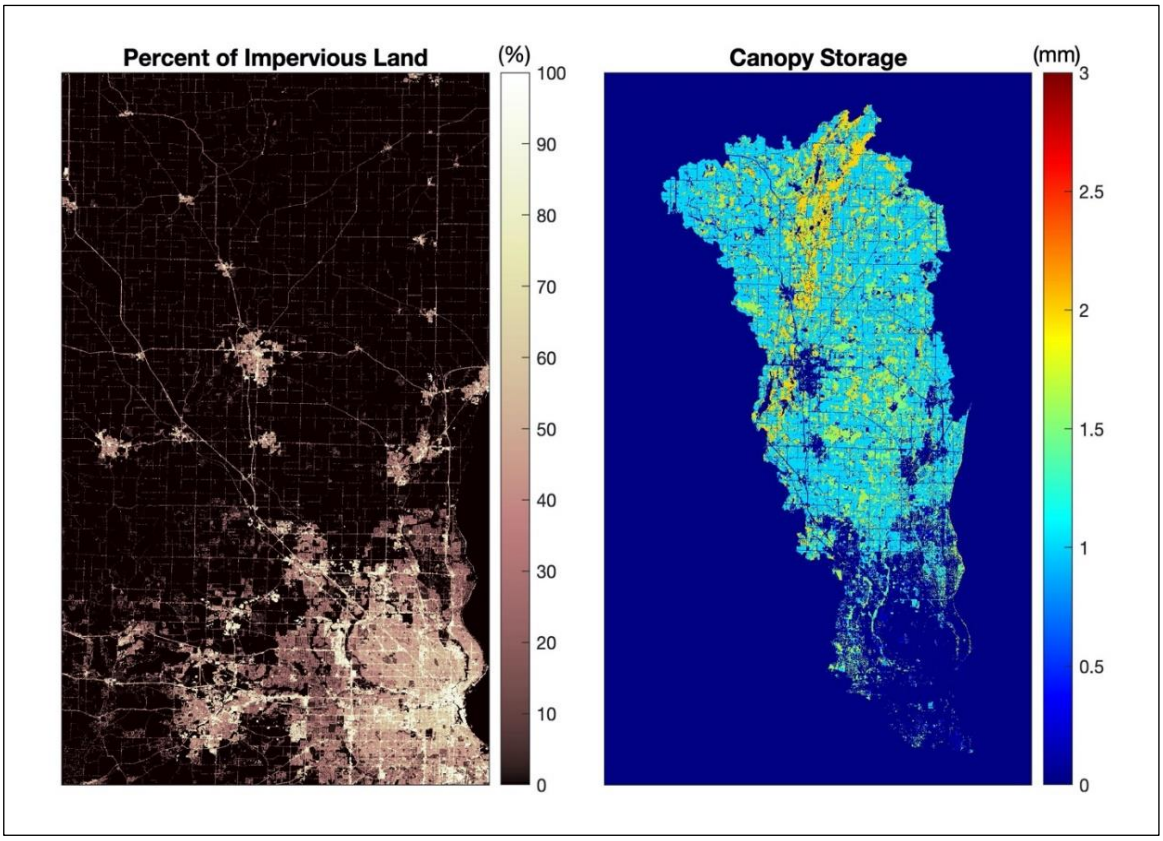


*Figure 4.6 Raster image of percent of impervious land (processed from NLCD data) and canopy storage (from LANDFIRE data)*

4.4.2.2 Parameters estimated from SSURGO dataset

Most parameters that are required to model processes involved in the SMA method are available from the processed SSURGO soil data (*Section 2.2.5*). SSURGO dataset included a map of geographic regions (a polygon shape) with each region assigned with a map-unit (identified by mukey). Every map unit contains multiple soil components (identified by co-key). Each component is a single type of soil which has multiple soil layers (identified by chkey). The relations among map units, components and layers are presented in tables for lookup. Soil

properties, such as soil layer depth, saturated conductivity, soil capacity and porosity, are listed in the soil layer table. The hierarchy SSURGO data structure is illustrated through *Figure 4.7*.

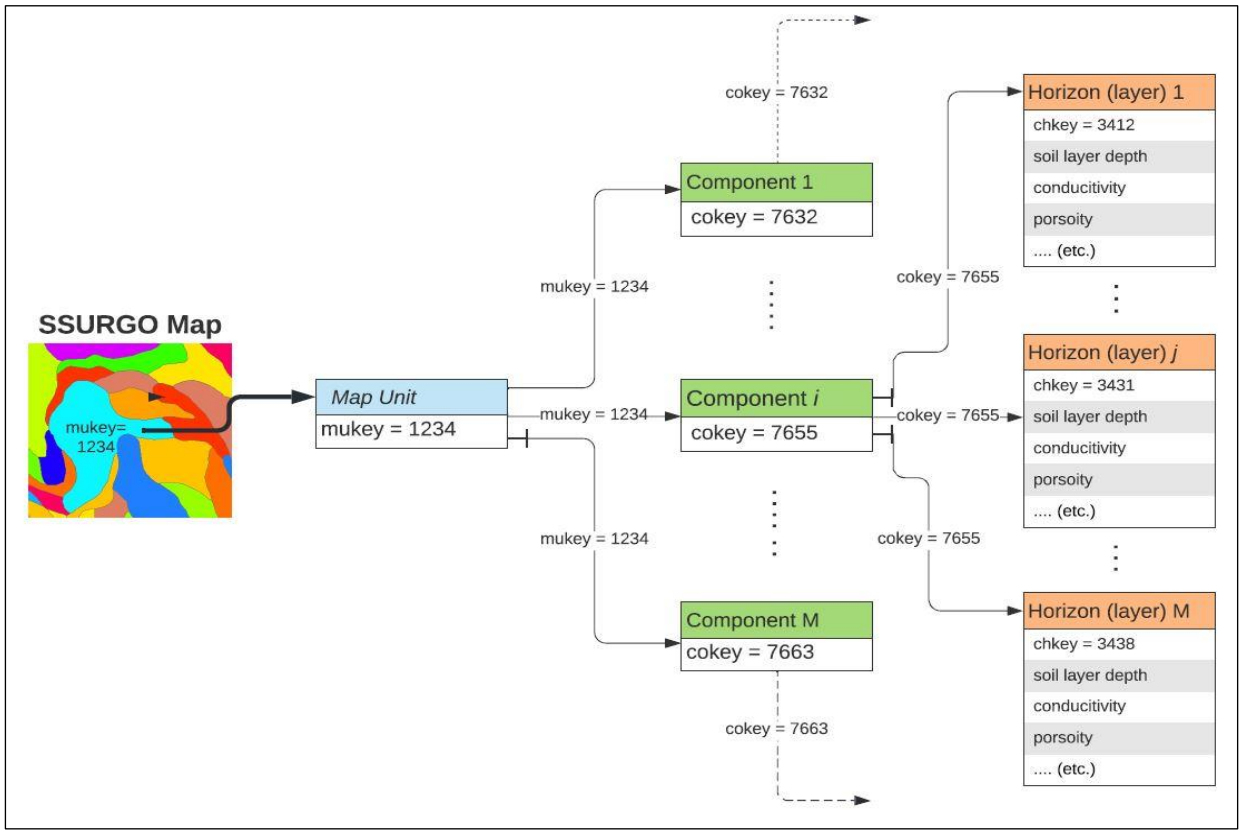


*Figure 4.7 Structure of SSURGO soil data*

In this study, a MATLAB program was developed to read the SSURGO map (shape files) and data tables, process the data following their relations, and to compute relevant soil properties for HEC-HMS modeling. The calculation methods for soil parameters were similar to those reported by (J. Holberg 2015). Specifically, the following soil properties were calculated with weighted averaging for each map unit according to the percentage of various components in the unit and the depth of each layers in a component:

- **Maximum Infiltration Rate ($\boldsymbol{Infil}$)** is the fastest rate at which precipitation seeps from the ground surface into the soil profile. It is calculated as the saturated hydraulic conductivity of the top soil layer ($K_{top}$) multiplied by the component percentage ($Pc$).

$$Infil = \sum_{i=1}^{M} K_{top_i} Pc_i \tag{4.1}$$

- **Maximum Percolation Rate ($\boldsymbol{Perc}$)** is the velocity with which water is transferred through the soil profile and groundwater layer(s). In this study, the maximum percolation rate is taken as the weighted average of the layer-averaged (layer thickness is denoted as $b$) saturated hydraulic conductivity ($K$) for all components in a map unit, following that described in Bennett (1998) and Fleming (2002).

$$Perc = \sum_{i=1}^{M} \left( Pc_i \frac{\sum_{j=1}^{N_i} K_{ij} b_{ij}}{\sum_{j=1}^{N_i} b_{ij}} \right) \tag{4.2}$$

- **Maximum Soil Profile Storage ($\boldsymbol{S_P}$)** is the storage depth available in voids and soil pores when the soil is dry. Soil voids can be drained by gravity or evaporation (HEC 2000). The soil profile storage is calculated by multiplying the component percent, average porosity ($\alpha$), and the soil layer thickness ($b$) together for each component and then summing these values to reach a total for each map unit.

$$S_P = \sum_{i=1}^{M} \left( Pc_i \frac{\sum_{j=1}^{N_i} \alpha_{ij} b_{ij}}{\sum_{j=1}^{N_i} b_{ij}} \right) \tag{4.3}$$

- **Maximum Tension Zone Storage ($\boldsymbol{S_T}$)** is the storage depth available in the form of water attached to soil particles. This water can only be removed through evaporation, suction, or

contact with a dry, porous material (Jury and Horton 2004). Field capacity is the amount of water left in the soil profile after water has stopped draining from the soil; it is analogous to the tension zone (Veihmeyer and Hendrickson 1931). The tension zone storage is calculated by multiplying the component percent, average field capacity ($Cap$), and the soil layer thickness together for each component and then summing these values to reach a total for each map unit.

$$S_T = \sum_{i=1}^{M} \left( Pc_i \frac{\sum_{j=1}^{N_i} Cap_{ij} b_{ij}}{\sum_{j=1}^{N_i} b_{ij}} \right) \tag{4.4}$$

In all equations presented above, subscript $i$ represents the i-th component of the current map unit, and subscript $j$ represents the j-th soil layer (horizon) of a component. $M$ is the total number of components in the map unit, and $N_i$ is the number of layers in the i-th component.

Calculated soil parameters for all map units in the watershed were converted to raster maps (*Figure 4.8* ), and the MATLAB program computed the regional average of the raster images for each sub-basin of the HEC-HMS model.

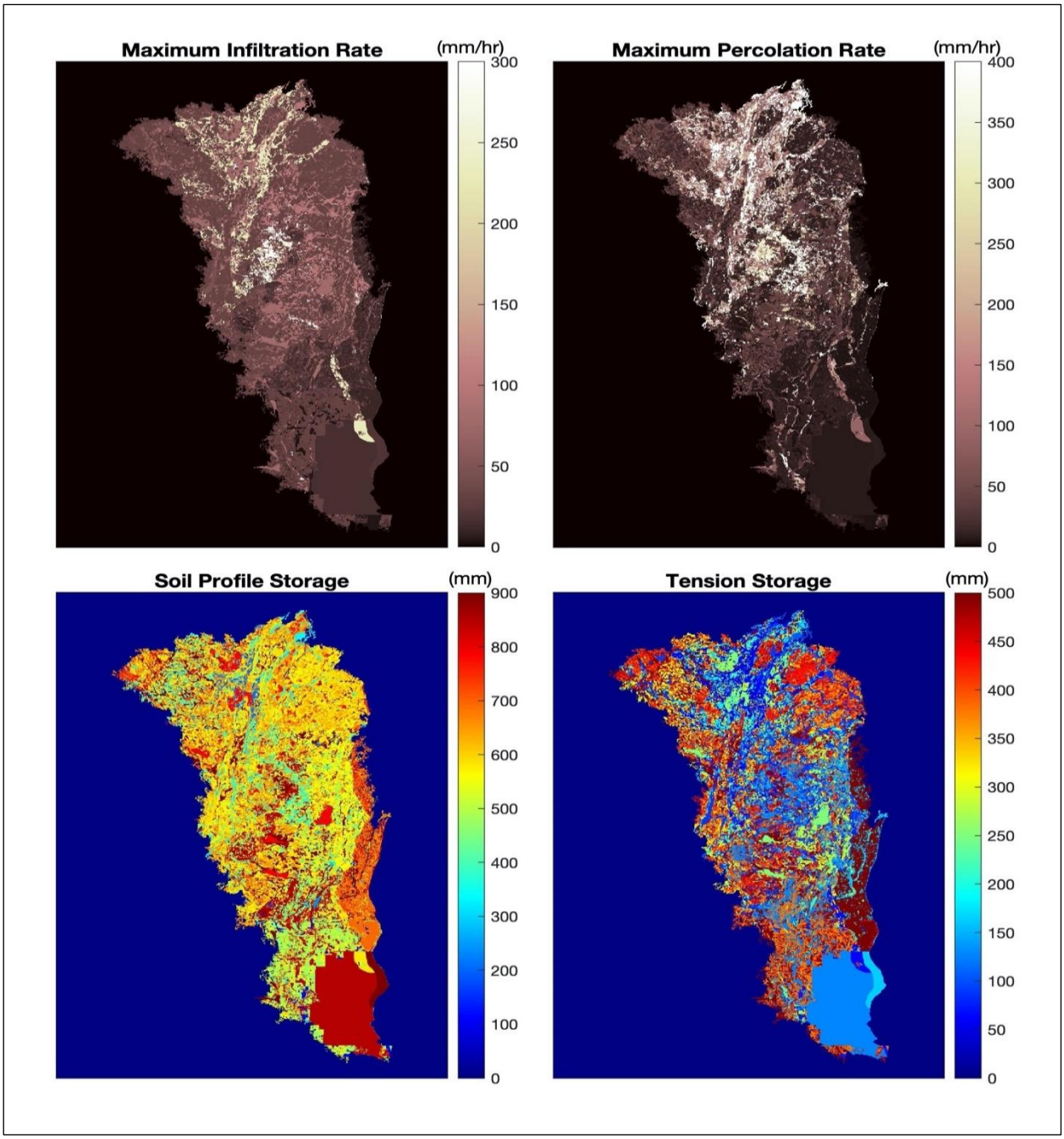


*Figure 4.8 Raster images of processed SSURGO soil data: maximum infiltration rate, maximum percolation rate, soil maximum profile storage, and soil maximum tension storage.*

4.4.2.3 Parameters estimated from Streamflow Analysis

In this project, the following SMA parameters were determined from the analysis of USGS Stream flow:

- **Groundwater 1 and groundwater 2 storage coefficients ($ST_{GW1}$ and $ST_{GW2}$)** are parameters that control the time scale of interflows and baseflows. In the SMA method, stream interflows originate from groundwater 1 storage and baseflows originate from groundwater 2 storage, as groundwater becomes saturated in the two storage compartments. For a typical stream hydrograph after an isolated storm event, the tail end of the receding "limb" represents effects of interflows and baseflows. Following the method described in (J. Holberg 2015), exponential functions can be applied to fit the receding "limbs" of a stream hydrograph and subtracted from the original hydrograph to isolate interflow and baseflow successively. The time scale of the exponential fit is considered as an estimate of groundwater storage coefficient. Since hydrograph data were not available for most river reaches in the model, a regional regression method was applied to scale the storage coefficient with the drainage area. Specifically, hydrograph data from 25 regional USGS stream gages were applied to estimate the storage coefficients by selecting isolated storm-runoff events at each station. The best-fitted storage coefficients were plotted against the drainage area. A linear trend was evident in the log-log scale graph, which suggested power-law relations for both $ST_{GW1}$ and $ST_{GW2}$ (*Figure 4.9*) as

$$ST_{GW1} = 2.02A^{0.621} \quad (4.5)$$

$$ST_{GW2} = 5.54A^{0.664} \quad (4.6)$$

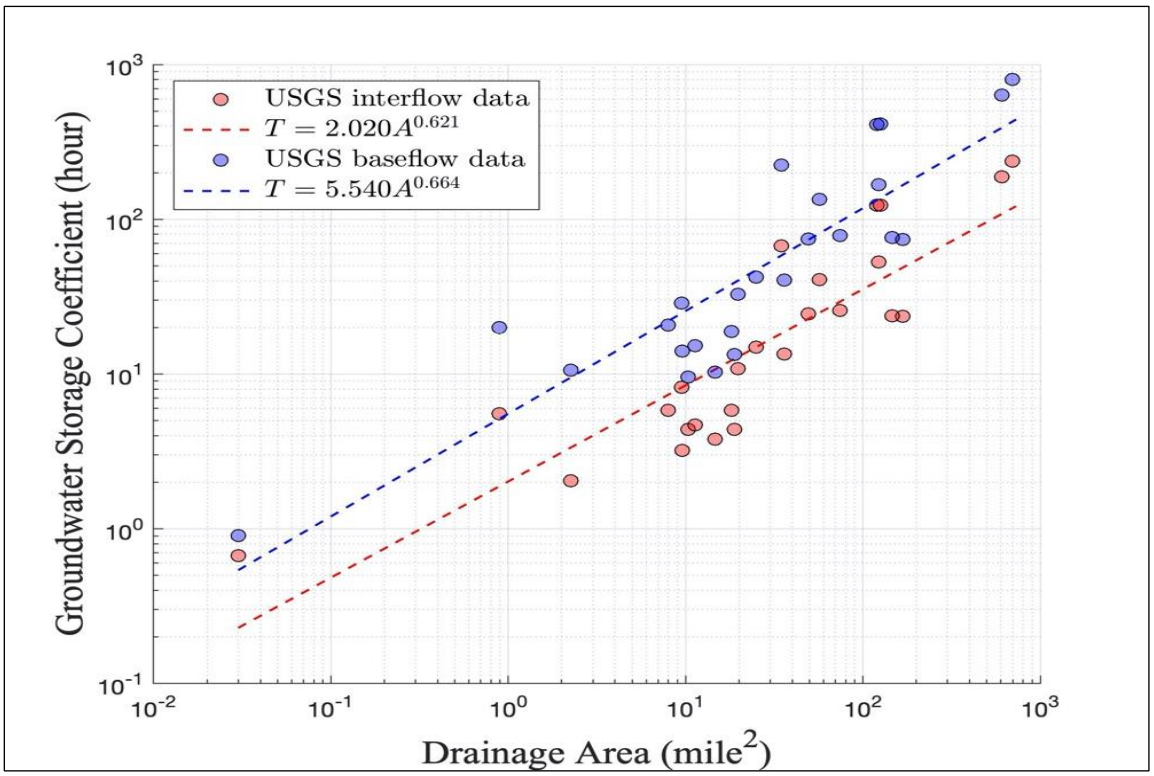


*Figure 4.9 Regional regression analysis of USGS stream gage interflow and baseflow data for the estimation of groundwater storage coefficients.*

where storage coefficients are in (hours) and the drainage area $A$ is in (mi$^2$). Equation (4.5) and (4.6) were subsequently applied to all sub-basins in the HEC-HMS model to calculate $ST_{GW1}$ and $ST_{GW2}$ according to sub-basin areas.

4.4.2.4 Parameters Estimated from Calibration

- **Groundwater 1 ($GW_1$) and groundwater 2 ($GW_2$) maximum storage** are the maximum amount of precipitation that can be stored in the upper and lower groundwater storage compartments, respectively. The two parameters are not available from soil data. They

were considered to be proportional to the soil storage depth in this project, and the proportionality were treated as tuning parameters during the calibration process (*Section 4.7*). It was found that the following relations produced good calibration results:

$$GW_1 = 0.9S_P \tag{4.7}$$

$$GW_1 = 1.2S_P \tag{4.8}$$

- **Groundwater 1 and groundwater 2 maximum percolation ($Perc_{GW1}$ and $Perc_{GW2}$)** are the maximum rate at which groundwater leaves the upper storage and enter the lower storage, and leaves the lower groundwater storage to deep aquifer, respectively. They were also treated as "tunning" parameters in this project, which were set as the following after calibration:

$$Perc_{GW1} = 0.1Perc \tag{4.9}$$

$$Perc_{GW2} = 0.5\ Perc_{GW2} \tag{4.10}$$

4.4.2.5 Modeling surface depression storage

In HEC-HMS the surface is a sub-basin component which represents the ground surface where water may accumulate in surface depression storage. In this project, a "Simple Surface" method was selected to model the surface depression storage. A storage capacity was assigned for each sub-basin. Water storage on surface will infiltrate into soil even when the capacity is not full. Surface runoff will start when the precipitation rate exceeds the infiltration rate. As suggested by

(Bennett 1998), ground surface storage is related to the ground slope. For paved impervious areas, the surface storage is between 3.18 and 6.35 mm. Otherwise, it is 50.8 mm for slope between 0 ~ 5%; 5-30 mm for slope between 5 ~ 30%; and 1.02 mm for slope greater than 30%. Following this reference, maximum surface storage was assigned based on average slope of each sub-basin, which was available from the results of GeoHMS procedures.

## 4.5 Clark Unit Hydrograph Approach for Transformation

The Clark unit hydrograph is a synthetic unit hydrograph method. A time versus area curve (time-area curve) built into HEC-HMS is used to develop the translation hydrograph resulting from a burst of precipitation. The resulting translation hydrograph is routed through a linear reservoir to account for storage attenuation effects across the subbasin. The Clark unit hydrograph requires two parameters for each sub-basin: (1) the time of concentration ($T_c$) defines the maximum travel time in the subbasin; and (2) the storage coefficient ($S_c$) is used in the linear reservoir that accounts for storage effects.

Data needed to estimate $T_c$ and $S_c$ were readily available through the GeoHMS analysis (see section **Error! Reference source not found.**), which prepares geographic parameters necessary for the Soil Conservation Service (SCS) TR-55 model (Cronshey 1996). The TR-55 method considers water moves through a catchment as (1) sheet flow; (2) shallow concentrated flow; and (3) open channel flow. Therefore, time of concentration of a sub-basin is the summation of travel time values for the three consecutive flow segments, i.e.,

$$T_c = T_{sheet\ flow} + T_{concentrated\ sheet\ flow} + T_{channel\ flow} \tag{4.11}$$

and

$$T_{\text{sheet flow}} = 0.007 \frac{(nL_S)^{0.8}}{P_{24}^{0.5} S_S^{0.4}} \tag{4.12}$$

$$T_{\text{concentrated sheet flow}} = \frac{L_{CS}}{16.13\sqrt{S_{CS}}} \quad \text{or} \frac{L_{CS}}{20.33\sqrt{S_{CS}}} \tag{4.13}$$

$$T_{\text{channel flow}} = \frac{nL_C}{1.49 R^{\frac{2}{3}} \sqrt{S_C}} \tag{4.14}$$

where $L_S, L_{CS}$ and $L_C$ are flow lengths of sheet flow, concentrated sheet flow and channel flow, respectively; $S_S, S_{CS}$ and $S_C$ are slopes of the three segments, respectively. Flow lengths and slopes were all calculated by GeoHMS for each sub-basin. The Manning's roughness was set to be $n = 0.03$ for both sheet flows and channel flows. The hydraulic radius $R$ of channel flows was manually set for each sub-basin channels with values varying between 0.1 ~ 0.5 m, depending on the drainage area. In equation (4.13) coefficients 16.13 and 20.33 are for unpaved and paved land surfaces, respectively. They were specified for each sub-basin based on the percentage of imperviousness.

Field studies suggest that the storage coefficient is correlated with the time of concentration, specifically,

$$\frac{S_c}{S_c + T_c} = 0.5 \sim 0.6 \tag{4.15}$$

over a region. This correlation was applied to calculation $S_c$ for all sub-basins.

## 4.6 River Routing

River routing process for reach (river) components in HEC-HMS accounts for attenuation of flood waves. The Muskingum-Cunge method was selected for routing in this project. The method is a combination of the conservation of mass and a diffusion representation of the conservation of momentum. Parameters need to be specified for Muskingum-Cunge includes channel length, slope, cross-section geometry, and the Manning's roughness. Channel length and slope of all reaches were readily available from GeoHMS output. All channels were assumed to have a trapezoidal cross-section. Since it is beyond the scope of this study to acquire cross-section geometry for every channel reach, it was assumed that side slopes of all channels equal to 2 (horizontal vs vertical), and channel width varies between 5 and 70 meters, which scales with the drainage area of each reach. The Manning's roughness was assumed as $n = 0.035$ uniformly for all channels.

## 4.7 Model Calibration

To calibrate the HEC-HMS model for the Milwaukee River watershed, simulated hydrograph at locations where USGS streamgage data are available. Model runs were conducted to simulate precipitation-runoff processes between 2010 and 2019. In this study, the meteorological components in the model included precipitation and evapotranspiration processes only. Stream flows simulated by HEC-HMS were calibrated by comparing the hydrograph with that recorded

by USGS stream gages between the simulation period, i.e., from May 1st to Nov 30th between 2010 and 2019 (section 2.2.8).

For model calibration, precipitation input between 2010 and 2019 over the entire watershed was an interpolated map based on available land-based rain gauge data. The “inversed distance” method was selected as the interpolation scheme, where the precipitation depth at a particular location is essentially a weighted average of data from nearby gages. The weighting factor is proportional to the inverse of the squared distance to those gauges. A searching distance of 60 km was selected in this study for the inverse distance method. To model evapotranspiration a simple Monthly Average Method was selected in HEC-HMS which estimates the rate in mm of water depth per month (section 2.2.6).

The reservoir function of beaver dams was switched off and changed to “junction” point for the calibration process. Most model parameters, particularly those in the Soil Moisture Accounting loss method and unit hydrograph transformations were obtained directly from realistic geodata and standard engineering approaches. These parameters were left as is. The groundwater storage, percolation rates and routing coefficients were considered as “tuning” parameters, since they were obtained through empirical regression relations. The “tuning” parameters were adjusted systematically, i.e., uniformly scaled by a common factor, such that the simulated hydrography matched best with that observed at the 11 USGS stream stations.

As a preliminary study, runoff due to snow falls and subsequent snow melting were not included. Therefore, calibration time window was limited to be between May 1st and November 30th. For each of the calibration year (2010 ~ 2019), simulation started on March 15th with initial soil and groundwater storage set as 20% of their corresponding maximum capacity, which allowed model to "warm up" for 1.5 months. Model results are presented starting at May 1st.

The time step of model simulation was set to 2 hours. Since the time resolution of USGS stream flow data was 15 minutes, they were smoothed by a 2-hour "moving average" window for comparison with simulation results. In addition, daily average flow data from USGS were also presented for comparison with the model.

Since the focus of the present study is to evaluate the potential of beavers on river flood abatement, calibration results for 2010, 2014, 2018 and 2019 are selected for presentation. Only in the four selected years, annual peak flow exceeded 100 m3/s at the Milwaukee River station (USGS 04087000), which is equivalent to a 2-year flow according to historic data recorded by this station.

## 4.8 Calibration Results

Modeled hydrograph curves are shown in *Figure 4.10~ Figure 4.13*, along with the USGS 2-hour average and daily flow series.

Total 7-month discharge volume between May 1st and Nov 30th was integrated from both observed and simulated hydrograph at 11 stream stations and for the 10 years. Their correlation is shown in *Figure 4.14*. A linear regression with a forced 1:1 relation suggested a very good

correlation with the coefficient of determination $R^2 = 89.7\%$. Linear regression with a forced zero-intercept indicated that

$$V_{Model} = 0.97 V_{USGS}\,, \tag{4.16}$$

where $V$ represents the 7-month discharge volume at every calibration station. This suggested that model results slightly underestimate the runoff volume overall.

Relation between modeled and observed annual peak flow rate at the 11 stations over the 10 years is shown in *Figure 4.15*. A linear regression with a forced 1:1 relation also demonstrated a good correlation with $R^2 = 84.6\%$. A linear regression with a forced zero-interception shows that

$$Q_{P_{Model}} = 0.99 Q_{P_{USGS}}\,, \tag{4.17}$$

where $Q_P$ represents the peak discharge. This suggested a nearly zero bias error. It should also be noted that better correlation is found at higher peak flow rate, i.e., when $Q_P > 100$ ($m^3/s$). Greater scattering is presented at lower flow rates, particularly for the case of the Little Menomonee River station near Freistadt, WI (USGS 04087050), where annual peak flow had never exceeded 10 $m^3/s$ over the 10 years.

Overall, calibration tests demonstrated that HEC-HMS with the parameterization reconstructed in this study was able to reproduce stream flow hydrograph with good accuracy as measured by the peak flow rates and the total runoff volume.

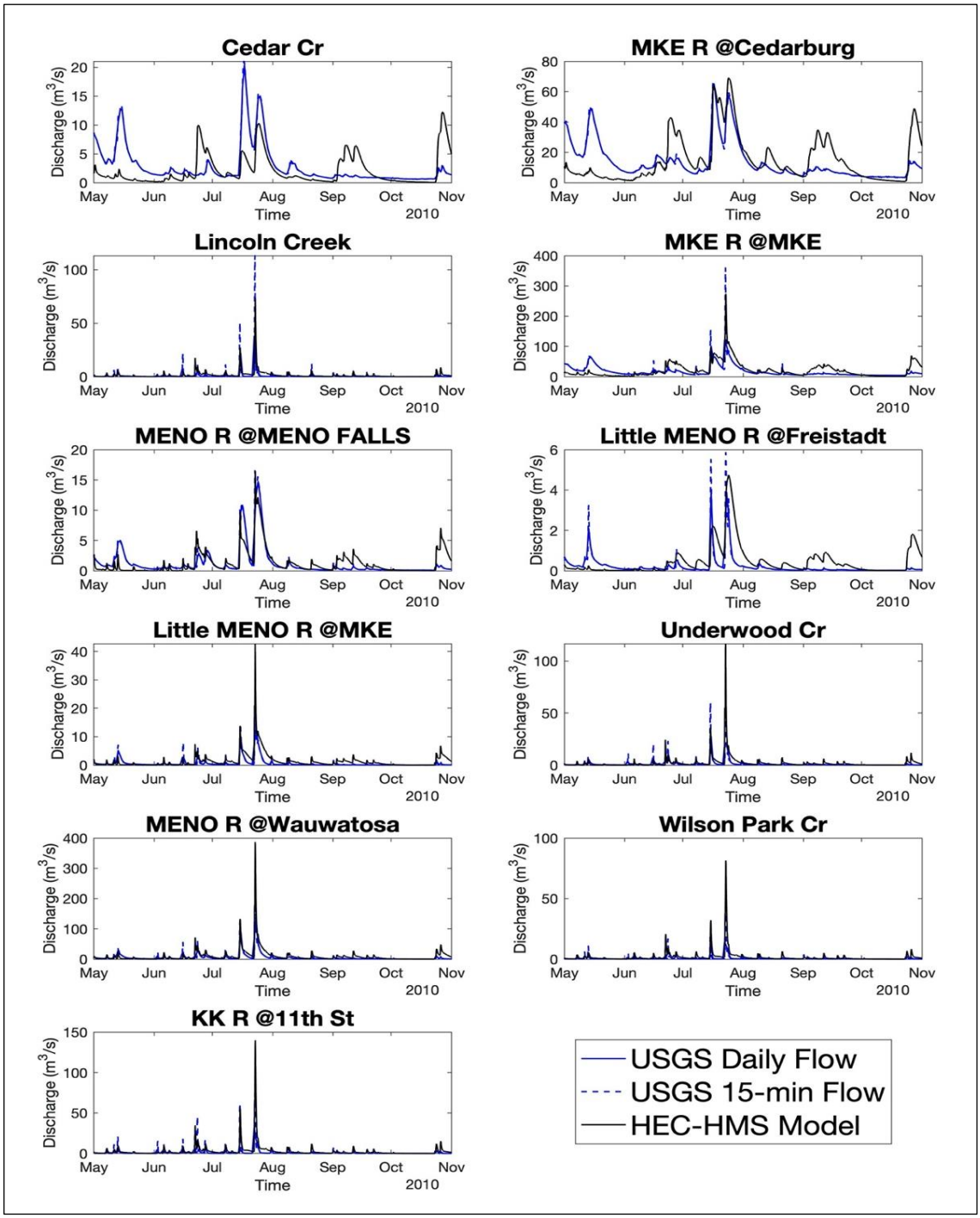


*Figure 4.10 Modeled hydrograph and observed discharge time series between May 1st and Nov 30th 2011 at 11 USGS stream stations.*

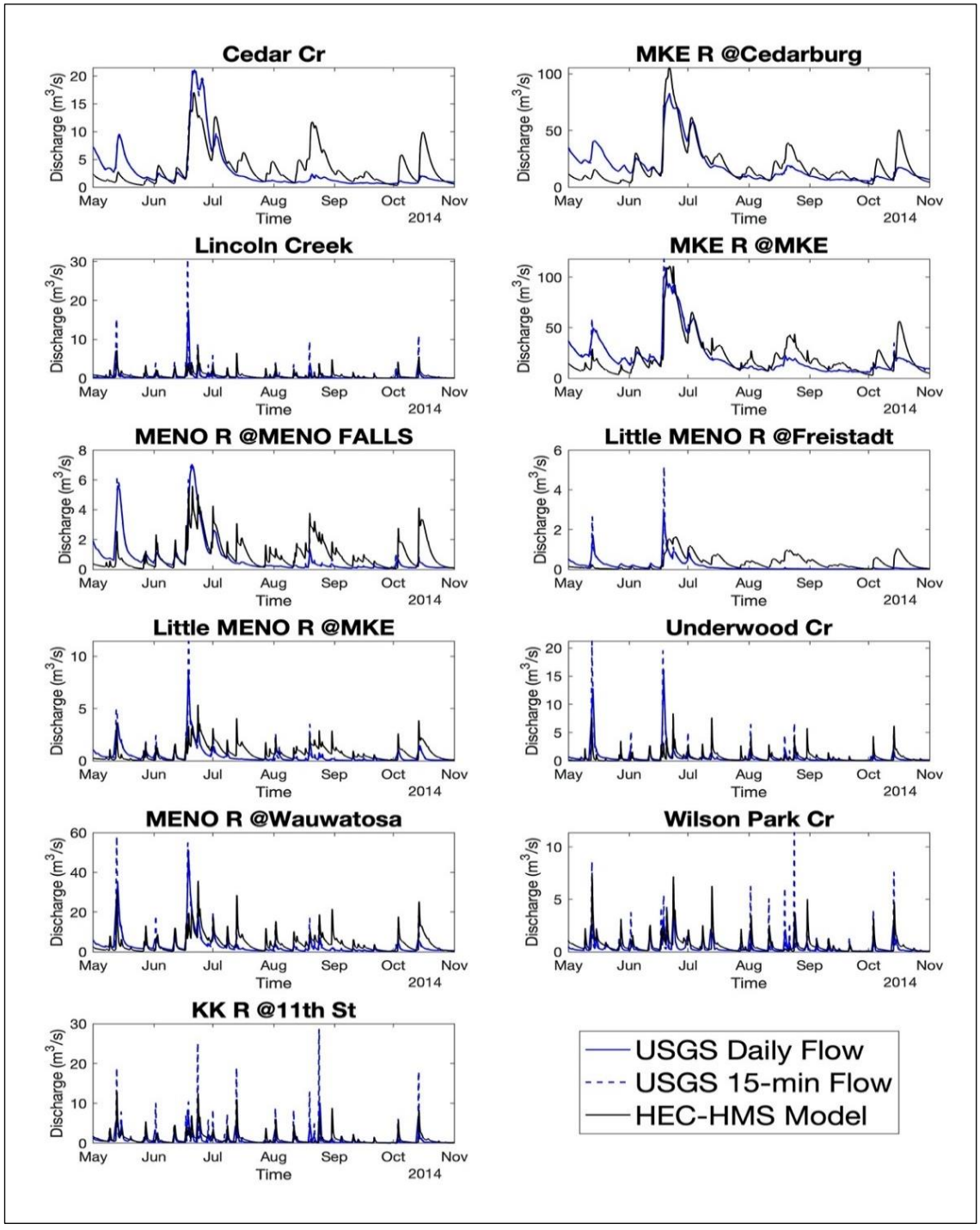


*Figure 4.11 Modeled hydrograph and observed discharge time series between May 1st and Nov 30th 2014 at 11 USGS stream stations*

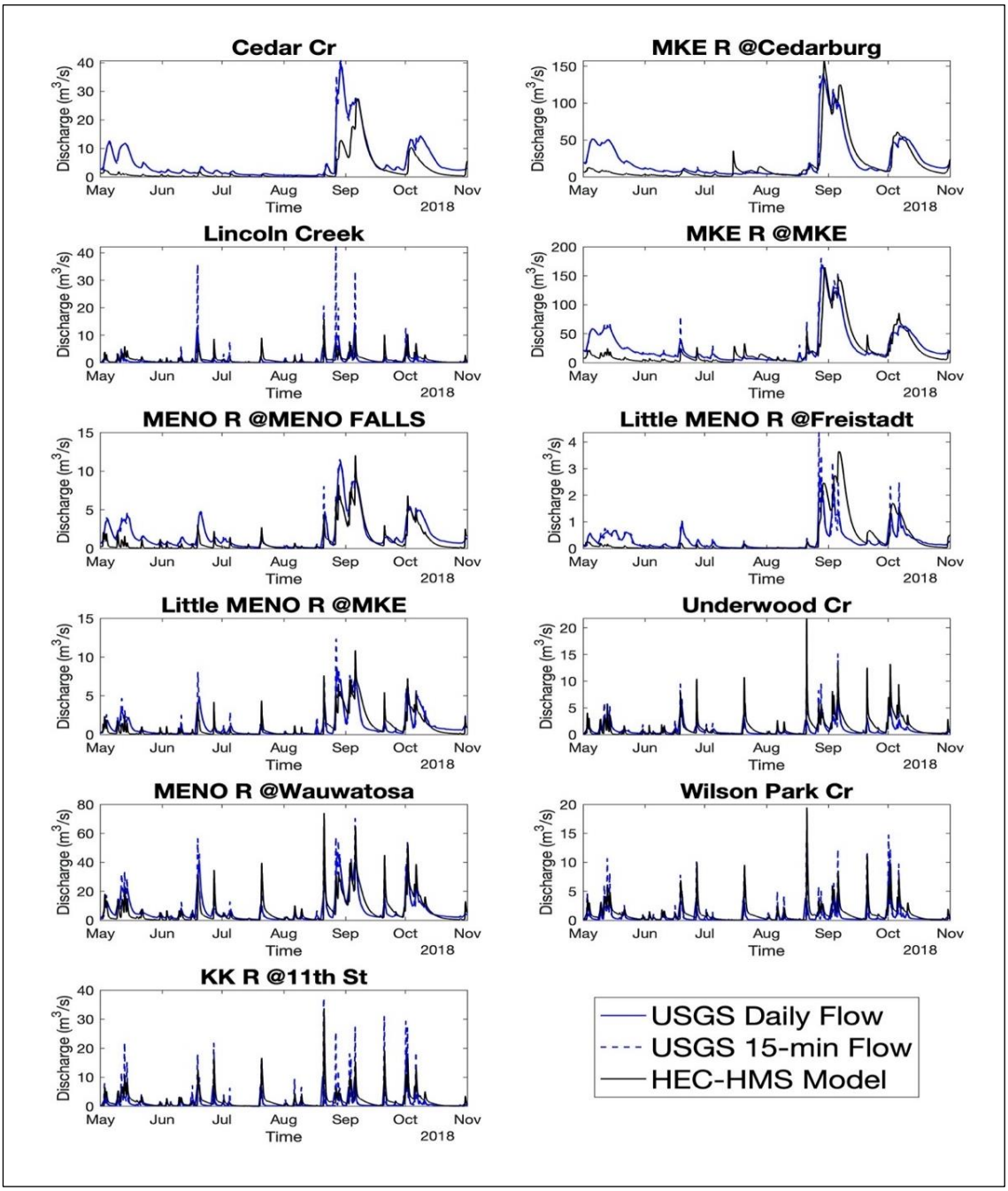


*Figure 4.12 Modeled hydrograph and observed discharge time series between May 1st and Nov 30th 2018 at 11 USGS stream stations*

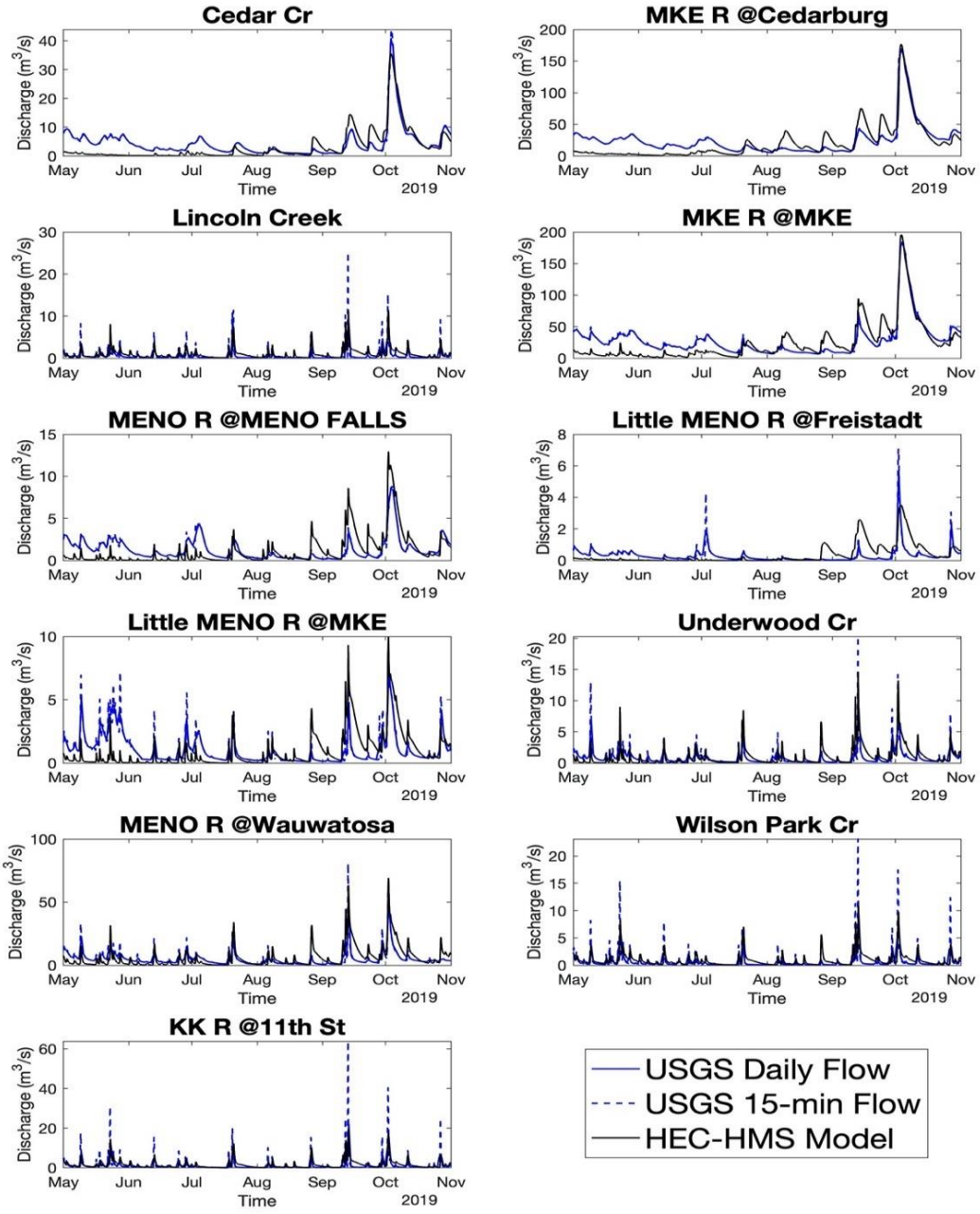


*Figure 4.13 Modeled hydrograph and observed discharge time series between May 1st and Nov 30th 2019 at 11 USGS stream stations*

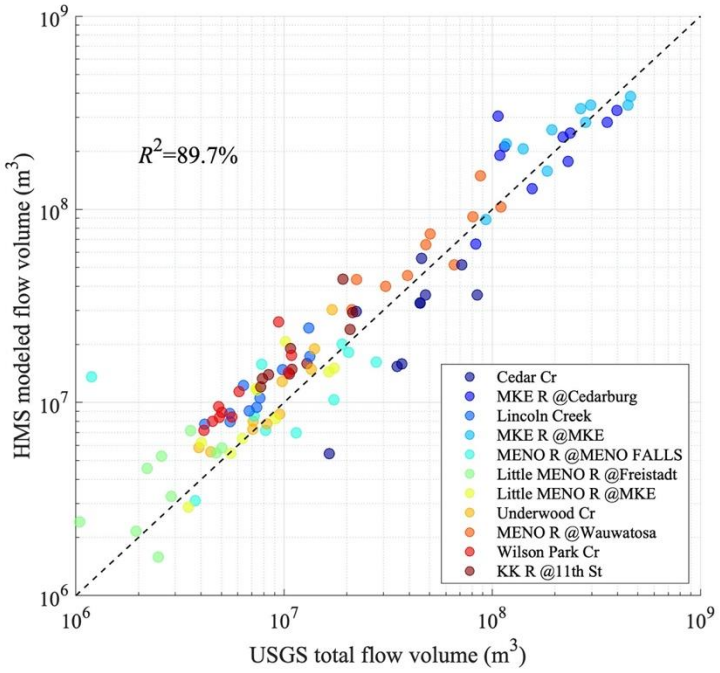


*Figure 4.14 Modeled vs. observed total discharge volume between May 1st and Nov 30th 2010~2019 at 11 USGS stream stations*

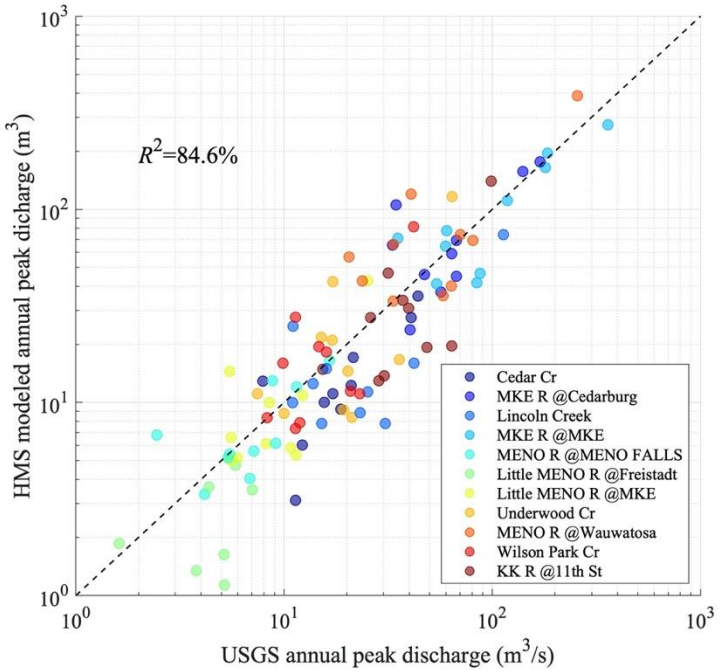


*Figure 4.15 Modeled vs. observed annual peak discharge at 11 USGS stream stations*

# CHAPTER 5

# RESULTS & DISCSSION

## 5.1 Model Reconstruction with Beaver Dam and Simulation Run

Beaver dams were modeled as “Reservoir” elements in HEC-HMS, and the “Outflow Structures” reservoir method was selected to simulate the effects of dams. Specifically, dams were modeled as a “Broad-Crested Spillway” with its crest length and elevation set to be equal to the dam width and height, respectively. The spillway method allows water to flow over the dam top in a controlled manner. The spillway coefficient, which accounts for energy loss as flow approaching the dam, was set to the maximum value of 1.66, considering the fact that beaver dams are generally constructed with a rough surface of logs and mud materials.

In HEC-HMS, reservoir storage relation can be specified through either elevation-storage or elevation-area methods, where the elevation refers to the ponded water surface elevation. The two rating curves developed for each dam can be applied for the two methods, respectively. Although the volume of ponded water is more important for mass balance of the rainfall-runoff simulation, the elevation-storage method does not account for water evaporation from the beaver pond. In this project, the elevation-area option was selected, which enables evaporation calculation. HEC-HMS automatically transforms the specified elevation-area curve into an elevation-volume curve using a conic formula.

Studies showed that active beaver dams are nearly impervious, thus dam overflow and evaporation are the major loss terms to a beaver pond (Woo and Waddington 1990). However, dams may become porous over time due to decaying materials. Water seeps out from beaver dams were included in the model using the dam seepage function in HEC-HMS. An elevation-discharge curve was specified for the seepage method, which is a linear function with a maximum seepage flow rate of 5.3 $ft^3/s$ (or 0.15 $m^3/s$) that occurs at the highest water level (top dam), as suggested in previous studies (Devito and Dillon 1993) (Caillat, et al. 2014). The "Outflow Structure" method requires an initial condition for the pond water level. In this study, it was set to be 50% of the dam height for all simulation cases with past storm.

Two sets of model simulations were conducted to evaluate the impact of beaver dams on the watershed-scale hydrograph:

a. simulation of hydrograph with past storm events in 2010, 2014, 2018 and 2019, with the same precipitation inputs used in the calibration runs, and
b. simulation of hydrograph with synthetic storm events of varied durations and recurrence intervals (return periods).

Hydrograph of river discharge in the river reach that drains each of the five sub-watersheds with modeled beaver establishments was extracted from model results. They represented the flows at the outlets of the five sub-watersheds, with their locations illustrated in *Figure 5.2*. Hydrographs at these locations were compared among cases without beaver dams and with beaver dams. Comparison of hydrograph at the outlets of the East-West branch (East-West), North branch (North), Cedar creek (Cedar) and Menomonee River (Meno) allows evaluation of beaver impact

of each sub-watershed separately, while the hydrograph at the outlet of South Milwaukee (South) represents the integrated impacts of beaver dams in four sub-basins that contribute to the flow (East-West, North, Cedar and Meno).

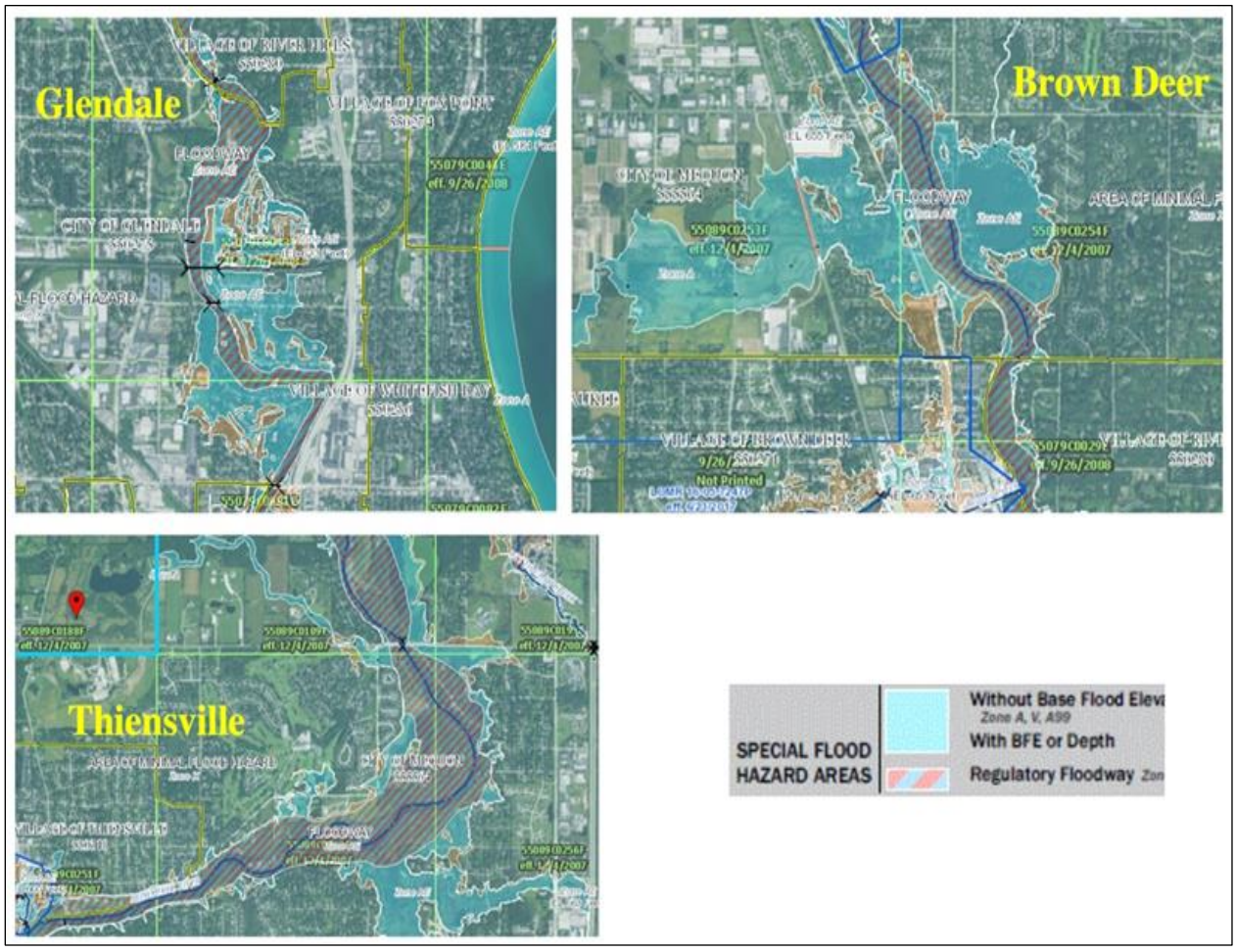


*Figure 5.1 Three urban flood zones in the South Milwaukee sub-watershed identified according to FEMA's flood map service (https://msc.fema.gov/portal/home)*

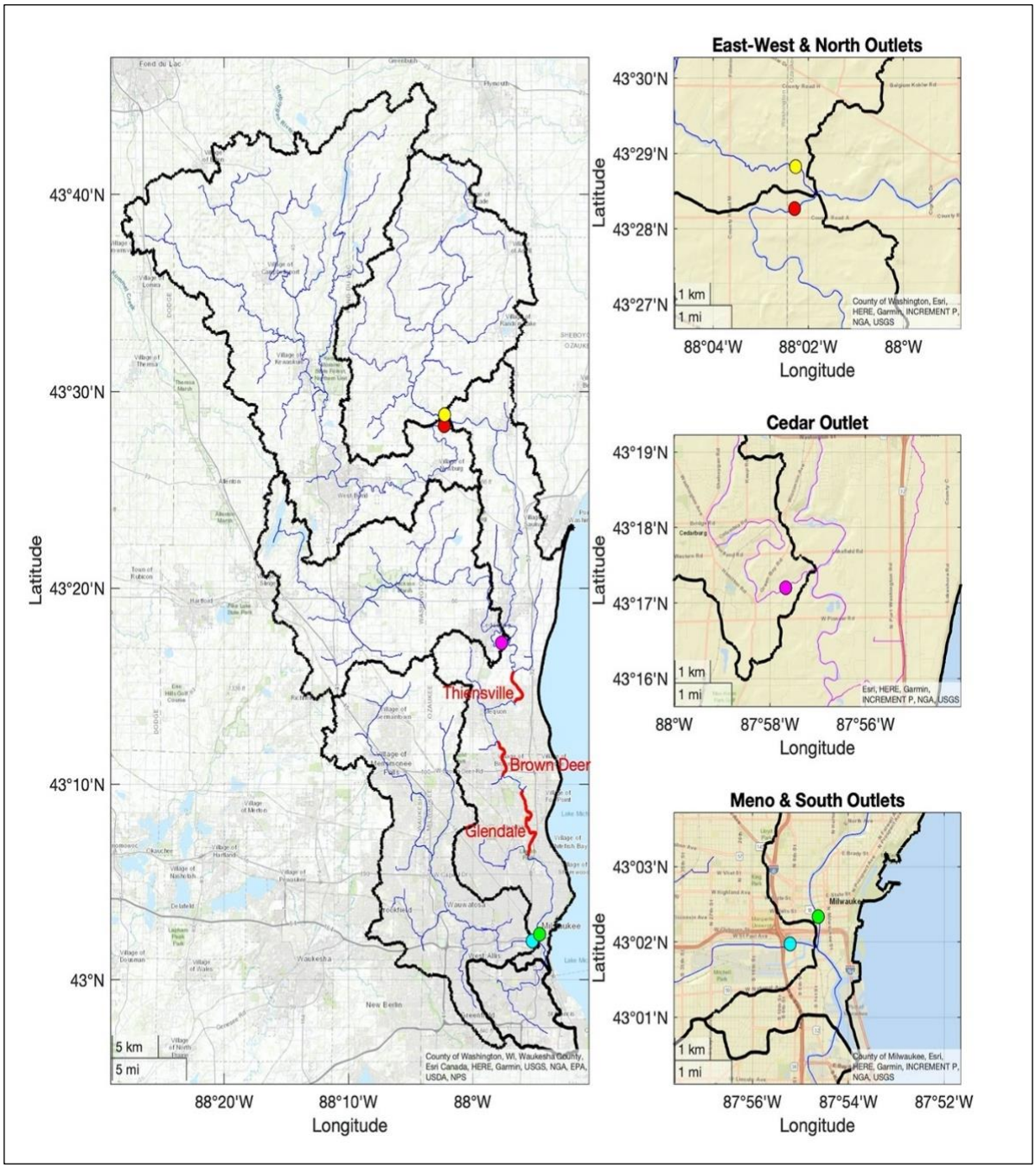


*Figure 5.2 Positions of outlets (colored circles) of five sub-watersheds (East-West, North, Cedar, Meno and South) and river reaches (bold red lines) of three urban flood zones (Thiensville, Brown Deer and Glendale) where hydrograph data were extracted from HEC-HMS model runs to evaluate flow reduction due to beaver dams*

## 5.2 Assess impact of beaver dams with past storm events

Model simulations of stream flows were conducted for the year of 2010, 2014, 2018 and 2019, using the same set of parameterizations as the calibration tests described in section 4.7. Simulation runs started on March 1st and ended on November 30th of each year. Results of the first two months are not included for analysis and presentation, i.e., two months of "ramp up" time to allow meteorological driving forces control the water budget of stream flow, groundwater, and beaver pond, or, to "forget" initial conditions which were set rather arbitrarily.

Simulated hydrographs at the outlets of the five sub-basins and the three flood zone reaches between May 1st and Nov 30th of each year are shown in *Figure 5.3 ~ Figure 5.10*. Details of high flow series during major storm events of each year are highlighted in these figures. Specifically, durations of major storm events of the four simulation years were identified as

- 2010: July 12th to August 9th
- 2014: June 14th to July 12th
- 2018: August 17th to October 28th
- 2019: September 29th to October 26th

The maximum flow rate and total discharged volume during the defined storm event durations were calculated from simulation results at these locations. They are presented as bar graphs shown in *Figure 5.11 ~ Figure 5.14*. Percentage reductions of peak flow and discharge volume due to beaver dams are also presented as bar graphs in these figures.

In addition, five beaver dam sites were selected, one in each sub-basin, to better illustrate hydrologic processes occurred in beaver ponds during storm events. Time series of water level behind beaver dams, discharge with and without dams are presented in *Figure 5.15 ~ Figure 5.18*.

Several important results are observed from simulations of past storm events:

1. As shown in *Figure 5.15 ~ Figure 5.18*, beaver pond can be filled up to its maximum capacity quickly after a major precipitation event. Excess water overflows above the dam, which may still effectively reduce flow rate due to overflow energy loss. During an interval of two major storm events, ponded water level gradually drops through evaporation and dam seepage flow, which helps to empty storage space for the next storm event.
2. Results suggest that beaver dams can significantly reduce both peak flows and discharge volume at most of the eight observation locations (5 outlet points and 3 river reaches), except for the peak flow event in 2019. The peak flow occurred on October 2nd, 2019 at all eight observation locations. However, several prior storm events during the month of August and September filled up most beaver ponds, leaving little storage capacity for the Oct 2nd event.
3. A flood event observed in the south branch of Milwaukee River on July 22nd, 2010 was a result of a heavy storm precipitation which poured 7.5 inch in two hours in the City of Milwaukee. Peak flows could be reduced only slightly by beaver dams at outlets of the South Milwaukee River (about 7%) and Menomonee River (about 2~3%) sub-basins. High flows at the two locations were results of precipitation concentrated in the southern

part of the watershed, while most beaver dams are in the northern watershed. River flows in the three northern urban flood zones were also relatively high during the July storms in 2010, and beaver dams could effectively reduce the flood levels: (about 25% peak reduction at Thiensville, 21% peak reduction at Brown Deer, and 14% at Glendale).

4. Based on simulated hydrographs at sub-basin outlets, beaver dams in the Cedar Creek sub-basin have the greatest potential for flow reduction. The peak reduction rate ranges from 15%~52% with an average of 41% and the volume reduction rate ranges from 15%~65% with an average of 43%. The peak reduction rate was above 50% both in 2010 and 2014. Similarly, the discharge volume reduction was maximum in the year 2010 about 65% and in 2014 it was about 50%. However, both peak reduction and discharge volume reduction were only 15% in year 2019, which is for limited storage capacity of beaver ponds due to several consecutive storm events as discussed earlier. The high rate of flood reduction is likely due to the high capacity per area of the sub-watershed.
5. Beaver dams in both the East-West branch and North branch Milwaukee river sub-basins are also very effective at reducing flood flow peak and volume at their corresponding outlets. At the outlet of the East-West branch, peak reduction rate ranged from 2~34% and volume reduction rate ranged from 3~28%. At the outlet of the North branch, peak reduction rate ranged from 2~52% and volume reduction rate ranged from 2~43%. Both peak and volume reduction were maximum in the year 2014 in North branch outlet.
6. River flood flows in the South Milwaukee river sub-basin are affected by beaver dams of four sub-basins, not including the Menomonee river sub-basin. Flood flows at the outlet of the sub-basin had a peak reduction rate of between 7~35% with an average of

19%. The volume reduction rate varied between 6~35% with an average of the 21%. The three flood zones in the northern suburban area of Milwaukee (Thiensville, Brown Deer and Glendale) had a peak reduction rate of between 5~45% with an average of 26%, and the volume reduction rate ranged between 6~37% with an average of 24%.

*Table 5.1 Summary of beaver-mitigated flood flow peak reduction and discharge volume reduction at outlets of five sub-basins and three urban flood zones in the south Milwaukee river sub-basin*

| **Locations** | **Peak flow reduction** | | | | | **Discharge Volume Reduction** | | | | |
|---|---|---|---|---|---|---|---|---|---|---|
| | *2010* | *2014* | *2018* | *2019* | *Avg* | *2010* | *2014* | *2018* | *2019* | *Avg* |
| East-West | 19% | 34% | 13% | 2% | 17% | 25% | 28% | 13% | 2% | 17% |
| North | 29% | 52% | 32% | 1.5% | 29% | 31% | 43% | 26% | 3% | 26% |
| Cedar Creek | 52% | 52% | 44% | 15% | 41% | 64% | 50% | 44% | 14% | 43% |
| Menomonee | 3% | 18% | 8% | 4% | 8% | 5.5% | 37% | 10% | 4.6% | 14% |
| South | 7% | 35% | 28% | 6% | 19% | 23% | 35% | 20% | 6% | 21% |
| Thiensville | 25% | 44% | 31% | 5% | 26% | 32% | 36% | 22% | 6% | 24% |
| Brown Deer | 21% | 45% | 32% | 6% | 26% | 31% | 37% | 22% | 6% | 24% |
| Glendale | 14% | 45% | 33% | 6% | 25% | 29% | 37% | 22% | 6% | 24% |

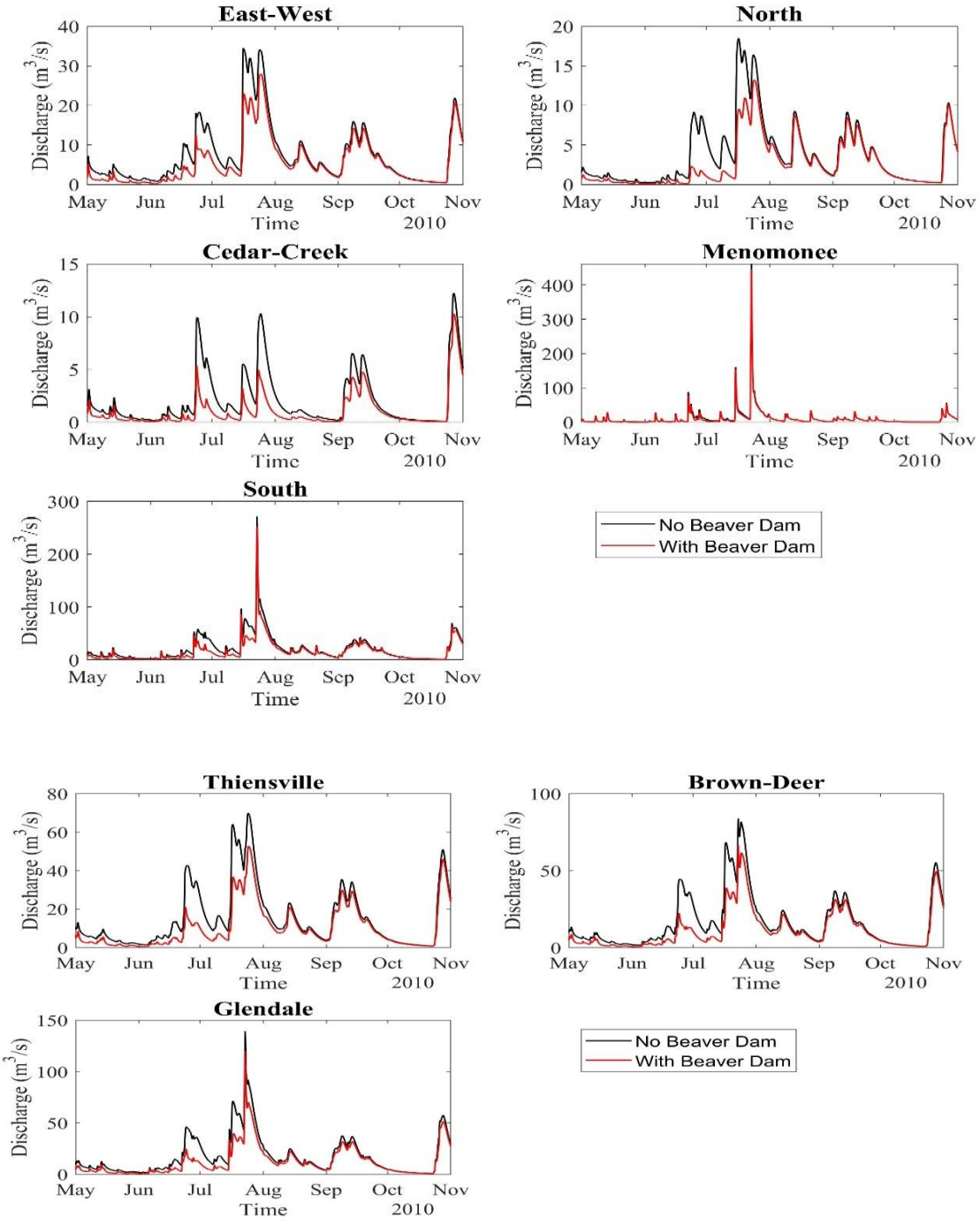


*Figure 5.3 Simulated hydrographs between May 1st and November 30th, 2010 at the outlets of five sub-basins and three flood zone river reaches in the South Milwaukee river sub-basin*

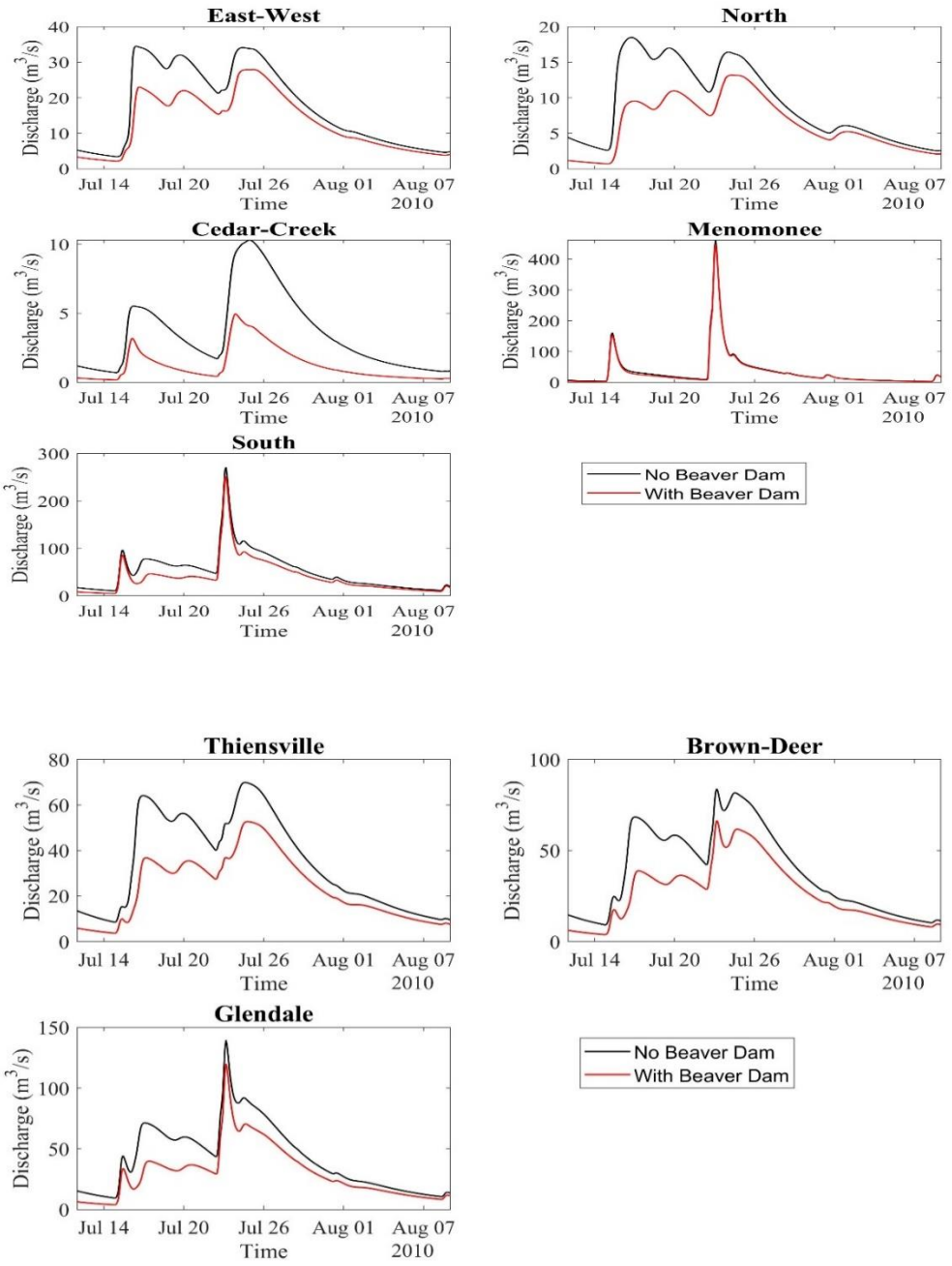


*Figure 5.4 Simulated hydrographs during the major storm events in 2010 (July 13th ~ August 7th) at the outlets of five sub-basins and three flood zone reaches in the South Milwaukee river sub-basin*

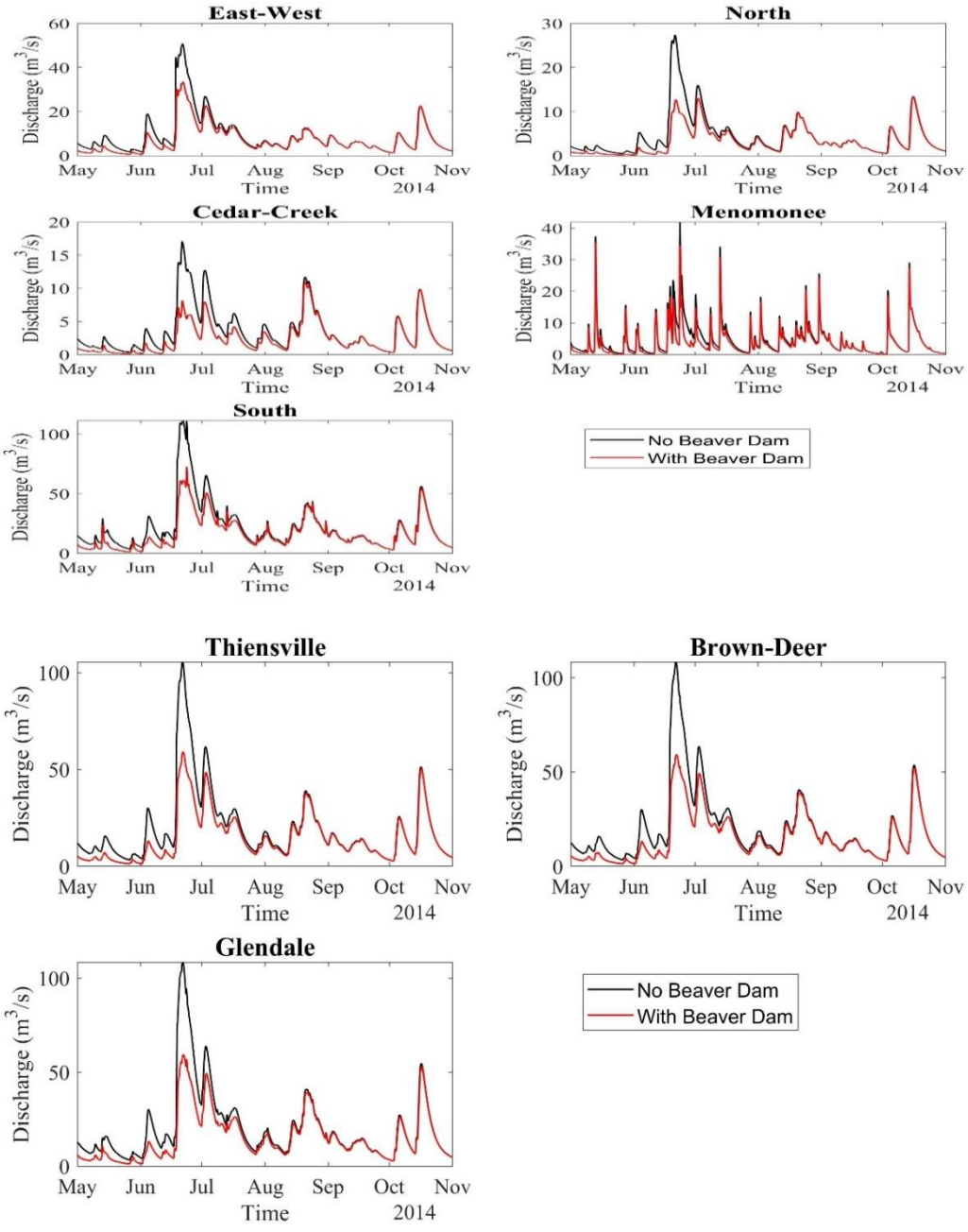


*Figure 5.5 Simulated hydrographs between May 1st and November 30th, 2014 at the outlets of five sub-basins and three flood zone river reaches in the South Milwaukee river sub-basin*

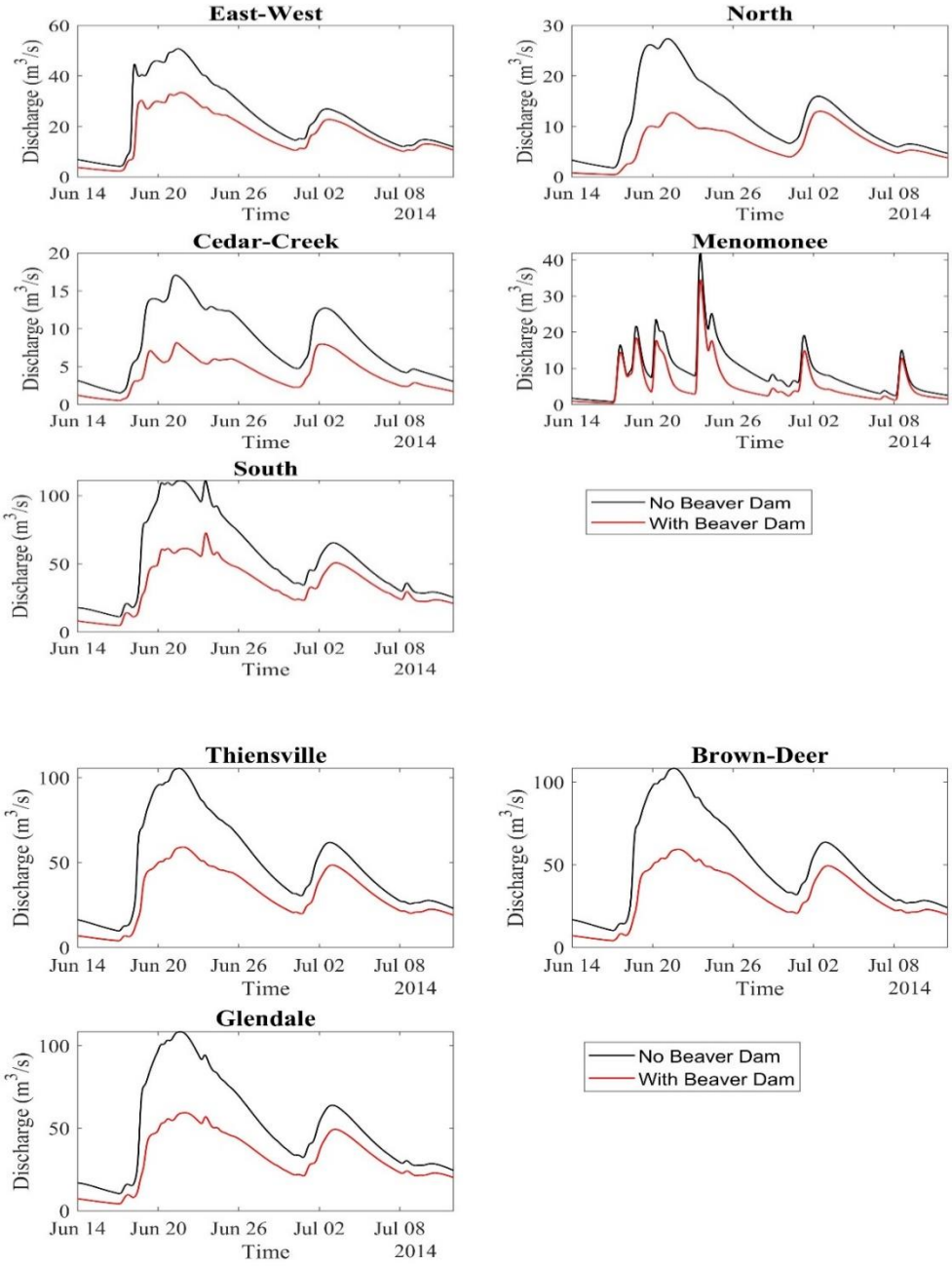


*Figure 5.6 Simulated hydrographs during the major storm events in 2014 (June 14th ~ July 12th) at the outlets of five sub-basins and three flood zone river reaches in the South Milwaukee river sub-basin*

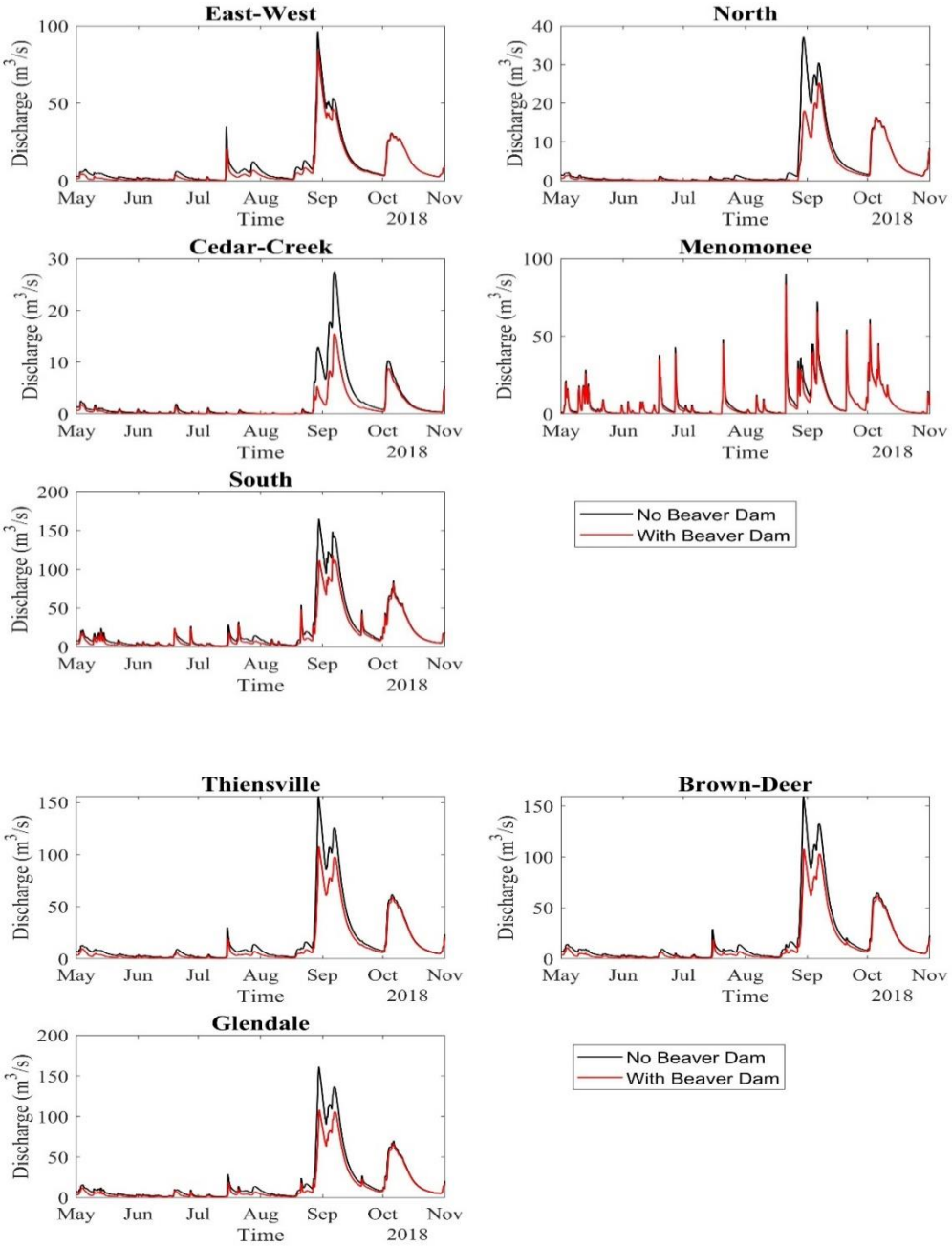


*Figure 5.7 Simulated hydrographs between May 1st and November 30th, 2018 at the outlets of five sub-basins and three flood zone river reaches in the South Milwaukee river sub-basin*

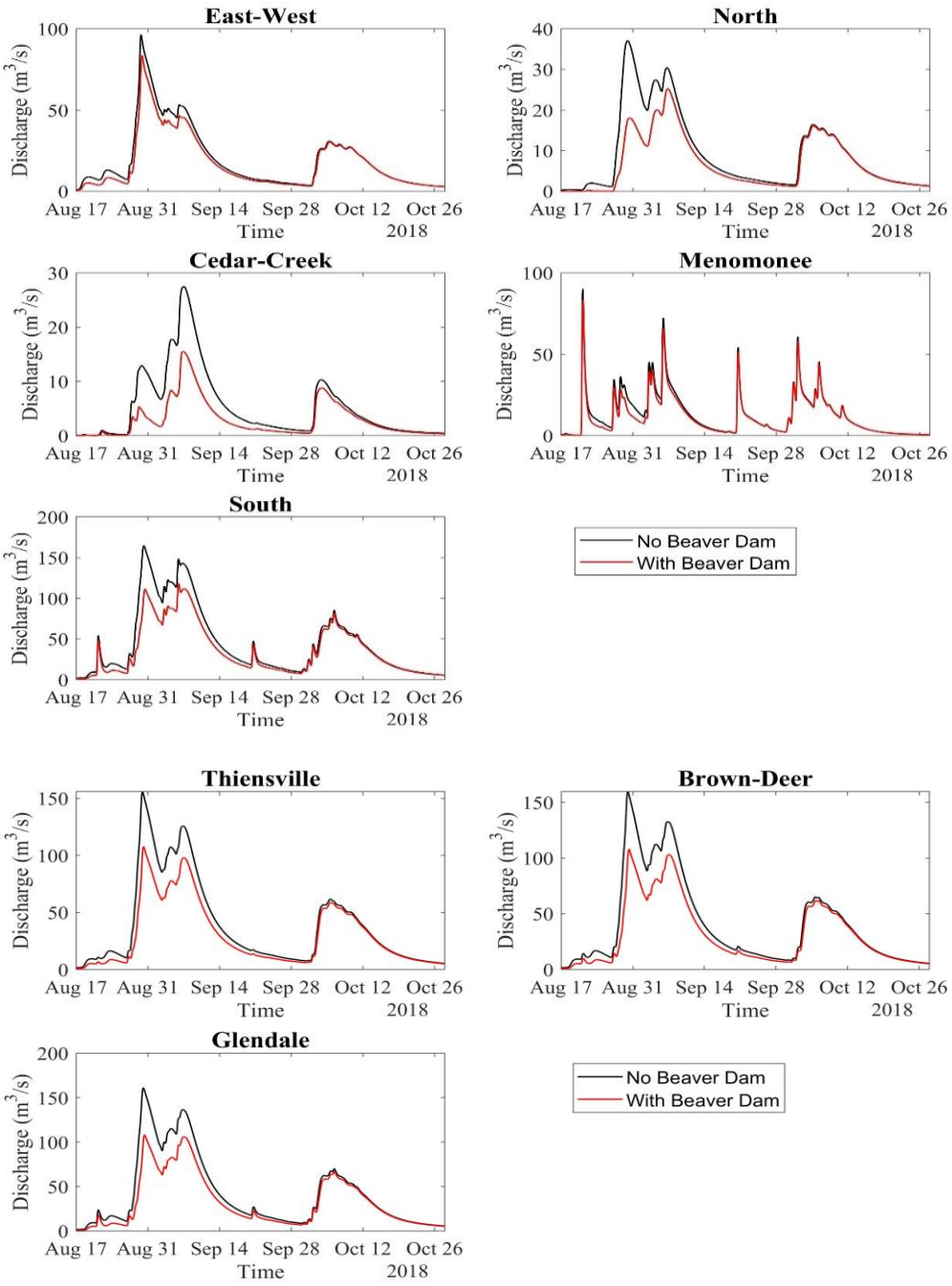


*Figure 5.8 Simulated hydrographs during the major storm events in 2018 (August 17th ~ October 26th) at the outlets of five sub-basins and three flood zone river reaches in the South Milwaukee river sub-basin*

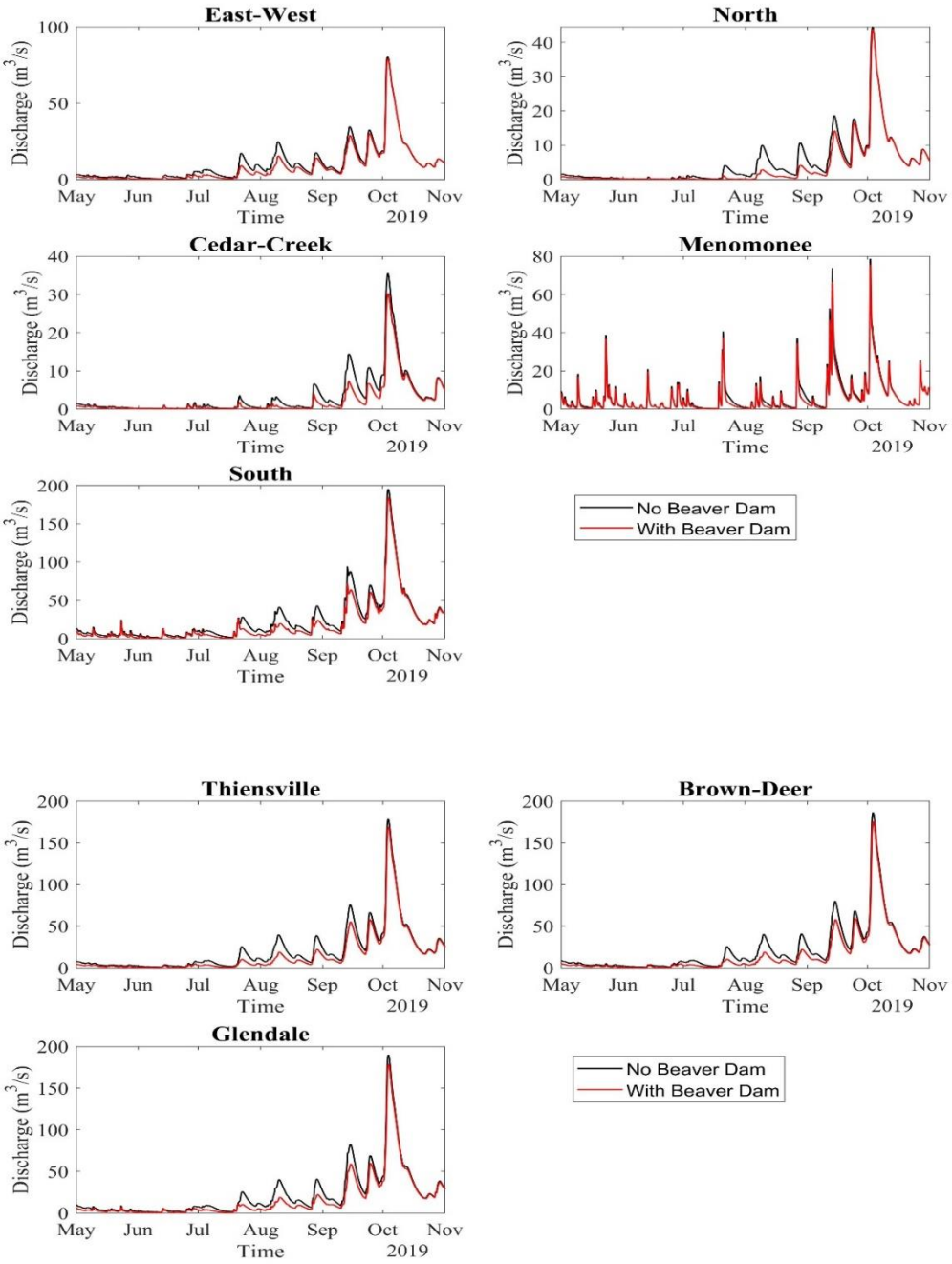


*Figure 5.9 Simulated hydrographs between May 1st and November 30th, 2019 at the outlets of five sub-basins and three flood zone river reaches in the South Milwaukee river sub-basin*

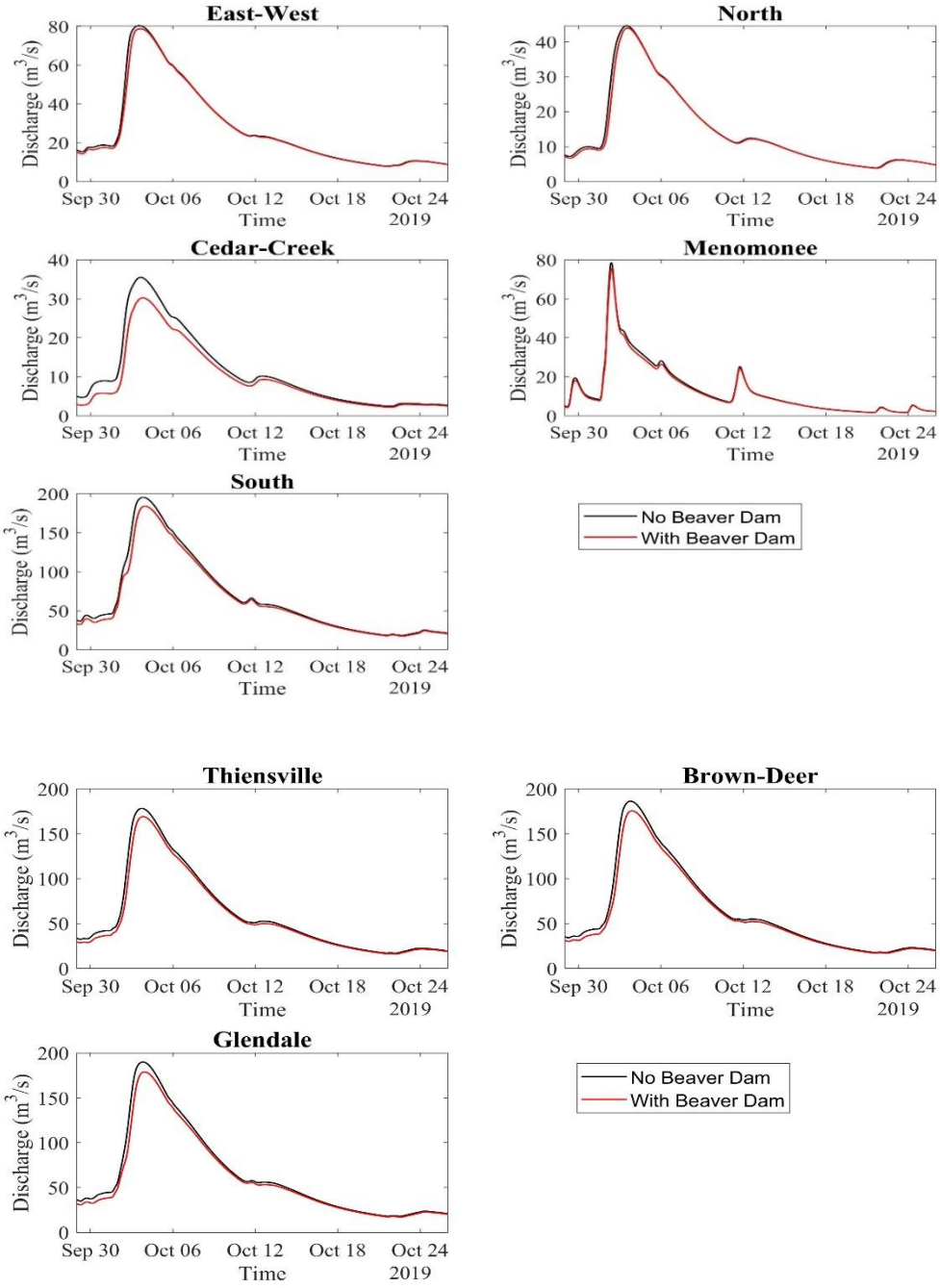


*Figure 5.10 Simulated hydrographs during the major storm events in 2019 (September 27th ~ October 26th) at the outlets of five sub-basins and three flood zone river reaches in the South Milwaukee river sub-basin*

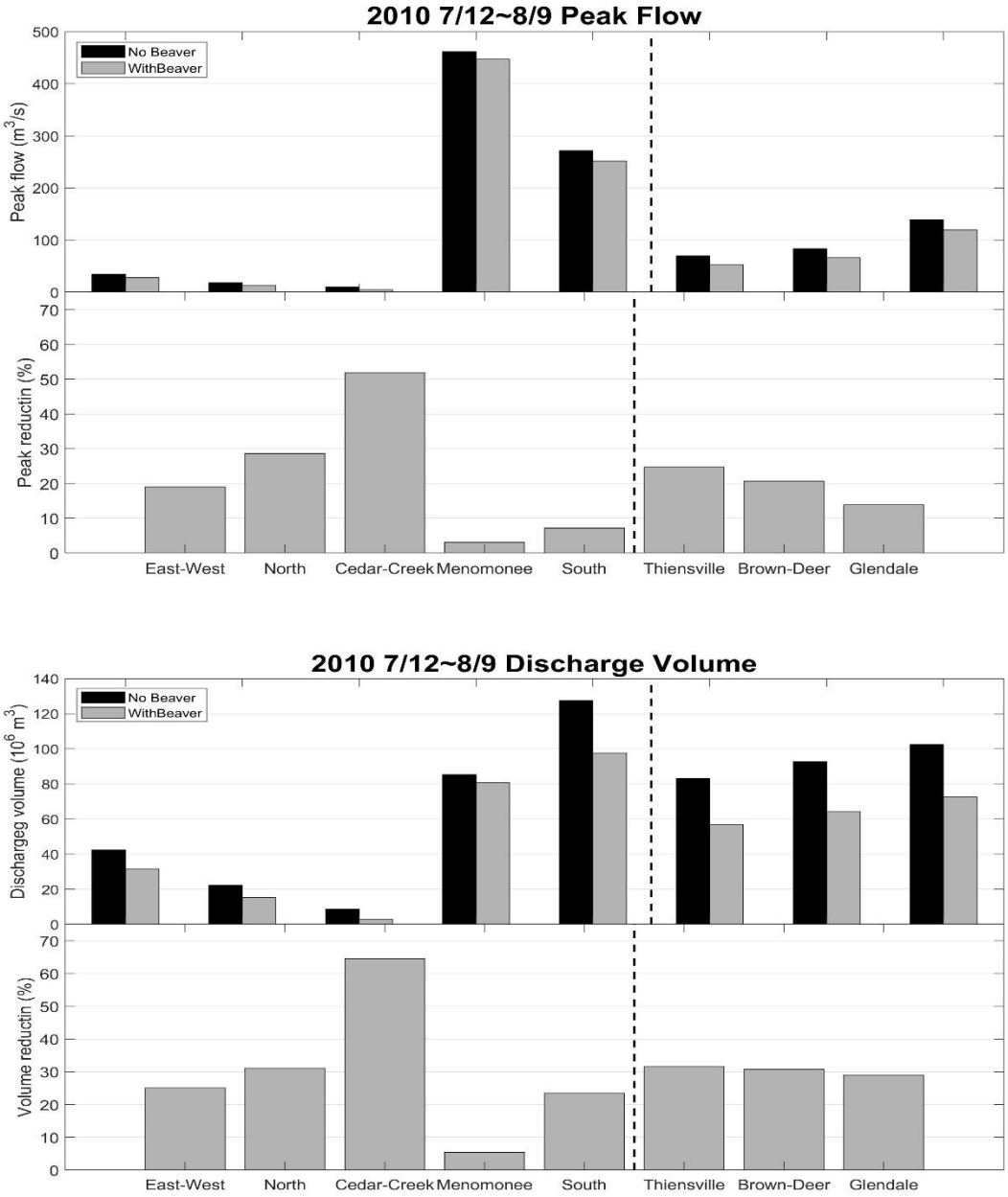


*Figure 5.11 Peak flow rate and discharge volume, and percentage of peak and volume reduction due to beaver dams during the major storm events in 2010, at the outlets of five sub-basins and three flood zone river reaches in the South Milwaukee river sub-basin*

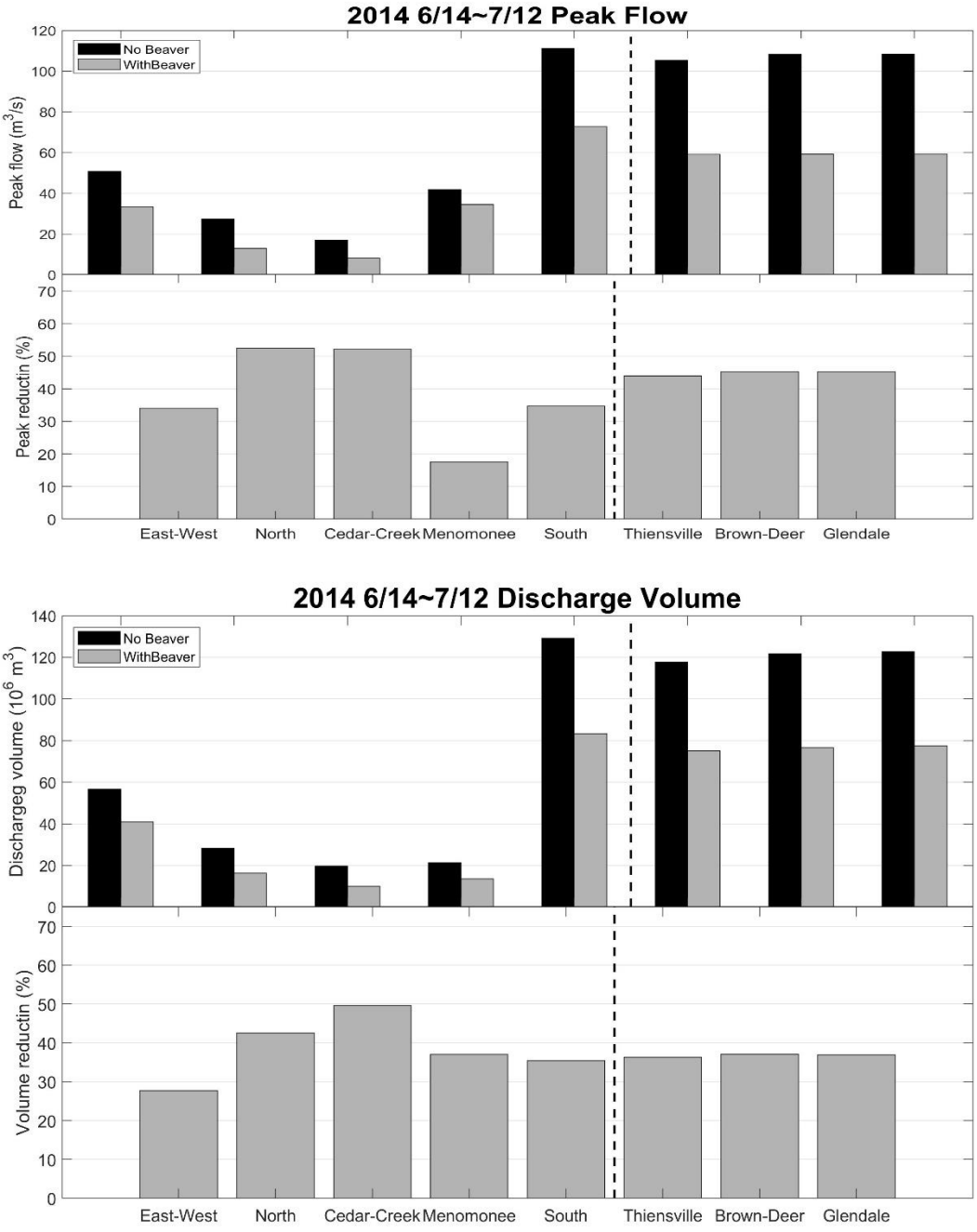


*Figure 5.12 Peak flow rate and discharge volume, and percentage of peak and volume reduction due to beaver dams during the major storm events in 2014, at the outlets of five sub-basins and three flood zone river reaches in the South Milwaukee river sub-basin*

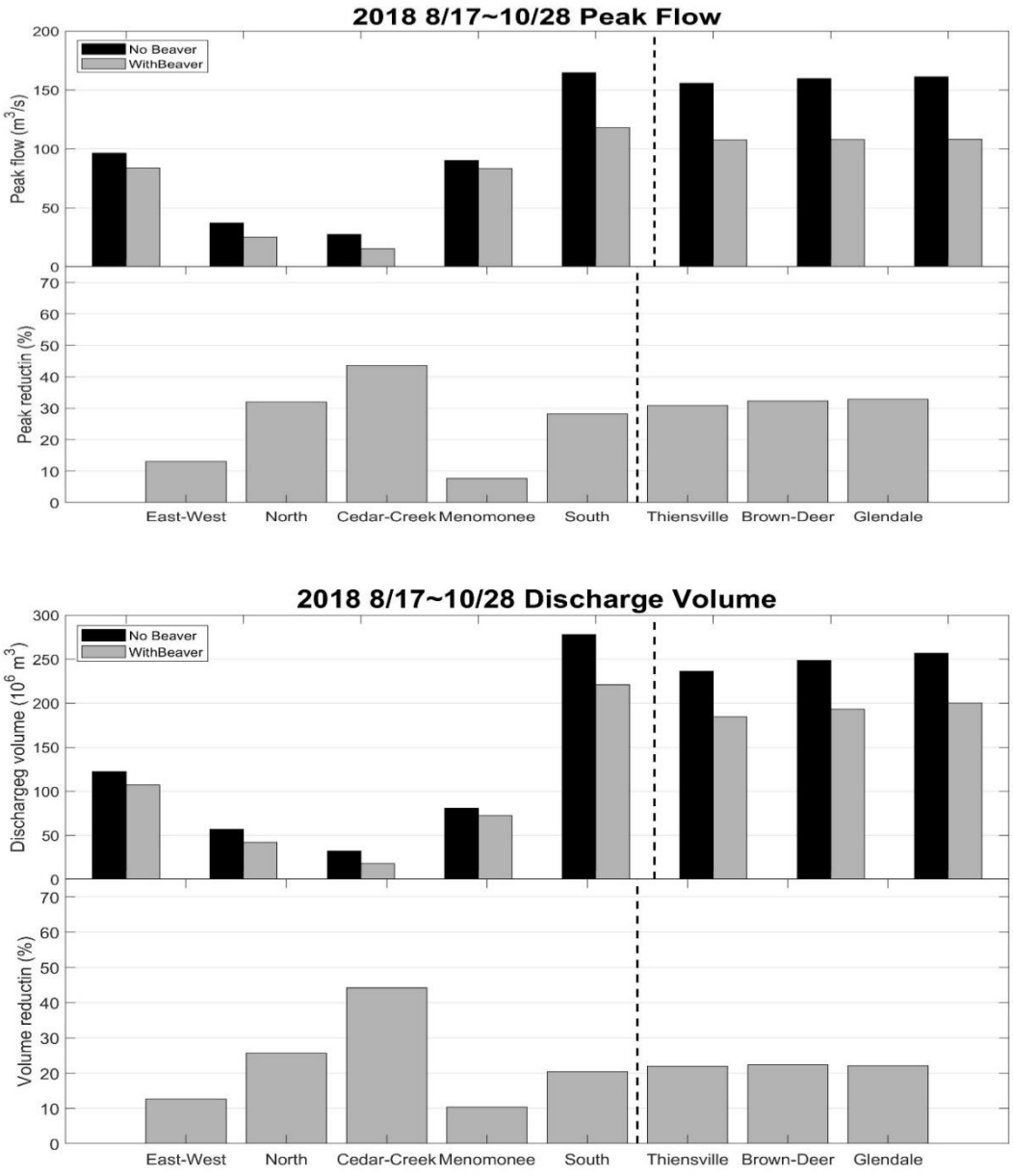


*Figure 5.13 Peak flow rate and discharge volume, and percentage of peak and volume reduction due to beaver dams during the major storm events in 2018, at the outlets of five sub-basins and three flood zone river reaches in the South Milwaukee river sub-basin*

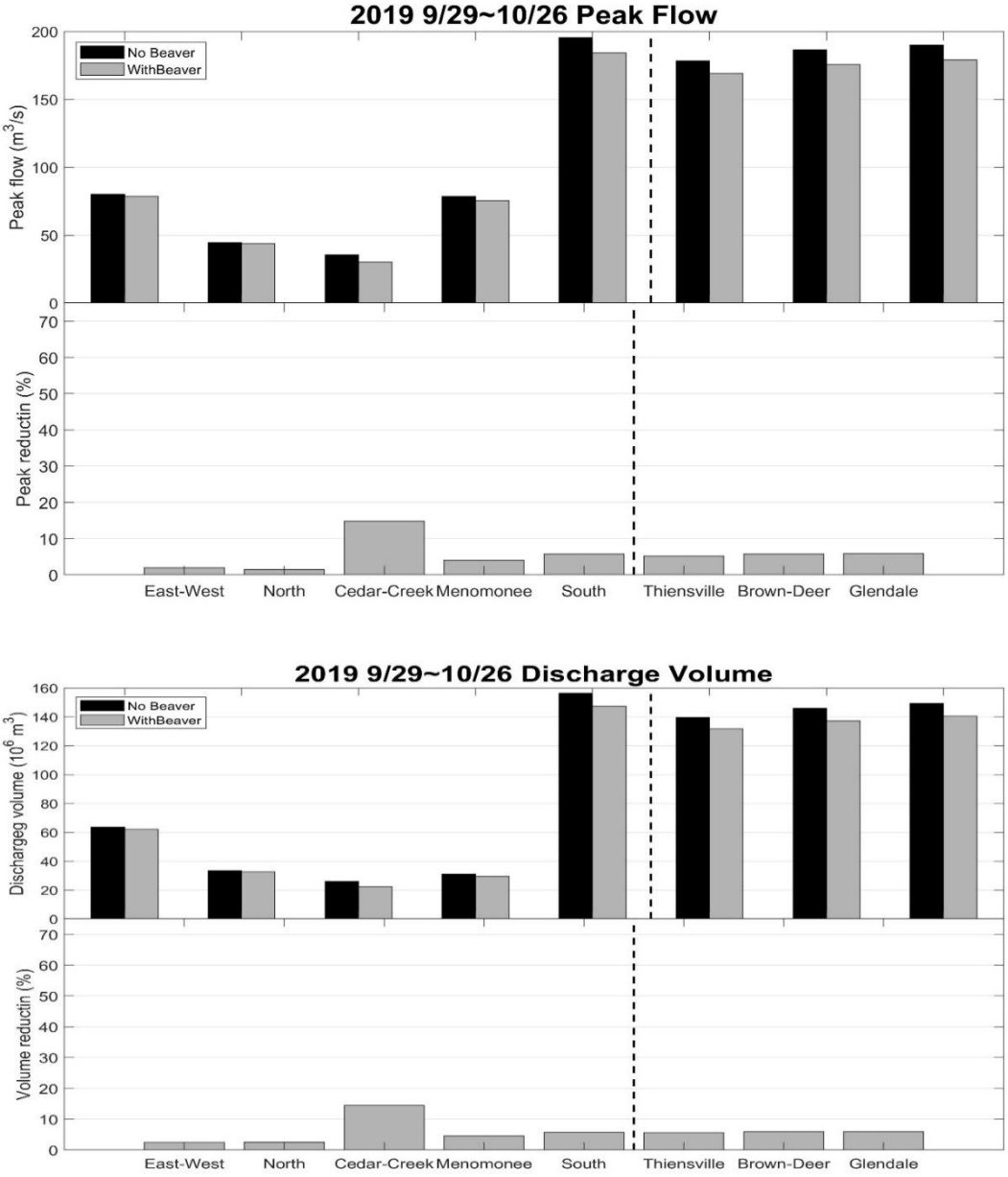


*Figure 5.14 Peak flow rate and discharge volume, and percentage of peak and volume reduction due to beaver dams during the major storm events in 2019, at the outlets of five sub-basins and three flood zone river reaches in the South Milwaukee river sub-basin*

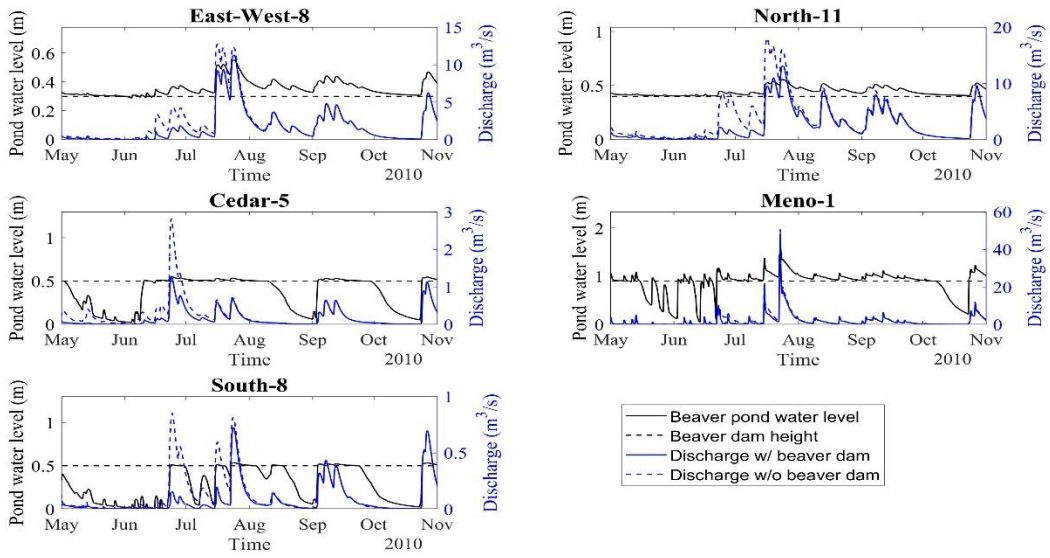


*Figure 5.15 Pond water level variation and hydrograph with or without beaver dams between May 1st and Nov 30th, 2010 at five selected beaver dam locations*

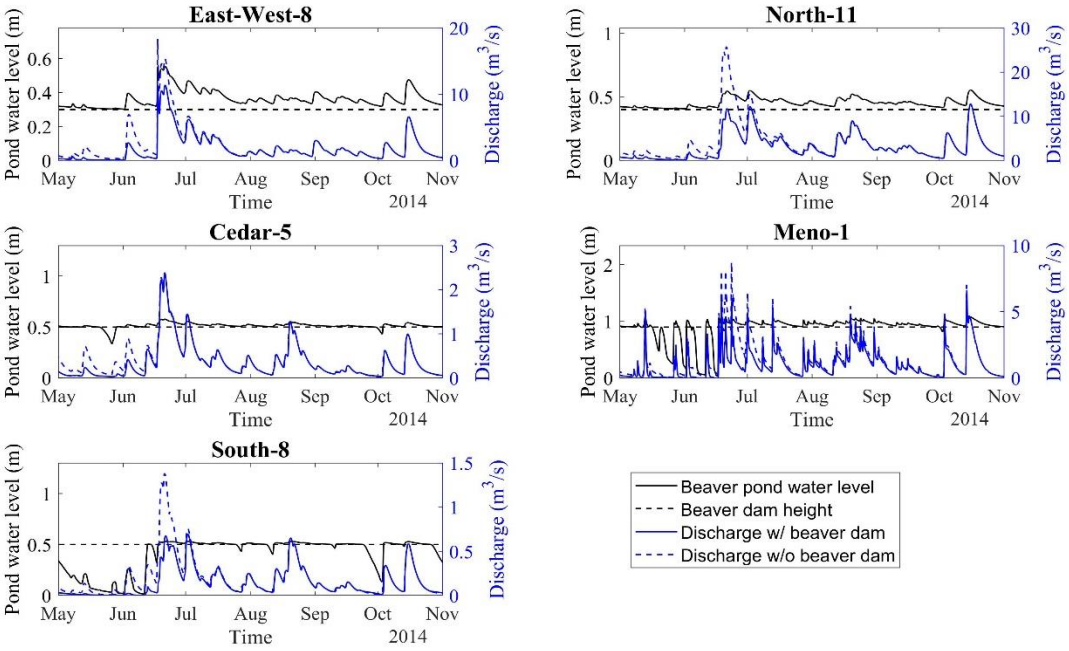


*Figure 5.16 Pond water level variation and hydrograph with or without beaver dams between May 1st and Nov 30th, 2014 at five selected beaver dam locations*

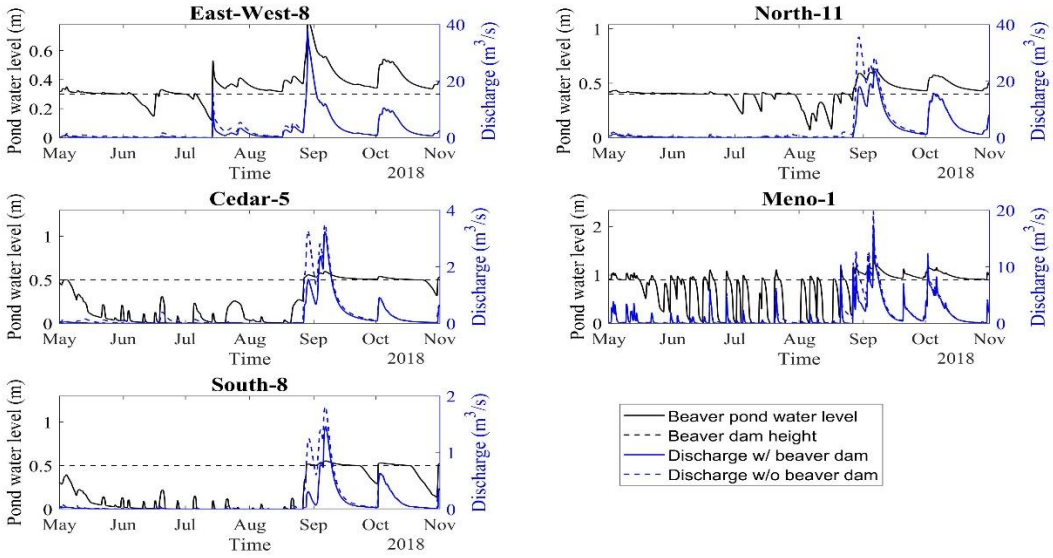


*Figure 5.17 Pond water level variation and hydrograph with or without beaver dams between May 1st and Nov 30th, 2018 at five selected beaver dam locations*

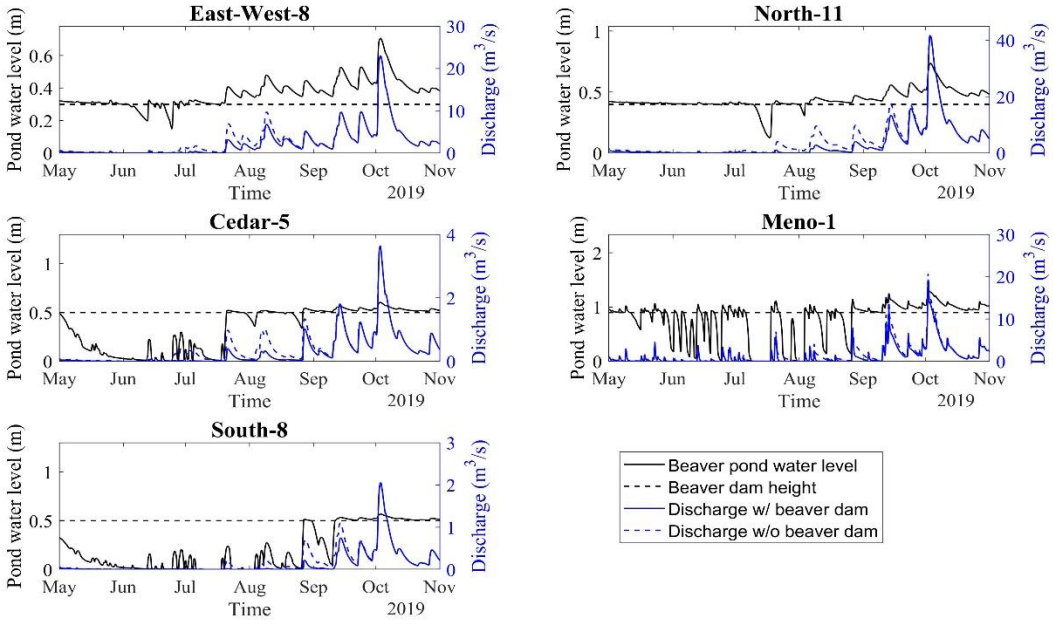


*Figure 5.18 Pond water level variation and hydrograph with or without beaver dams between May 1st and Nov 30th, 2019 at five selected beaver dam locations*

## 5.3 Assess impact of beaver dams with designed frequency storms

To evaluate impacts of beaver dams on future extreme storm events, synthetic storms were generated in HEC-HMS to simulate the hydrograph processes. The "Frequency Storm" method was selected as the meteorological input. Statistical precipitation data were acquired from US National Weather Service and supplied as input to the frequency storm method. Specifically, the precipitation duration-depth relation for the Milwaukee River watershed was obtained from NOAA's Precipitation Frequency Data Server (https://hdsc.nws.noaa.gov/hdsc/pfds/). In this study, synthetic storms included in simulations are 6-hour and 24-hour precipitation events with recurrence intervals (return period) of 10, 25 and 100 years, respectively. There were in total 10 synthetic storm events. Precipitation depths of these events (ranged from 2.96 to 6.46 inches, or 76 to 164 mm) are summarized in *Table 5.2Table 5.2*. Precipitation hyetograph was assumed to be uniformly distributed over all sub-basins

*Table 5.2 Precipitation depth (mm) of 6-hour and 24-hour storms with recurrence intervals of 10, 25 and 100 years of the Milwaukee River watershed. (Data source: NOAA Precipitation Frequency Data Server)*

| Duration | Recurrence Interval (Year) | | |
|---|---|---|---|
| | ***10*** | ***25*** | ***100*** |
| **6 Hour** | 76 | 94 | 125 |
| **24 Hour** | 97 | 120 | 164 |

All synthetic frequency storms were assumed to start on August 1st, 2020, and simulations runs for one full month with a time step of 30 minutes.

Simulated hydrographs at the outlets of the five sub-basins and the three flood zone reaches from the 10 synthetic storms are shown in *Figure 5.19 ~ Figure 5.24*. In these figures, results of the first six days are shown to focus on hydrographs of peak flows. The peak flood flow and total discharged volume were calculated from simulation results at these locations. They are presented as bar graphs shown in *Figure 5.25 ~ Figure 5.30* . Percentage reductions of peak flow and discharge volume due to beaver dams are also presented as bar graphs in these figures.

For most storm scenarios and observational sites, a short period of "plateau" can be observed on the rising "limbs" of simulated hydrographs for cases with beaver dams. This demonstrates the effect of flow interception by available storage space behind beaver dams. After beaver ponds were filled to their full capacity, the hydrograph rose again with a slope milder than that of the case without beaver dams. This observation demonstrates that energy loss due to dam overflow as a secondary mechanism of downstream peak flow reduction.

With modeled synthetic storms which uniformly cover the entire watershed, all beaver dams in the model can contribute to flood mitigation. Simulation results suggested a very significant effect of flow reduction at all eight observational sites. The range and average of peak reductions are summarized in *Table 2.1Table 5.3*. Peak reduction was maximum in the Cedar Creek sub basin i.e. 23% on average.

*Table 5.3 Summary of beaver-mitigated flood flow peak reduction and discharge volume reduction at outlets of five sub-basins and three urban flood zones in the South Milwaukee river sub-basin*

| **Locations** | **Peak flow reduction** | | |
|---|---|---|---|
| | *Minimum* | *Maximum* | *Average* |
| East-West | 6% | 12% | 8% |
| North | 7% | 7% | 7% |
| Cedar Creek | 20% | 25% | 23% |
| Menomonee | 9% | 13% | 11% |
| South | 5% | 9% | 8% |
| Thiensville | 4% | 8% | 6% |
| Brown Deer | 4% | 8% | 6% |
| Glendale | 4% | 8% | 7% |

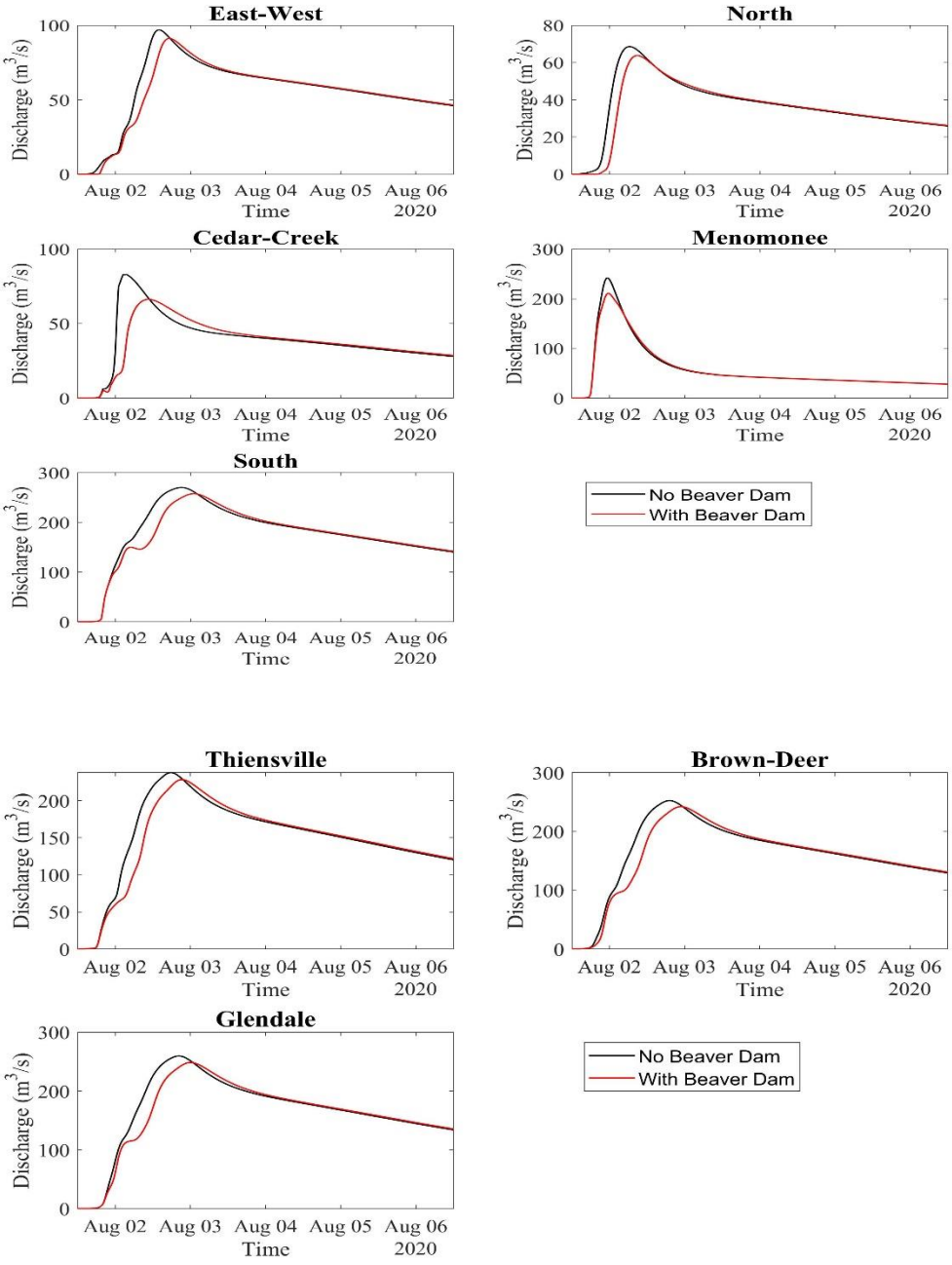


*Figure 5.19 Simulated hydrographs at the outlets of five sub-basins and three flood zone river reaches in the South Milwaukee river sub-basin in response to a 10-year 6-hour svnthetic storm*

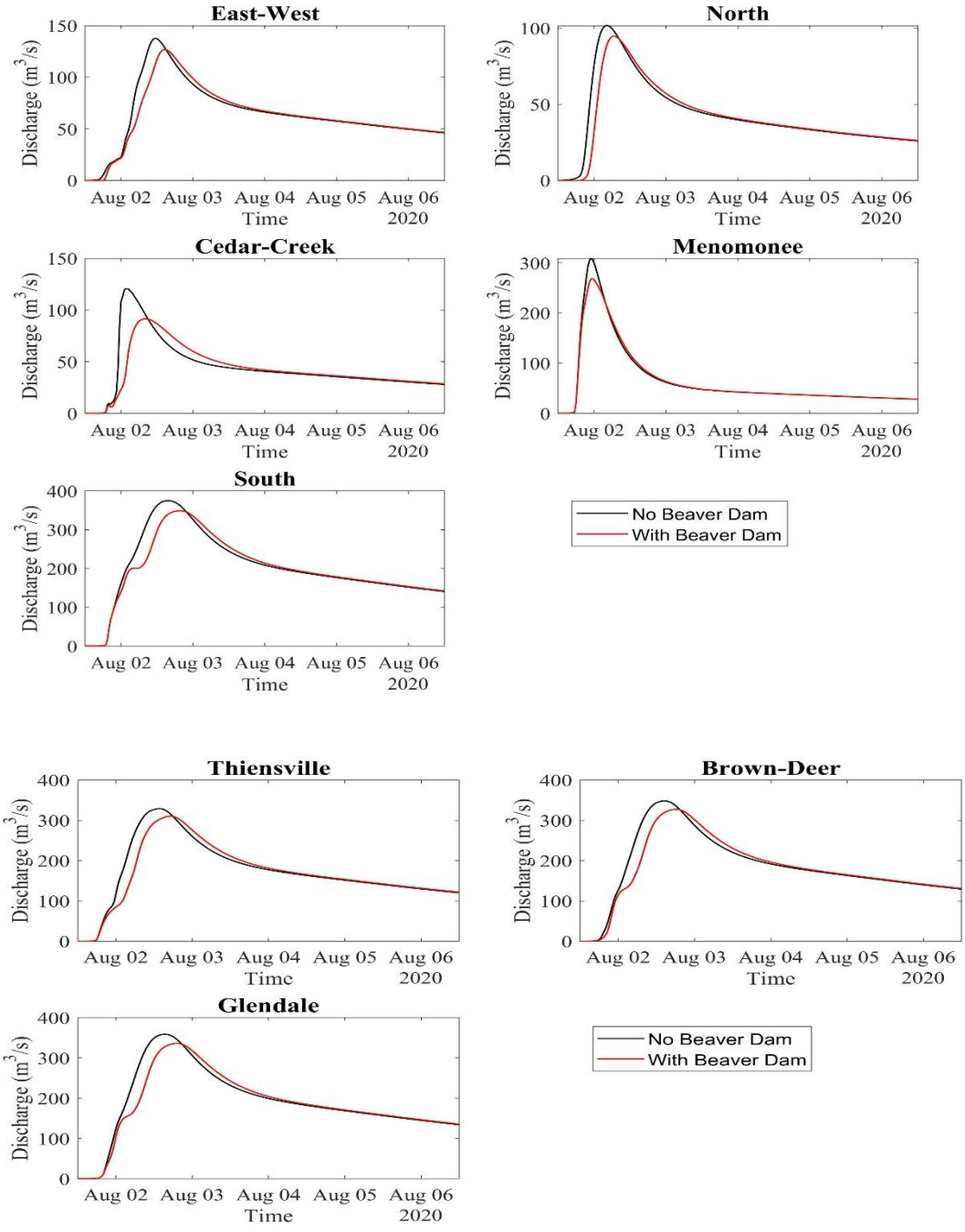


*Figure 5.20 Simulated hydrographs at the outlets of five sub-basins and three flood zone river reaches in the South Milwaukee river sub-basin in response to a 25-year 6-hour synthetic storm*

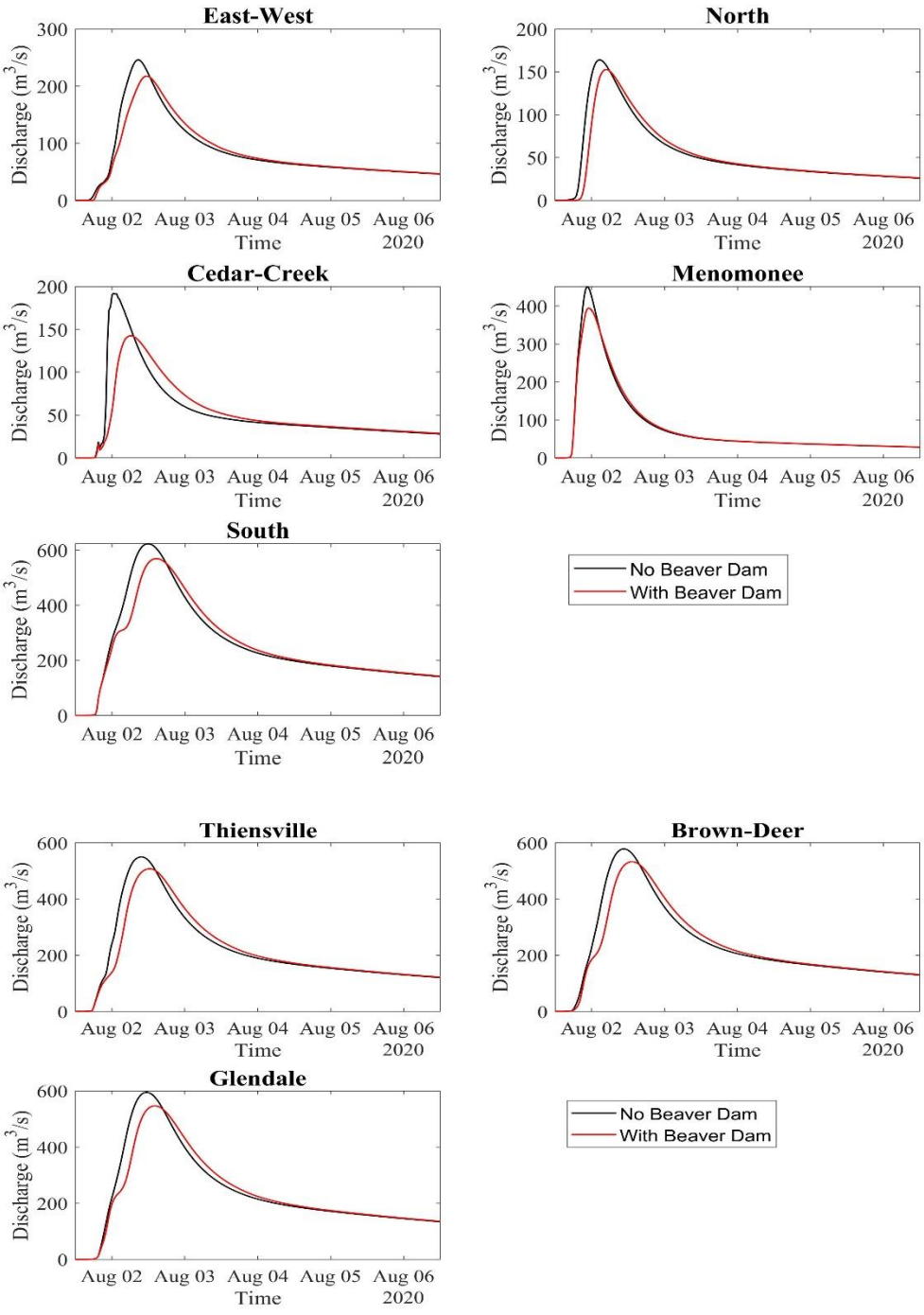


*Figure 5.21 Simulated hydrographs at the outlets of five sub-basins and three flood zone river reaches in the South Milwaukee river sub-basin in response to a 100-year 6-hour*

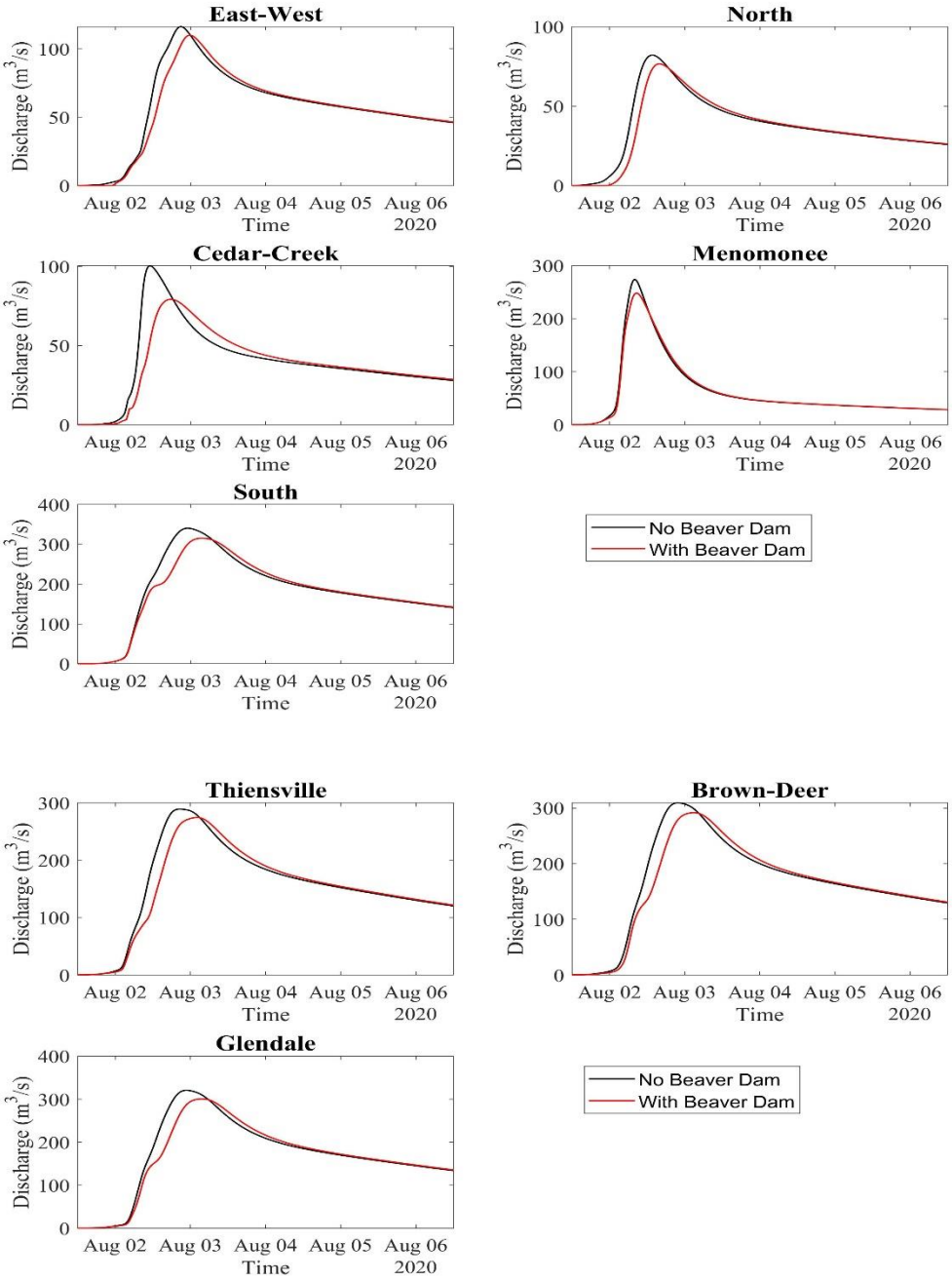


*Figure 5.22 Simulated hydrographs at the outlets of five sub-basins and three flood zone river reaches in the South Milwaukee river sub-basin in response to a 10-year 24-hour*

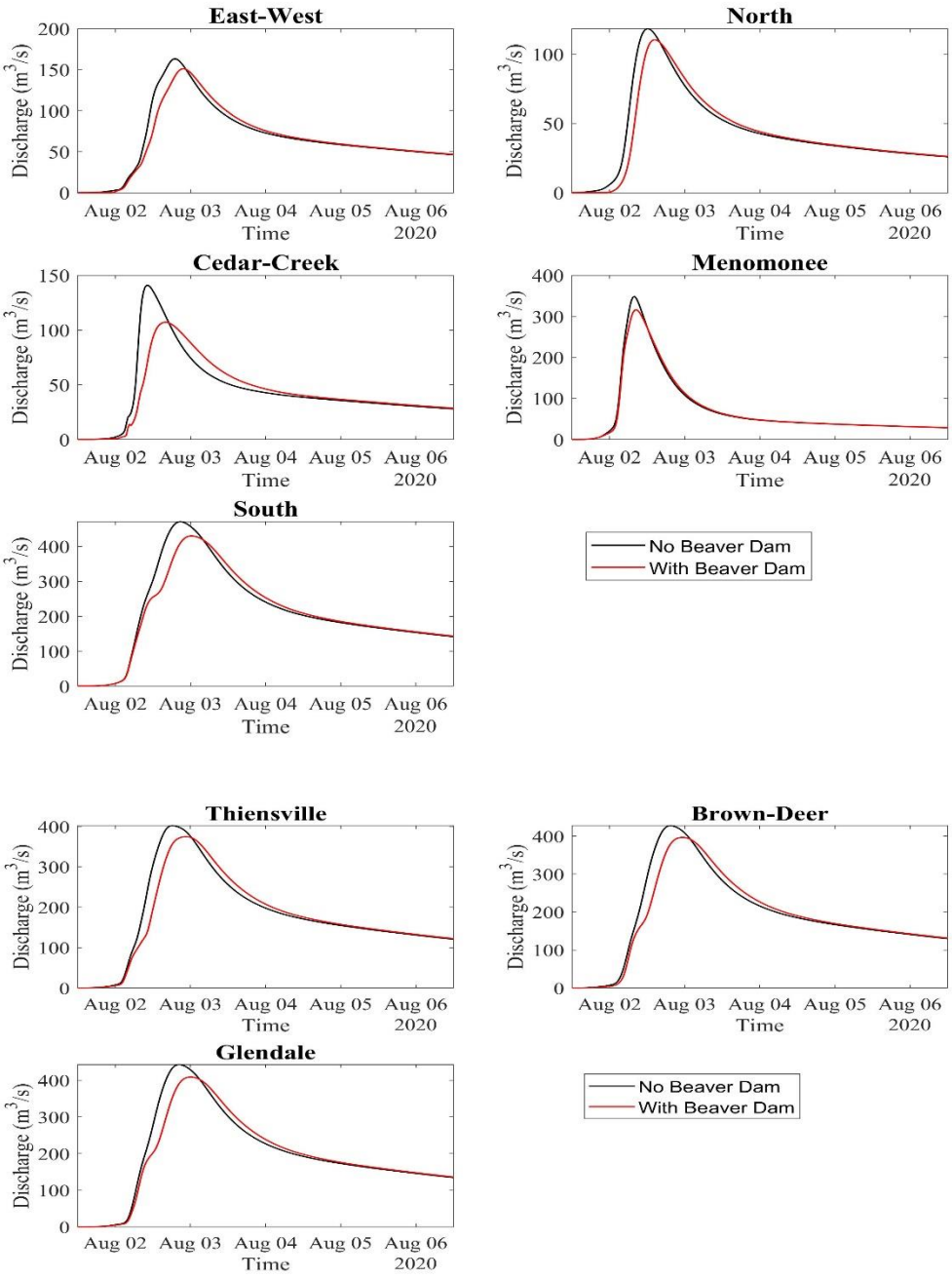


*Figure 5.23 Simulated hydrographs at the outlets of five sub-basins and three flood zone river reaches in the South Milwaukee river sub-basin in response to a 25-year 24-hour*

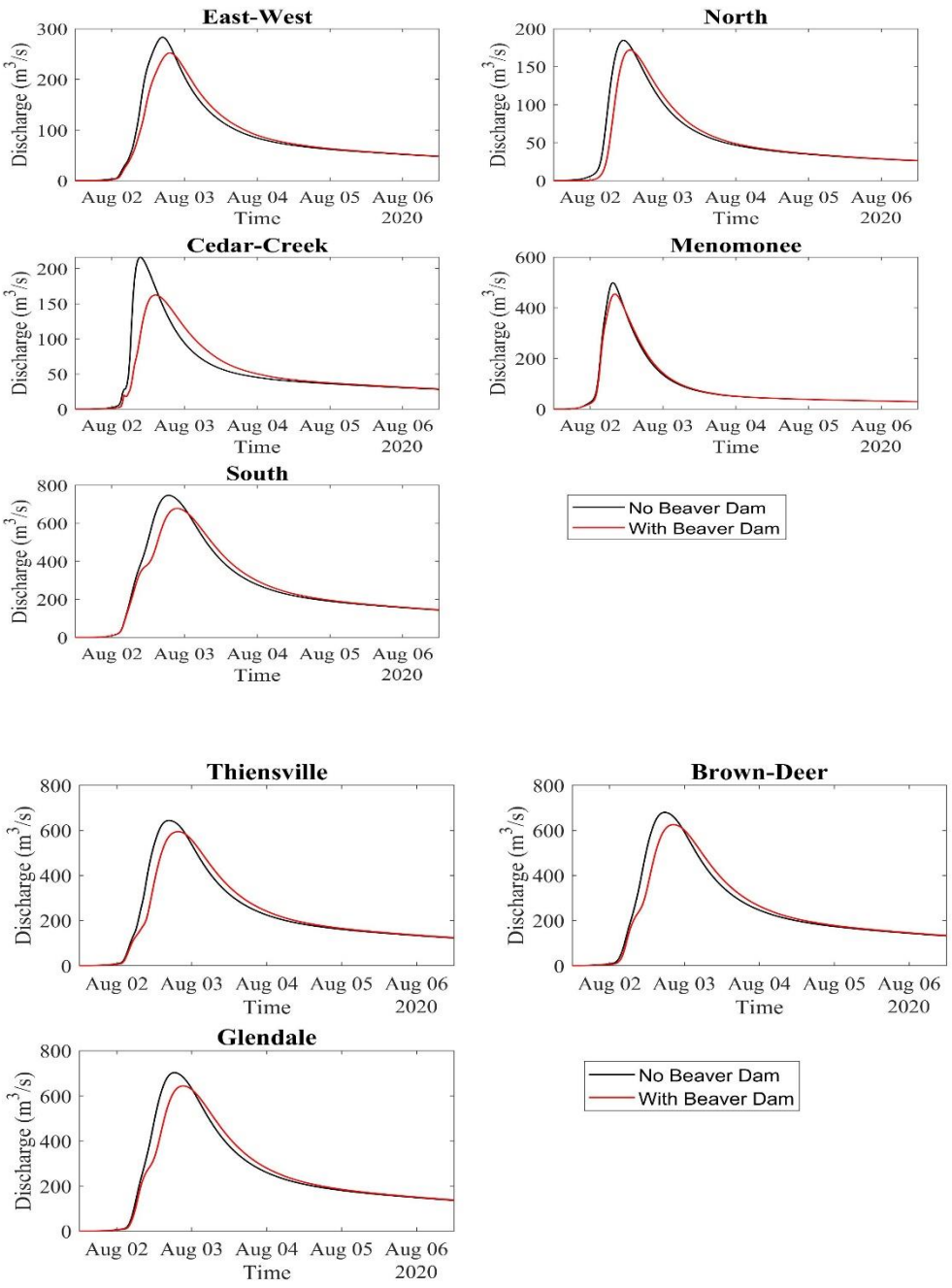


*Figure 5.24 Simulated hydrographs at the outlets of five sub-basins and three flood zone river reaches in the South Milwaukee river sub-basin in response to a 100-year 24-hour*

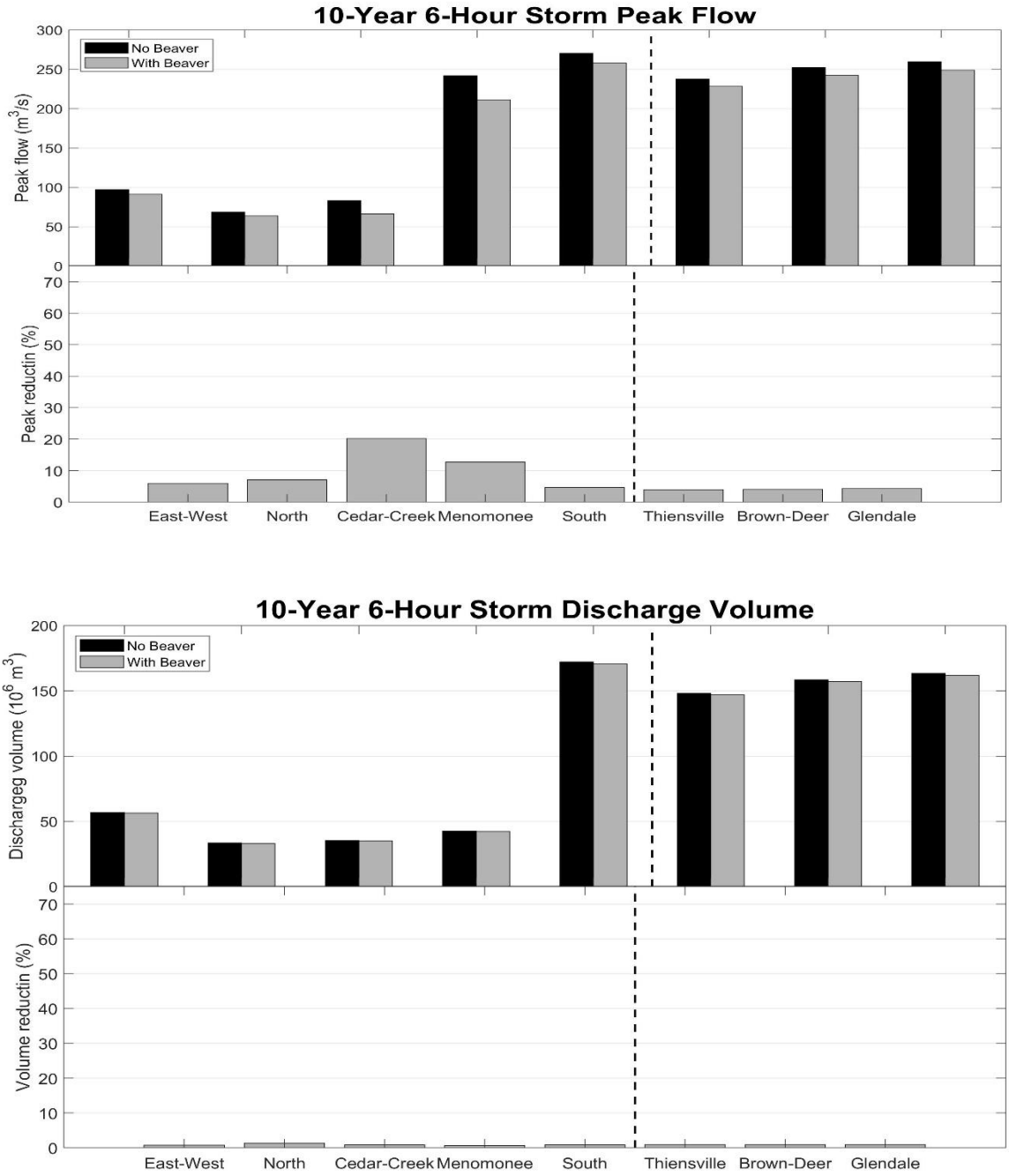


*Figure 5.25 Peak flow rate and discharge volume, and percentage of peak and volume reduction due to beaver dams at the outlets of five sub-basins and three flood zone river reaches in the South Milwaukee river sub-basin in response to a 10-year 6-hour synthetic storm*

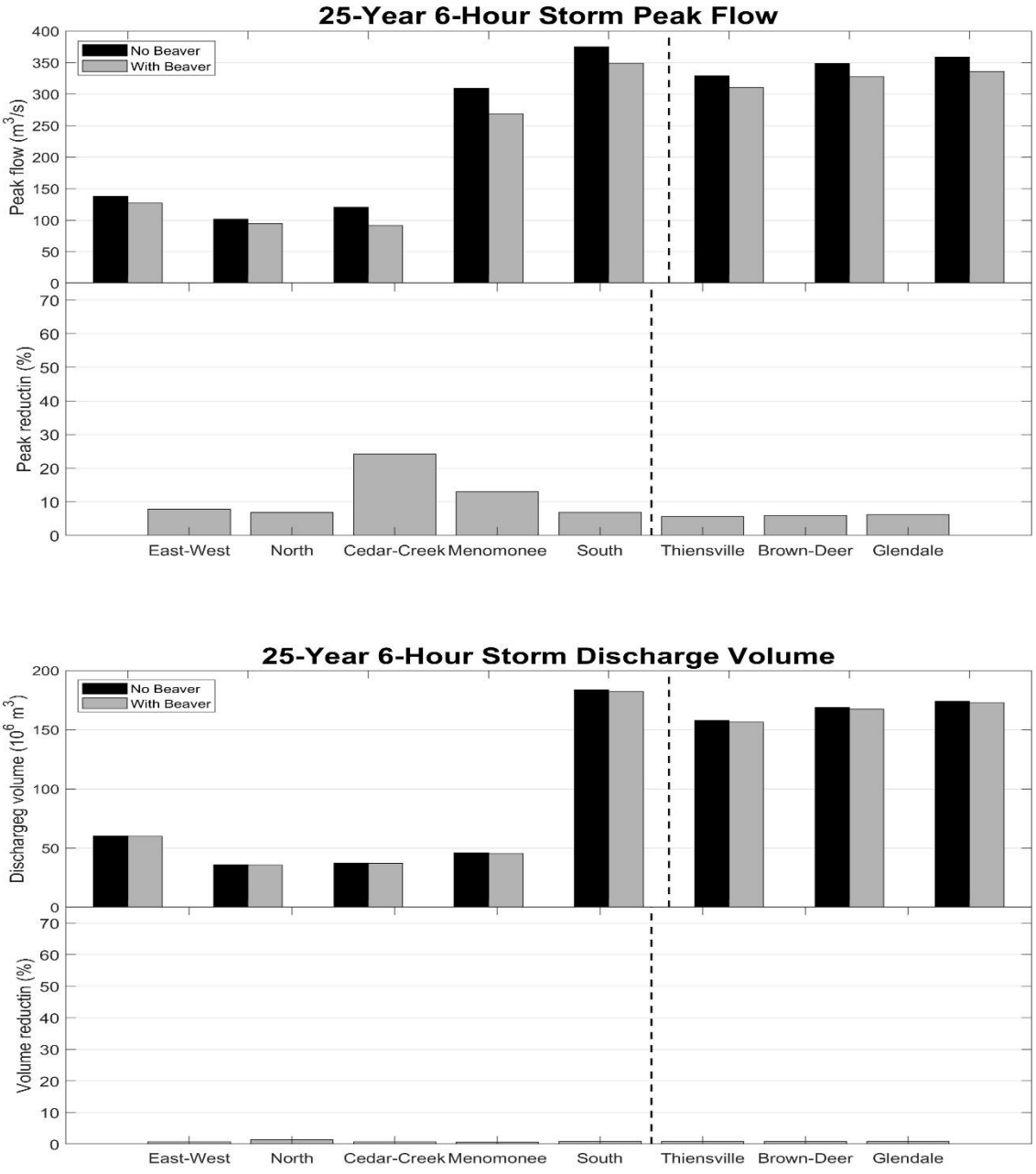


*Figure 5.26 Peak flow rate and discharge volume, and percentage of peak and volume reduction due to beaver dams at the outlets of five sub-basins and three flood zone river reaches in the South Milwaukee river sub-basin in response to a 25-year 6-hour synthetic storm*

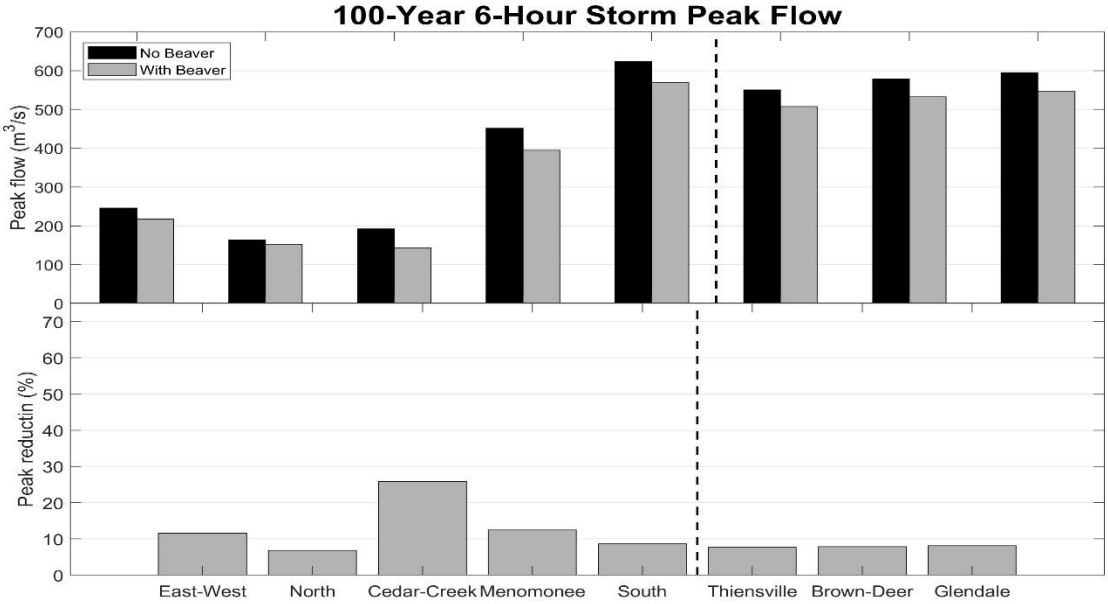


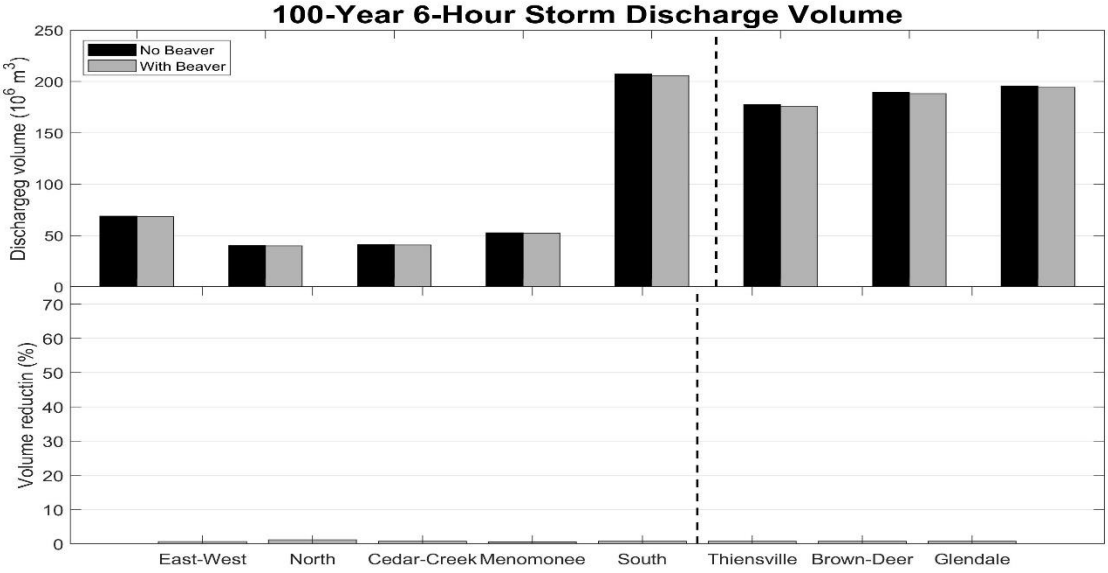


*Figure 5.27 Peak flow rate and discharge volume, and percentage of peak and volume reduction due to beaver dams at the outlets of five sub-basins and three flood zone river reaches in the South Milwaukee river sub-basin in response to a 100-year 6-hour synthetic storm*

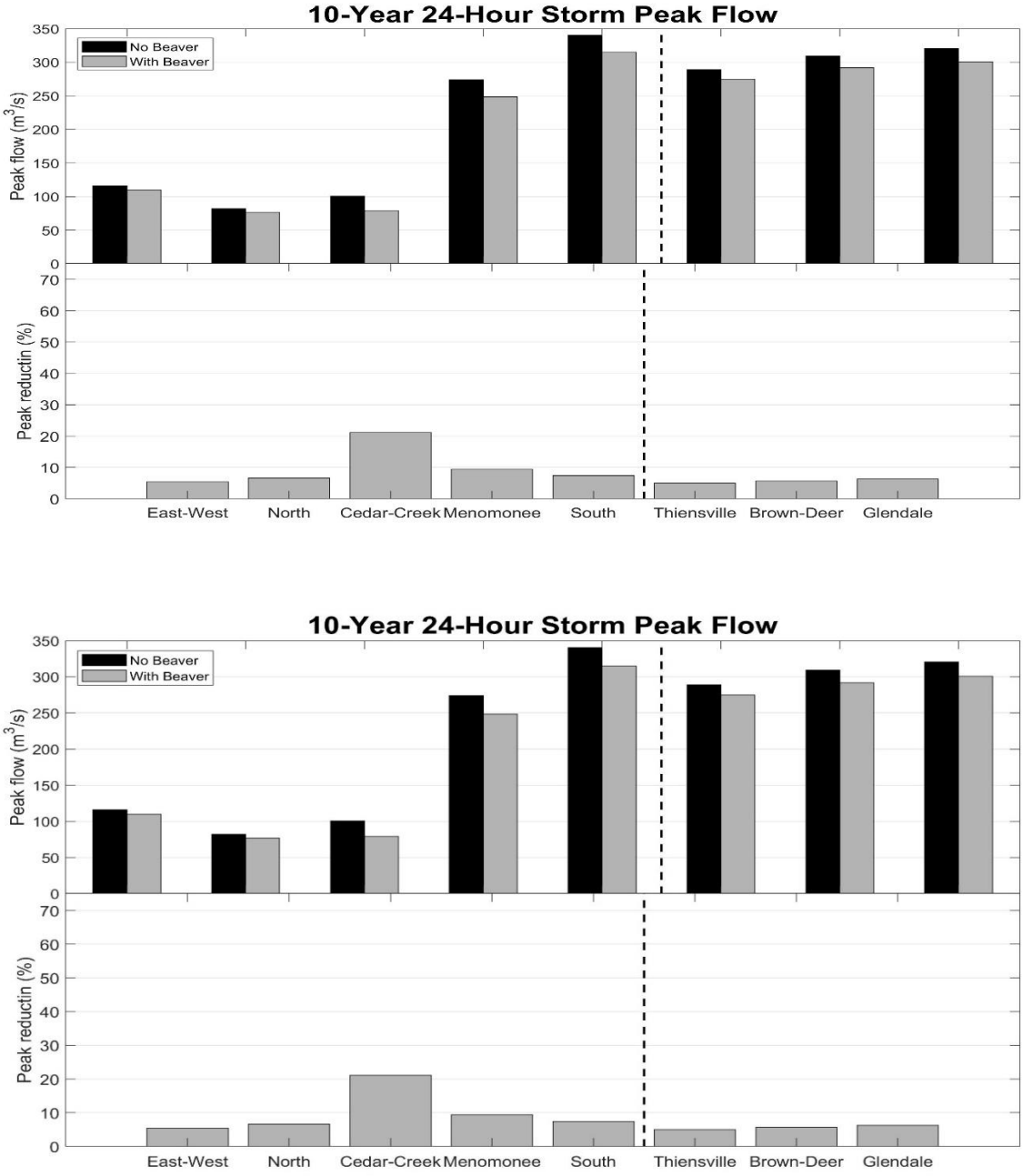


*Figure 5.28 Peak flow rate and discharge volume, and percentage of peak and volume reduction due to beaver dams at the outlets of five sub-basins and three flood zone river reaches in the South Milwaukee river sub-basin in response to a 10-year 24-hour synthetic storm*

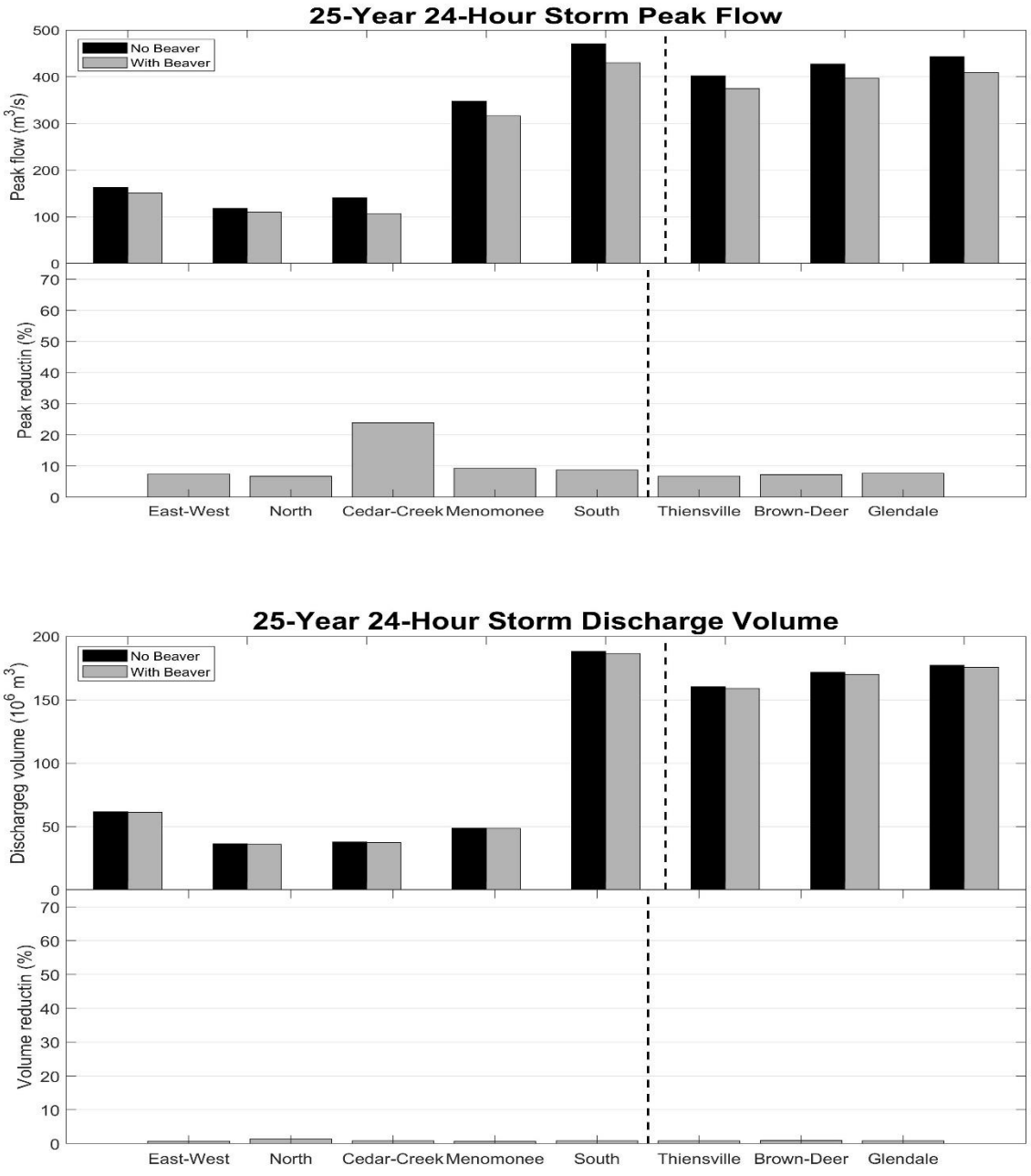


*Figure 5.29 Peak flow rate and discharge volume, and percentage of peak and volume reduction due to beaver dams at the outlets of five sub-basins and three flood zone river reaches in the South Milwaukee river sub-basin in response to a 100-year 24-hour synthetic*

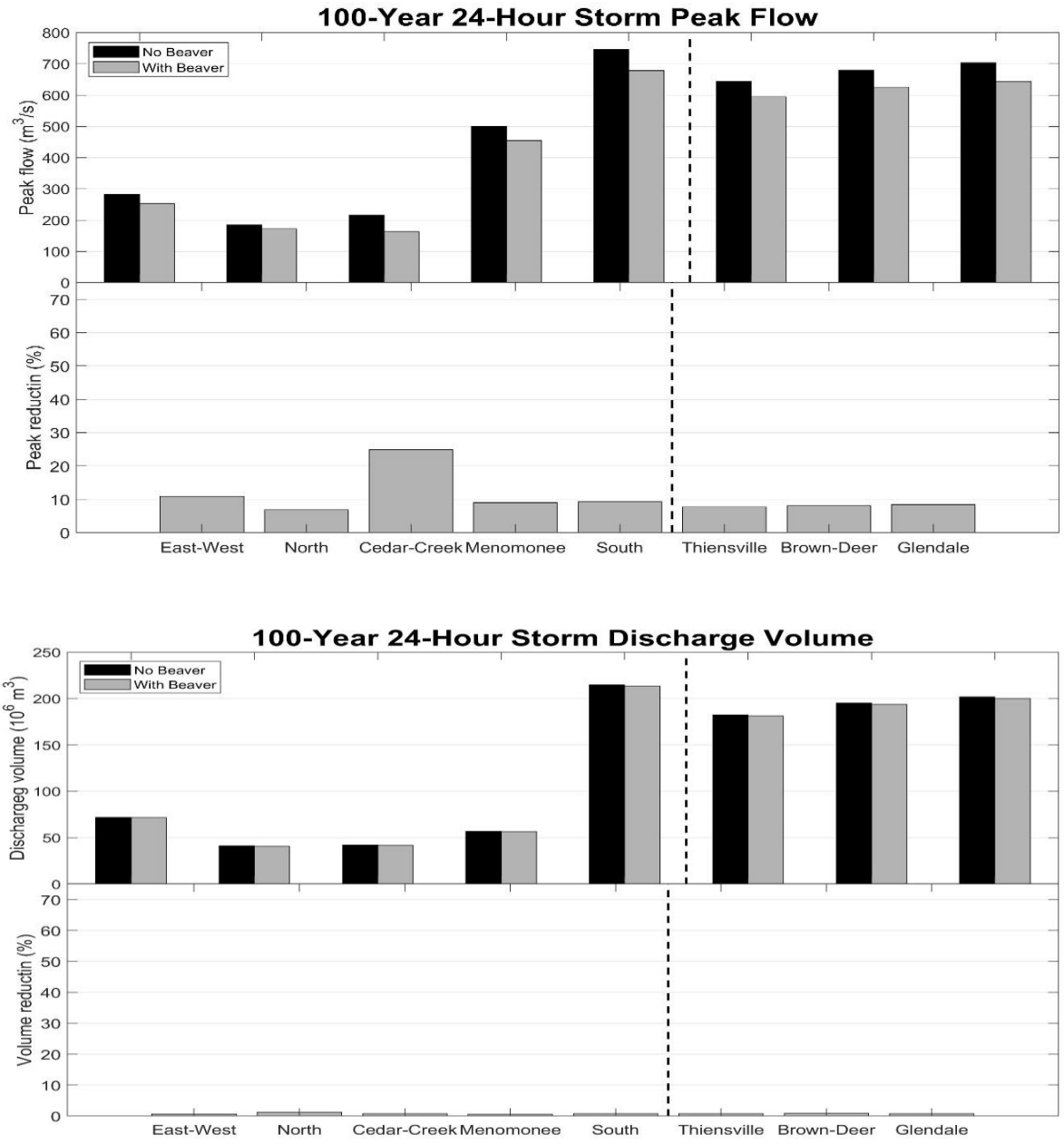


*Figure 5.30 Peak flow rate and discharge volume, and percentage of peak and volume reduction due to beaver dams at the outlets of five sub-basins and three flood zone river reaches in the South Milwaukee river sub-basin in response to a 100-year 24-hour synthetic storm*

# CHAPTER 6

# CONCLUSION

The primary objective of the thesis was to analysis the hypothesis that restoration of beaver habitats in the Milwaukee River watershed can significantly mitigate river flood flows, even for urban areas at the lower end of the watershed. In this process, the BRAT model was developed to assess the suitability of Milwaukee watershed for beaver restoration. Considering both vegetation cover and hydrologic conditions, the BRAT results suggest that three northern sub-basins including the East-West branch Milwaukee river, the North branch Milwaukee river and the Cedar Creek, are more suitable for beaver restoration, the Menomonee river sub-basin and the Milwaukee river South sub-basin can moderately support beaver habitations. The Kinnikinnic river sub-basin is generally not suitable for beaver restoration due to extensive developed land and lack of vegetation support along the streams. However, model predictions presented in this report has not been calibrated with ground truth. Present beaver colonies are rare to none in the Milwaukee River watershed, which brings difficulties for model calibration or validation.

To assess the hydrological impact of beaver dams in Milwaukee watershed, a distributed continuous model was developed in HEC-HMS to reproduce the hydrological processes such as soil infiltration, groundwater interflow and baseflow, as well as stream flows. Simulations of past storm and river flow events demonstrated that modeled hydrographs agreed fairly well with observed data, in terms of the peak flows and total discharge volume calculated over the period from late spring to early winter of each year. It was postulated that the main source of error of

simulation was precipitation data. Precipitation inputs to the model were land based rain gauge data which were interpolated to each sub-basin with the "inverse distance" method. Rain gauges are sparse, and the interpolation creates "smooth" variation of precipitation intensity over the watershed. This approach fails to represent the true spatial variability of a storm event, which is typically heterogeneous with rapidly moving "sharp" fronts. Therefore, it is expected that model performance will be improved if a "gridded" precipitation model is applied with radar image-based data.

With the calibrated HEC-HMS model, hypothetical analysis was conducted to evaluate effects of beaver dams on hydrology of the watershed. Locations of beaver dams were identified based on BRAT model results and validated through field surveys. 42 beaver restoration sites were selected representing those with highest potentials according to the field survey. A MATLAB program was developed to assist beaver dam reconstruction over high-resolution DEM data at selected sites. Through the reconstruction process, model parameters of dams were determined, including the height and length of dams, and the rating relations between water storage and water surface level behind dams. With beaver dams added as "reservoir" components in HEC-HMS, model runs were conducted with both past storm events and synthetic frequency storms. Simulated hydrographs were extracted at eight observation locations: the outlets of five sub-basins excluding the Kinnikinnic river sub-basin, and river segments in three urban flood zones in the South Milwaukee river sub-basin.

Simulation with realistic past storm events suggested that beaver dams can significantly reduce the peak flow and discharge volume at the eight observation locations. Two factors contribute to peak flow reduction: (1) flow interception by storage capacity of beaver dams makes the primary contribution (2) energy dissipation through dam overflow when the storage capacity is filled. Water evaporation from the impounded water is the primary loss that contributes to discharge volume reduction. The simulation results showed that average percentage of peak flow reduction ranged between 11% and 48%; and averaged percentage of volume reduction ranged between 15% and 48%. The minimum and maximum percentage reduction are at the outlet of the Menomonee River and the outlet of the Cedar Creek, respectively. A further investigation indicated that most beaver dams were near their full capacity before the occurrence of major storms, due to water accumulation through prior flow events. Among all the past storm simulation cases, the case with least flood flow reduction (7% average peak reduction) was observed for the October 2019 storm event. For this case, nearly all beaver dams were completely full due to a series minor storms prior to the October peak event.

Six synthetic frequency storms were generated for simulation, they are standard 6-hour and 24-hour storms with recurrence intervals ranged from 10 years and 100 years. Total precipitation depth of these storms varied between 2.99 and 6.5 inches. Since synthetic storms were designed with a uniform spatial distribution over the entire watershed, all beaver dams were able to contribute to flow reduction at river reaches at the lower end of the watershed. Consequently, a significant flow reduction were reported at the eight observational locations. Average flood peak

reduction ranged between 10% (24-hour 200-year storm) and 9% (6-hour 10-year storm). Modeling analysis with synthetic frequency storms approved the hypothesis that beaver dams that largely dispersed in the upper tributaries of the watershed may mitigate flood flows in urban flood zones at the lower end of the watershed. It should be noted that these conclusions are based on the assumption that storm precipitation was uniformly distributed over the entire watershed, and all beaver dams had at least 60% of their potential capacity for flow interception before the extreme but isolated storm event. For real storm events which are spatially inhomogeneous and may occur as a series of events, the effect of flood mitigation is expected to be less than that predicted by the synthetic storm simulation.

It is considered that the main source of uncertainty that may affect model results and conclusions is associated with how beaver dams reconstructed in the model can represent realistic ones. In this study, each beaver site was assigned a single dam that is relatively large in height and length, such that impounded water is comparable to a large beaver dam complex. Most pervasive beaver colonies are a complex that consists of a series of smaller beaver ponds with multiple dam structures. Cumulative hydraulic performance of a large dam complex may or may not be comparable to that of a single large dam structure modeled in this study. To reduce the uncertainty, future research should focus on detailed modeling of beaver complex structures. Model simulations can be conducted in similar watershed with known existing beaver complexes, which allows model calibration with realistic dam structures. Field experiments in real beaver structures that measures change of water level, inflow and outflow during high and low flow events are also

necessary to improve the simulation of hydraulic performances. These additional efforts may help to revise the current model that can better represent beaver effects on hydrology at the basin scale.

In the HEC-HMS model, groundwater storage and flow are treated for each sub-basin through a box model. Beaver dams (or reservoirs) are treated as hydraulic control nodes. Therefore, it is not able to account for the local pond-groundwater exchange, which is a rather important process that affect the water balance. This limitation needs to be acknowledged for future research considerations.

# CHAPTER 7

# REFERENCES


AR Nicholson, ME Wilkinson, GM O'Donnell, PF Quinn. 2012. "Runoff attenuation features: a sustainable flood mitigation strategy in the Belford catchment, UK." *Royal Geographical Society* https://doi.org/10.1111/j.1475-4762.2012.01099.x.

Beedle, D. L. 1991. *Physical dimensions and hydrologic effects of beaver ponds on Kuiu Island in southeast Alaska.* Master Thesis, Oregon State University.

Bennett, T. H. 1998. *Development and application of a continuous soil moisture accounting algorithm for the Hydrologic Engineering Center Hydrologic Modeling System (HEC-HMS).* Doctoral Dissertation, University of California, Davis.

Burzynski, M. 2001. *The State of the Milwaukee River Basin.* Wisconsin Department of Natural Resources.

Burzynski, Marsha. 2001. *The State of the Milwaukee River Basin.* Milwaukee: Wisconsin Department of Natural Resources. https://dnr.wi.gov/water/basin/milw/milwaukee_801.pdf.

C.Cuny, Frederick. 1991. "Living with floods: Alternatives for riverine flood mitigation." *Land Use Policy* 8 (4): 331-342.

Caillat, A., B. Callaway, D. Hebert, Nguyen A., and S. Petro. 2014. *Beaver (Castor Canaensis) Impact on Water Resources in the Jemez Waatershed, New Mexico.* Group Project Report, University of California, Santa Barbara.

Cherie J. Westbrook, Amanda Ronnquist, Angela Bedard-Haughn. 2020. "Hydrological functioning of a beaver dam sequence and regional dam persistence during an extreme rainstorm." *Hydrological Processes* 34 (18): 3726-3737.

Cronshey, R. 1996. *Urban hydrology for small watersheds.* Technical Relase 55, US Dept. of Agriculture, Soil Conservation Service, Engineering Division.

Devito, K. J., and P. J. Dillon. 1993. "Importance of runoff and winter anoxia to the P and N dynamics of a beaver pond." *Canadian Journal of Fisheries and Aquatic Sciences* 50: 2222-2234.

Feiner, K., and C. S. Lowry. 2015. "Simulating the effects of a beaver dam on regional groundwater flow through a wetland." *Journal of Hydrology: Regional Studies* 4: 675-685.

Flemming, M. and Neary, V. 2004. "Continuous Hydrologic Modelling Study with the hydrologic modeling system." *Hydrology* J. Hydrol. Eng., 2004, vol. 9, no. 3, pp. 175–183.

Green, K. C., and C. J. Westbrook. 2009. "Changes in riparian area structure, channel hydraulics, and sediment yield following loss of beaver dams." *Journal of Ecosystems and Management* 10 (1).

Hartenberg, R. S., and J. Denavit. 1965. In *Kinematic Synthesis of Linkages*, 435. New York: McGraw-Hill.

Holberg, J. 2015. "Downward model development of the soil moisture accounting loss method in HEC-HMS: Revelations concerning the soil profile." Master Thesis, Purdue University.

Holberg, Jessica. 2015. "Downward model development of the soil moisture accounting loss method in HEC-HMS." *Master's Thesis, Purdue University.*

J.Harrower, Michael. 2010. "Geographic Information Systems (GIS) hydrological modeling in archaeology: an example from the origins of irrigation in Southwest Arabia (Yemen)." *Journal of Archaeological Science* Volume 37, Issue 7, July 2010, Pages 1447-1452.

James Oloche Oleyiblo, Zhi-jia Li. 2010. "Application of HEC-HMS for flood forecasting in Misai and Wan'an catchments in China." *Water Science and Engineering* 3(1): 14-22; doi:10.3882/j.issn.1674-2370.2010.01.002.

Joshi, Neekita, Astha Bista, Indira Pokhrel, Ajay Kalra, and Sajjad Ahmad. 2019. "Rainfall-Runoff Simulation in Cache River Basin, Illinois, Using HEC-HMS." *World Environmental and Water Resources Congress* .

Kundzecz, Zbigniew W. 2002. "Non-structural Flood Protection and Sustainability." *Water International* 27 (1).

M.L. Anderson, Z.Q. Chen, M.L. Kavvas, Arlen Feldman. 2002. "Coupling HEC-HMS with Atmospheric Models for Prediction of Watershed Runoff." *Journal of Hydrologic Engineering* Volume 7, Issue 4.

M.R. Knebl, Z.L. Yang, K. Hutchison, D.R. Maidment. 2005. "Regional scale flood modeling using NEXRAD rainfall, GIS, and HEC-HMS/RAS: a case study for the San Antonio River Basin Summer 2002 storm event." *Journal of Environmental Management* Volume 75, Issue 4, June 2005, Pages 325-336.

Macfarlane, W. W., J. M. Wheaton, N. Bouwes, M. L. Jensen, J. T. Gilbert, N. Hough-Snee, and J. A. Shivik. 2017. "Modeling the capacity of riverscapes to support beaver dams." *Geomorphology* 277: 72-99.

Majerova, M., B. T. Neilson, N. M. Schmadel, J. M. Wheaton, and C. J. Snow. 2015. "Impacts of beaver dams on hydrologic and temperature regimes in a mountain Stream." *Hydrology & Earth System Sciences Discussions* 12 (1): 839-878.

Meentemeyer, R. K., and D. R. Butler. 1999. "Hydrogeomorphic Effects Of Beaver Dams In Glacier National Park, Montana." *Physical Geography* 20 (5): 436-446.

Nyssen, J., J. Pontzeele, and P. Billi. 2011. "Effect of beaver dams on the hydrology of small mountain streams: Example from the Chevral in the Ourthe Orientale basin, Ardennes, Belgium." *Journal of Hydrology* 402 (1-2): 92-102.

Pollock, Michael, Gregory Lewallen, Kent Woodruff, Chris Jordan, and Janine Castro. 2015. *The Beaver Restoration Guidebook: Working with Beaver to Restore Streams, Wetlands, and Floodplain.* Portland, Oregon: United States Fish and Wildlife Service. http://www.fws.gov/oregonfwo/ToolsForLandowners/RiverScience/Beaver.asp.

Puttock, A., H. A. Graham, A. M. Cunliffe, M. Elliott, and R. E. Brazier. 2017. "Eurasian beaver activity increases water storage, attenuates flow and mitigates diffuse pollution from intensively-managed grasslands." *Science of the total environment* 576: 430-443.

Salwa Ramly, Wardah Tahir. 2016. "Application of HEC-GeoHMS and HEC-HMS as Rainfall–Runoff Model for Flood Simulation." *Proceedings of the International Symposium on Flood Research and Management 2015.*

Samady, Khalid. 2017. "Continuous Hydrologic Modeling for analyzing the effects of drought on the lower Colorado river in Texas." *Master's Thesis, Michigan Technological University.*

Westbrook, C. J., D. J. Cooper, and B. W. Baker. 2006. "Beaver dams and overbank floods influence groundwater–surface water interactions of a Rocky Mountain riparian area." *Water Resources Research* 42 (6): https://doi.org/10.1029/2005WR004560.

Woo, M. K., and J. M. Waddington. 1990. "Effects of beaver dams on subarctic wetland hydrology." *Arctic* 223-230.

Woonsup Choi, Changshan Wu. 2016. "Impacts of climate change and urban growth on the streamflow of the Milwaukee River (Wisconsin, USA)." (Regional Environmental Change, 17, pages889–899(2017)).

Xuefeng Chu, A.M.ASCE, Alan Steinman. 2009. "Event and Continuous Hydrologic Modelling with HEC-HMS." *ASCE.*

Yves Tramblay, Christophe Bouvier, Claude Martin. 2010. "Assessment of initial soil moisture conditions for event-based rainfall–runoff modelling." *Journal of Hydrology* Volume 387, Issues 3–4, 15 June 2010, Pages 176-187.